Functional Characterization of Interaction Partners of the Co-Chaperone BAG3

Dissertation

zur

Erlangung des Doktorgrades (Dr. rer. nat.)

der

Mathematisch-Naturwissenschaftlichen Fakultät

der

Rheinischen Friedrich-Wilhelms-Universität Bonn

vorgelegt von

Claudia Zeidler

aus Karlsruhe

Bonn, Oktober 2017

Angefertigt mit der Genehmigung der Mathematisch-Naturwissenschaftlichen Fakultät
der Rheinischen Friedrich-Wilhelms-Universität Bonn

1. Gutachter: Herr Prof. Dr. Jörg Höhfeld

2. Gutachter: Herr Prof. Dr. Dieter Fürst

Tag der Promotion: 06.04.2018

Erscheinungsjahr: 2018

Für meine Schwester Betty,

und all den lieben Menschen in meinem Leben,

die die Welt ganz langsam wieder bunt gemacht haben.

Table of Content

Abstract

Protein homeostasis describes the cellular balance between protein synthesis, function and degradation. The stress inducible co-chaperone BAG3 is a key factor in proteostasis in particular under mechanical stress. In cooperation with the actin binding protein Synaptopodin 2 (SYNPO2), BAG3 is a central element of filamin (an actin crosslinking protein) homeostasis in muscle cells. Here BAG3 is involved in the degradation of defective filamin via chaperone assisted selective autophagy (CASA) as well as in the induction of filamin transcription via the Hippo pathway. SYNPO2 can directly bind to the WW-domain of BAG3 and is enabled to recruit complexes mediating the formation of autophagosomes via its N-terminal PDZ-domain.

SYNPO2 belongs to the SYNPO family of actin binding proteins. Four isoforms of SYNPO2 exist of which three contain an N-terminal PDZ-domain, whereas all four isoforms have a centrally located proline-rich motif (PPXY-motif). SYNPO2 was identified to interact with BAG3 via its PPXY-motif in a peptde screen for novel binding partners of the BAG3 WW-domain. Another SYNPO family member, Synaptopodin (SYNPO), was also identified in this peptide screen. SYNPO has three isoforms of which all contain two subsequent PPXY-motifs. Furthermore, SYNPO has been described to interact with the PDZ-domain containing protein MAGI-1 (Membrane Associated Guanylate Kinase Inverted 1).

In this work SYNPO could be confirmed as novel BAG3 binding partner. Because SYNPO2 is not expressed ubiquitously in all cell types, it should be clarified whether SYNPO, together with BAG3, is similarly involved in autophagic protein degradation as shown for SYNPO2. In HeLa cells, which do not express SYNPO2, SYNPO turnover was monitored in the context of inhibition of the proteasome or autophagy. In contrast to SYNPO2, which is rapidly degraded via autophagy upon inhibition of the proteasome or mechanical stress, SYNPO protein levels remained stable upon inhibiton of the proteasome or autophagy. Furthermore, no association of SYNPO with autophagic marker proteins such as LC3 or p62 could be observed in HeLa cells. These findings imply that SYNPO functions differently from SYNPO2 under the chosen experimental conditions. Challenging the cells with increased cellular stress to enhance the induction of BAG3 mediated degradation could potentially have a different effect on SYNPO turnover. Thus similar functions of SYNPO and SYNPO2 in protein degradation can not be excluded.

Immunofluorescent staining of SYNPO in HeLa cells reveals a punctate pattern. These SYNPO punctae are largely increased in size upon overexpression of the largest of the three SYNPO isoforms: SYNPOc. These SYNPOc punctae often show small pointed protrusions and sometimes appear as ring like structures. Furthermore, BAG3 is recruited to these SYNPOc punctae in immunofluorescence experiments. For elucidation of the molecular functions of SYNPO punctae and the role of SYNPO – BAG3 interaction, immunofluorescent co-staining experiments with several marker proteins for e.g. aggresomes, the cytoskeleton, lysosomes or endosomes were conducted. A co-localization of SYNPOc punctae with the early endosome marker EEA1 (early endosome antigen 1) could be observed pointing to a potential involvement of SYNPO in endosomal transport or processing. In addition new binding partners of SYNPO could be identified via immunoprecipitation followed by mass spectrometry, one of them being the actin associated protein Annexin A2 (ANXA2). These findings further underscore a potential involvement of SYNPO in endosomal transport, as ANXA2 has been previously described to play a role in endosomal trafficking. The exact mechanism of SYNPO involvement in endosomal transport, and how BAG3 might contribute to this process, remains to be a topic for further investigation.

Besides confirming SYNPO as a novel binding partner of BAG3, this work provides fundamental information on SYNPO behavior in HeLa cells. The nature of BAG3 – SYNPO interaction could be further characterized and new interaction partners of SYNPO could be identified. In addition, this work provides first experimental data linking SYNPO, possibly together with BAG3, to endosomes, shedding light in potential molecular functions of SYNPO in HeLa cells.

1. Introduction

1.1 Protein homeostasis

Specificity and accuracy are essential for every cell and the organism it is part of. Depending on the context, cells need to grow, divide, migrate, polarize or even die to ensure an organism's viability. To do so, cells are equipped with an intricate network of signaling pathways which allow a cell to constantly adapt to its ever changing surroundings. In the transduction of such signals, proteins are the key players. The entity of all proteins of a cell is called its proteome and comprises a vast amount of different proteins each having (a) specific function(s). Proteins can interact with each other, react to changes in and outside of the cell, bind to cellular membranes and much more. Importantly, all these interactions are either highly specific or tightly controlled and depend on the three dimensional structure and charge of the respective proteins. Minor defects in protein conformation can already result in a loss of its function or its aggregation with other proteins. Here molecular chaperones come into play. They are a group of enzymes, with various cofactors, aiding in protein folding, function in protein quality control and ultimately can direct proteins to be degraded whenever the correct native protein structure cannot be attained. The constant effort of a cell to maintain the balance between protein synthesis, function and degradation is called protein homeostasis, or proteostasis (figure 1.1).

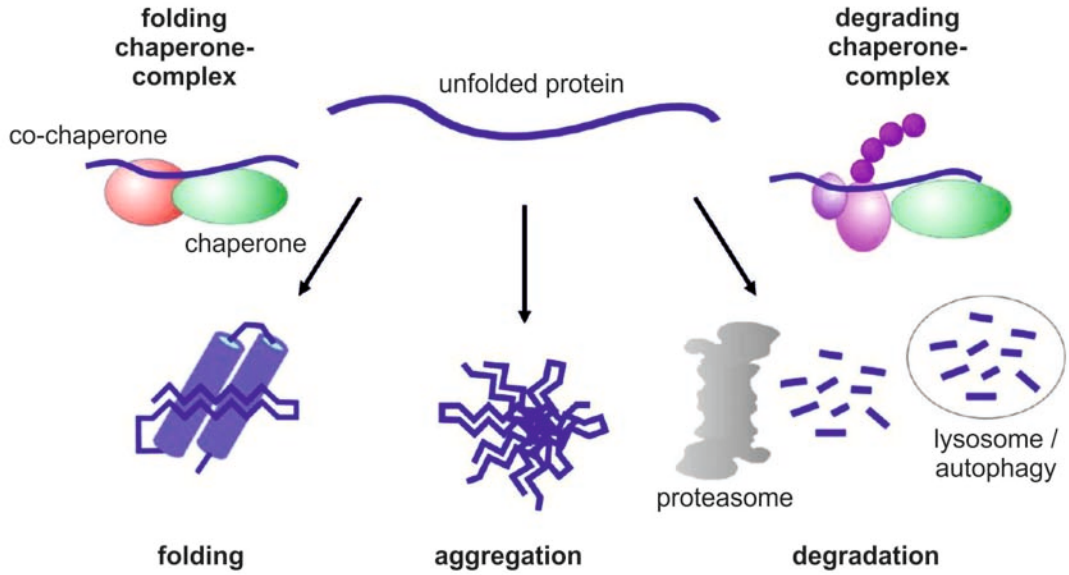

Figure 1.1: Overview proteostasis. Chaperones assist in folding of newly synthesized or unfolded proteins. Under pathophysiological conditions unfolded proteins may aggregate. To prevent aggregation, irreversibly damaged or unfolded proteins need to be degraded. Degrading chaperone-complexes assist in degradation of client proteins by either the proteasomal or the lysosomal / autophagy pathway.

Protein misfolding can have many reasons such as mutations in their genetic code or cellular stress e.g. nutrient deprivation, oxidative stress or mechanical force. Misfolding leads to exposition of hydrophobic residues within the amino acid sequence of the protein, which are hidden inside of the protein when folded in its correct tertiary structure. Thus it is essential that protein folding is tightly and thoroughly controlled, as an accumulation of misfolded proteins may lead to the formation of potentially toxic aggregates. Many severe diseases are associated with protein aggregation such as Huntington's disease or Alzheimer's disease (reviewed by Bates *et al.* 2015 and Kumar *et al.* 2015). Aggregate formation however is not necessarily irreversible. Usually misfolded proteins are detected by chaperones, which help unfolded proteins to fold correctly or mark them for degradation through the attachment of one or many ubiquitin moieties, eventually leading to their degradation via the ubiquitin-proteasome pathway. For the degradation of larger protein compounds including aggregates or even entire cellular organelles, like mitochondria, another pathway exists, namely the autophagic-lysosomal pathway (Glick *et al.* 2010). The lysosome provides an acidic pH and an array

of proteases, which specifically cleave target proteins into small peptides leading to their degradation.

Three types of autophagy have been defined, being macro-autophagy, micro-autophagy and chaperone-mediated autophagy. In micro-autophagy the lysosome directly takes up cytosolic components for degradation by invagination of its membrane (Li *et al.* 2012). In chaperone-mediated autophagy the client protein is bound by chaperones and their respective cofactors for direct deliverance to the lysosome without preceding formation of an autophagosome. These chaperone-client complexes are recognized by lysosomal surface receptors and translocated across the lysosomal membrane to be degraded inside (Cuervo and Wong 2014). The only type of autophagy that involves an intermediate step is macro-autophagy. Here cargo is delivered to the lysosome through a double-membrane vesicle, called the autophagosome, which ultimately fuses with a lysosome (Feng *et al.* 2014) (figure 1.2).

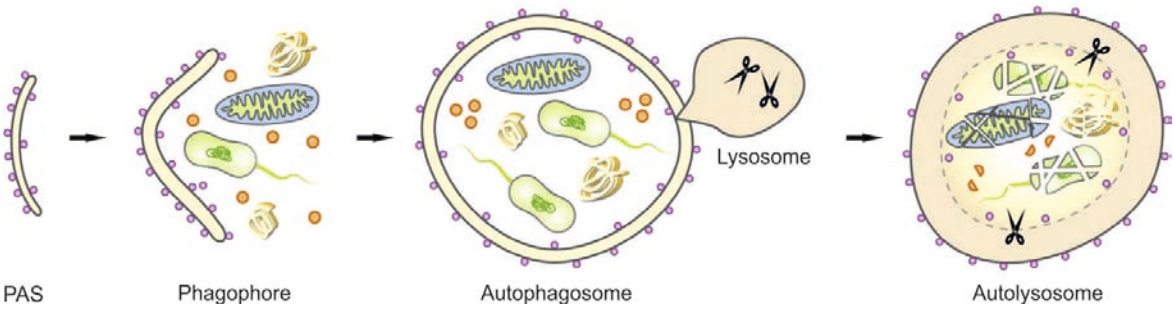

Figure 1.2: Formation of Autophagosomes. Macro-autophagy involves multiple steps ultimately resulting in the autolysosome in which intracellular substrates are degraded. First a phagophore begins to form at the phagophore assembly site (PAS). The phagophore membrane continuously expands and thereby engulfs its substrates leading to a mature autophagosome. The autophagosome then fuses with a lysosome which provides acidic hydrolases and proteases to generate an autolysosome capable of degrading its content (Figure is modified and taken from Behl (2016)).

Recent findings also show an involvement of chaperones and their cofactors in the macro-autophagy pathway, where they initiate or facilitate autophagosome formation. This supports the hypothesis that autophagy is a highly selective process, rather than a random uptake of cytosolic components (Arndt *et al.* 2010, Crippa *et al.* 2010, Carra *et al.* 2008).

1.2 HSP70 and the BAG family

A major, and well characterized, family of chaperones is the HSP70 family (heat shock protein 70 kDa). It comprises constitutively expressed HSP70, termed HSC70 and stress-inducible forms (Murphy 2013). In general, one can regard HSP70 as a small machine driven by hydrolysis of ATP. This reaction is possible due to the N-terminally located ATPase domain of HSP70 which is coupled to the C-terminal peptide-binding domain, consisting of an α-helical lid and a β-sandwich subdomain. Unfolded proteins are recognized via their hydrophobic residues by the β-sandwich. Peptides can stably be bound by HSP70 through hydrolysis of ATP to ADP, leading to a conformational change in the β-sandwich and closure of the α-helical lid (Rüdiger *et al.* 1997). The hydrolysis of ATP and therefore stable substrate binding is supported by HSP40 (heat shock protein 40 kDa) which accelerates the reaction. HSP40 belongs to a family of co-chaperones which, besides enhancing HSP70 function, can also deliver unfolded protein substrates to HSP70 (Fan *et al.* 2003). Substrate release from HSP70 is catalyzed by nucleotide exchange factors exchanging ADP for ATP and thereby promote opening of the α-helical lid of HSP70 (reviewed by Hartl *et al.* 2011, Mayer 2010).

For the selectivity of chaperone function their cofactors or co-chaperones play an important role as they facilitate recognition and release of client proteins, recruitment of ubiquitin ligases, substrate delivery to the autophagic machinery and many more processes (Caplan 2003, Edkins 2015, Arndt *et al.* 2010). Among the vast variety of thus far identified co-chaperones is the Bcl-2 associated athanogene 3 (BAG3).

BAG3 is one of six proteins, which constitute the human BAG family. BAG1 was the first family member to be identified in 1995 as a Bcl-2 (B-Cell lymphoma 2) binding protein. It could be shown that BAG1 has an anti-apoptotic effect, especially in combination with Bcl-2. This anti-apoptotic function of BAG1 also gave rise to its name as the term "*athano*" is derived from the Greek word "*athanos*" which means anti-death (Takayama *et al.* 1995). Another four members of the BAG family (BAG 2 – 5) were identified shortly afterwards by a yeast two-hybrid screen with the ATPase domain of HSC/HSP70 as bait. The conserved binding domain responsible for the interaction of BAG family members with the HSC/HSP70 ATPase domain was termed BAG domain and is shared by all members of the BAG family (Takayama *et al.* 1999) (figure 1.3). Only two years later it could be shown, that BAG1 promotes release of substrate from HSP70 by binding to the ATPase domain via its BAG domain (Sondermann *et al.* 2001). Therefore BAG family members act as nucleotide exchange factors assisting HSC/HSP70 in substrate release, making BAG family members co-chaperones.

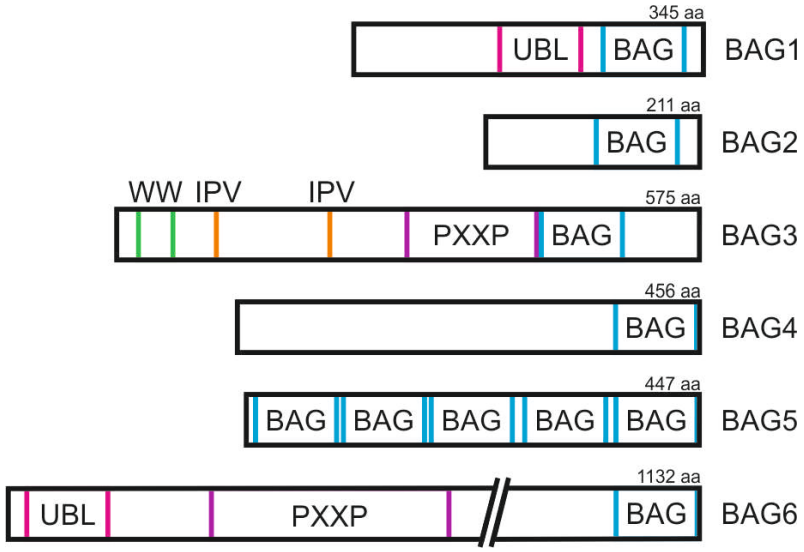

Figure 1.3: The BAG protein family. Schematic representation of the human family of BAG proteins. Each member has a C-terminally located BAG domain and differing domains and motifs throughout their N-termini and central sequence. UBL – ubiquitin-like domain, WW – WW-domain, IPV – IPV (Ile-Pro-Val) motif, PXXP – proline rich region. Data shown in this figure was obtained from the UniProt database (http://www.uniprot.org).

1.3 The co-chaperone BAG3

In this work, focus was laid on the BAG family member 3 (BAG3). Two isoforms have been reported for BAG3, which can be detected by Western Blot at roughly 80 and 40 kDa (Rosati *et al.* 2011, Bruno *et al.* 2008). BAG3 expression could be shown in various tissues under cellular stress conditions, whereas BAG3 is constitutively expressed in skeletal muscle, the heart and cancer cells (Homma *et al.* 2006). Interestingly BAG3 expression is induced under cellular stress such as oxidative stress, HIV-1 infection or mechanical stress (Bonelli *et al.* 2004, Rosati *et al.* 2007 and 2009, Ulbricht *et al.* 2015). Like all BAG family members also BAG3 can interact with Bcl-2 via its BAG domain and acts as an anti-apoptotic protein (Lee *et al.* 1999). Furthermore BAG3 contains various other motifs and domains for protein-protein interactions such as an N-terminally located WW-domain, two IPV (Ile-Pro-Val) motifs and a centrally located proline rich (PXXP) repeat region, completed by a C-terminal LEAD motif for Caspase 9 cleavage (Merabova *et al.* 2015, Fuchs *et al.* 2010, Chen *et al.* 2013, Virador *et al.* 2009) (figure 1.4). Being equipped with these diverse domains and motifs, BAG3 shows high potential to be involved in various cellular pathways. This potential has been proven true by linkage of BAG3 to biological processes ranging from apoptosis, cytoskeleton arrangement, cell

adhesion and migration, to developmental processes, protein folding and autophagy (Lee *et al.* 1999, Iwasaki *et al.* 2007 and 2010, Shi *et al.* 2016, Choi *et al.* 2006, De Marco *et al.* 2011, Behl 2016, Arndt *et al.* 2010, Gamerdinger *et al.* 2011).

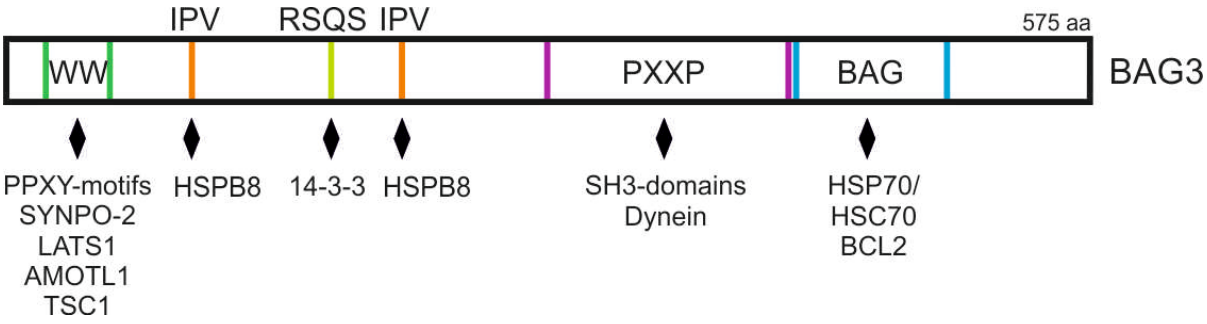

Figure 1.4: The human co-chaperone BAG3. BAG3 comprises various domains and motifs for protein-protein interaction being an N-terminal WW-domain with the capability of interaction with proteins like SYNPO2 or AMOTL1. Two IPV motifs for interaction with the small heat shock protein HSPB8, two RSQS motifs in close proximity for interaction with 14-3-3 (here indicated by only one light green line), a proline rich region which mediates binding to the motor protein dynein and a C-terminal BAG-domain for interaction with HSP70/HSC70 and Bcl-2. Additional protein binding partners of BAG3 are given below each domain / motif. Data obtained from the UniProt database (http://www.uniprot.org).

1.4 BAG3 in cancer

Many studies describe BAG3 to play a role in various types of cancer. In non-small cell lung cancer BAG3 is described to promote resistance to apoptosis (Zhang *et al.* 2012). This anti-apoptotic activity of BAG3 in tumors has also been reported for other types of tumors like thyroid carcinomas (Chiappetta *et al.* 2006), neuroblastoma cells (Gentilella *et al.* 2008), colon cancer (Aaron *et al.* 2009), kidney cancer (Wang *et al.* 2009) and pancreatic cancer (Liao *et al.* 2001). In hepatocellular carcinomas increased BAG3 levels can inhibit cellular proliferation via an interaction with glucose-6-phosphate dehydrogenase, a pentose phosphate pathway enzyme (Kong *et al.* 2016). Through the function as a co-chaperone of HSP70, BAG3 is involved in many additional cancer cell signaling pathways. For example the transcription factor nuclear factor κB (NF-κB) signaling, an essential pathway for cellular survival, or the cell cycle regulator p21 (Colvin *et al.* 2014). The many roles of BAG3 in tumor development and progression make it a potential target for cancer therapy. A small molecule inhibitor, YM-1, which disrupts the HSP70-BAG3 complex has been identified and successfully used in mice to

suppress tumor growth (Colvin *et al.* 2014). Furthermore JG-98, an allosteric inhibitor of the HSP70-BAG3 protein interaction, was tested in xenograft models revealing elevated p21 levels and limited tumor growth (Li *et al.* 2015).

1.5 BAG3 knockout mice and myopathies

In the model organism *Drosophila melanogaster* only one BAG family protein is expressed called Starvin. Homozygous mutant alleles of Starvin lead to an early death of *Drosophila* larvae during the first larval instar. This is due to their inability to take up food resulting in the lack of body size increase and death by starvation (Coulson *et al.* 2005, Arndt *et al.* 2010). Flies with a heterozygous knockout for Starvin reach adulthood, but develop a progressive myopathy (Arndt *et al.* 2010). This could also be shown in BAG3 deficient homozygous knockout mice which develop normally, but postnatally develop a severe myopathy and die by 4 weeks of age (Homma *et al.* 2006). Together this indicates that BAG3 / Starvin is not essential for muscle development during embryogenesis but crucial for postnatal skeletal muscle homeostasis (Coulson *et al.* 2005, Arndt *et al.* 2010). BAG3 knockout mice generated with the cre-LoxP system by Youn *et al.* (2008) also showed growth retardation and death by three weeks of age. Furthermore, it was shown that the mice showed hypoglycemia, a reduction of white blood cells, splenocytes and thymocytes and a reduction of weight of the thymus and spleen (Youn *et al.* 2008).

In humans several mutations of the BAG3 gene are described in myopathies predominantly affecting the heart (dilated cardiomyopathy) eventually resulting in heart failure (Norton *et al.* 2011, Villard *et al.* 2011, Franaszczyk *et al.* 2014). Patients with a point mutation in the BAG3 gene which leads to an amino acid substitution of proline 209 to leucine (BAG^{P209L}) show a combination of cardiomyopathy and myofibrillar myopathy with very early onset in childhood. On cellular level BAG^{P209L} patients show disintegration of Z-discs and myofibrils with additional aggregation of BAG3 and other Z-disc proteins like desmin or filamin (Kostera-Pruszczyk *et al.* 2015, Selcen *et al.* 2009).

Together this leads to the conclusion that BAG3 is important for postnatal growth and survival, with a considerable effect on food uptake and muscle function.

1.6 BAG3 in protein homeostasis

Through its interaction with HSP70, BAG3 is directly involved in protein homeostasis. Like all BAG family members it acts as a nucleotide exchange factor aiding in substrate release from HSP70 (Sondermann *et al.* 2001, Arndt *et al.* 2010). In addition to this, several studies show an involvement of BAG3 in selective macro-autophagy pathways, where it assists substrate selection. BAG3 directly links HSP70 to these selective macro-autophagy pathways and has also been shown to be able to recruit autophagic adaptor proteins to sites of phagophore assembly (Ulbricht *et al.* 2013, Kathage *et al.* 2017) A peptide screen for BAG3 interaction partners which specifically bind to its WW-domain resulted in the identification of Synaptopodin 2 (SYNPO2) (PhD thesis Ulbricht 2013). It could be shown, that interaction of BAG3 with SYNPO2 is important for autophagosome formation during tension-induced chaperone assisted selective autophagy (CASA) in muscle cells (Arndt *et al.* 2010, Ulbricht *et al.* 2013 and 2015). Here, unfolded / damaged filamin, a cytoskeletal protein responsible for cross-linking of actin filaments in the cytoskeleton and at the Z-disk of striated muscle, is specifically recognized by a complex consisting of HSP70, HSPB8 and BAG3 (Nakamura *et al.* 2011, Ulbricht *et al.* 2013). HSP70 recruits the ubiquitin ligase CHIP which, together with the ubiquitin conjugating enzyme 4/5, mediates poly-ubiquitination of filamin and thereby labels it for degradation via the autophagic pathway (Arndt *et al.* 2010, Murata *et al.* 2001). With the help of its N-terminal PDZ-domain, SYNPO2 is able to interact with the membrane tethering proteins VPS18 and VPS16 (Vacuole Protein Sorting 18 and 16), key components of membrane tethering complexes responsible for recognition and interaction of two independent membranes (Chia and Gleeson, 2014). Furthermore the SNARE-protein (soluble NSF attachment receptors) Syntaxin 7, a catalysator of membrane fusion (Mullock *et al.* 2000) was identified to be in a complex with SYNPO2. Interaction of BAG3 with SYNPO2 therefore enables recruitment of a complex mediating the formation of autophagosomes to the CASA machinery (Ulbricht *et al.* 2013).

The specific recognition and degradation of filamin is important since filamin functions as a cross-linking agent of actin and is under extra- and intracellular strain. This strain causes a partial, reversible unfolding of filamin. However, unfolded filamin is prone to aggregation which leads to loss of its ability to refold to its native conformation. Cytoskeletal maintenance therefore requires a constant degradation and replacement of irreversibly unfolded filamin which involves BAG3 as described above. Intriguingly, BAG3 does not only mediate the specific disposal of damaged filamin, but also is involved in stimulating filamin transcription. Via its WW-domain BAG3 can interact with LATS1 (Large Tumor Suppressor Kinase 1) and AMOTL1 (Angiomotin Like 1) (Ulbricht *et al.*

2013), which are inhibitors of the transcription factors YAP (Yes Associated Protein 1) and TAZ (WW Domain Containing Transcription Regulator 1 (WWTR1)) of the Hippo signaling pathway (reviewed by Salah and Aqeilan, 2011 and Wang *et al.* 2017). By BAG3 binding to LATS1 and AMOTL1 respectively, YAP and TAZ are released and can translocate into the nucleus to initiate, next to many other target genes, filamin transcription (Dupont *et al.* 2011, Ulbricht *et al.* 2013) (figure 1.5).

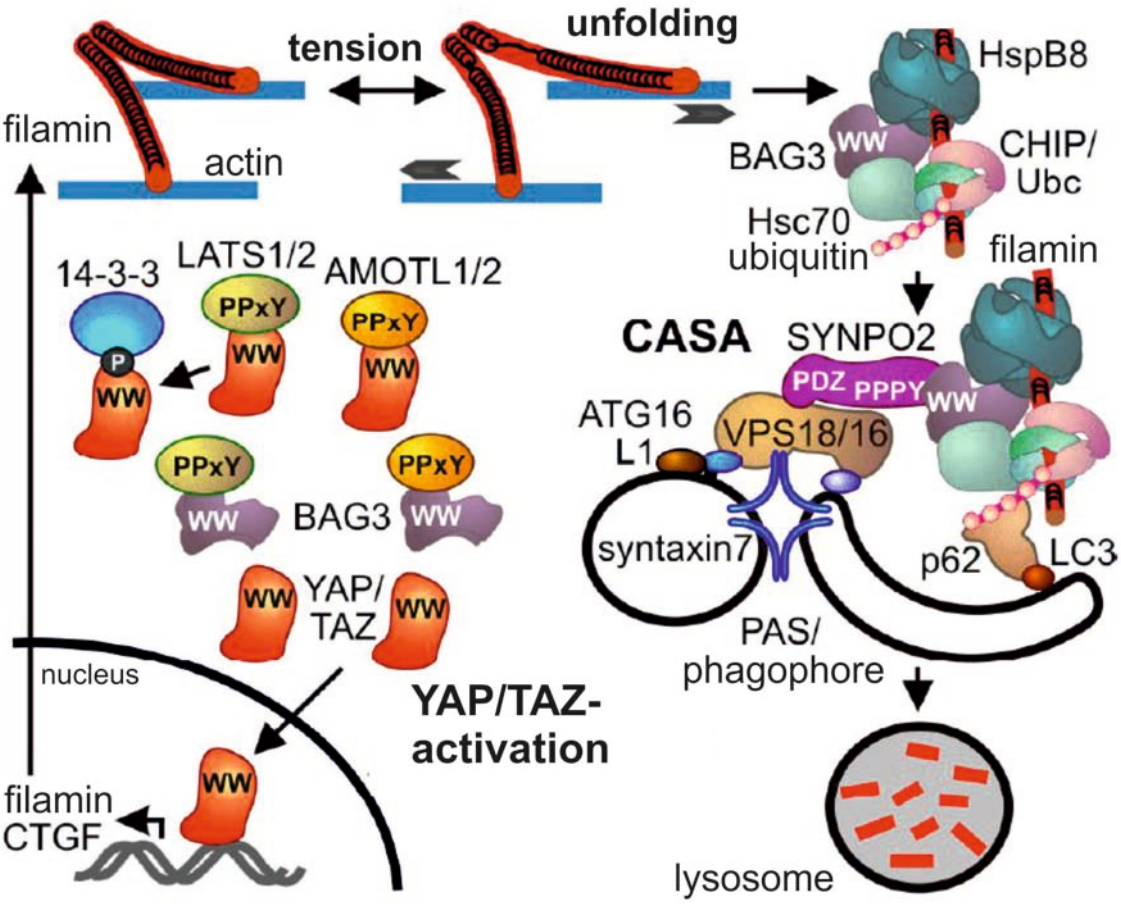

Figure1.5: BAG3 in chaperone assisted selective autophagy (CASA) and filamin transcription. Overview of specific filamin degradation in muscle cells mediated by BAG3 in complex with HSC70, HSPB8, CHIP and SYNPO2. Unfolded filamin is recognized by the CASA machinery and delivered to the autophagosome via BAG3 – SYNPO2 and ubiquitin – p62 interaction. On the left side involvement of BAG3 in YAP/TAZ activation is depicted. BAG3 binds to the YAP/TAZ inhibitors LATS1/2 and AMOTL1/2 via its WW-domain and thereby releases YAP/TAZ for translocation to the nucleus where they act as transcription factors for filamin and other proteins. Figure was modified and taken from Ulbricht *et al.* 2013.

It has been long known that under cellular stress, like nutrient deprivation, mechanical strain or oxidative stress, autophagy is employed for recycling of nutrients and other

cellular components to ensure survival (reviewed by Bento *et al.* 2016, Navarro-Yepes *et al.* 2014, Ulbricht *et al.* 2013). Interestingly, BAG3 expression is up-regulated under acute cellular stress, in aged cells or by the inhibition of the proteasome (Gamerdinger *et al.* 2009). Under physiological conditions BAG-family member dependent degradation of proteins is mediated by BAG1 and HSP70 which guide client proteins to the ubiquitin-proteasomal-pathway (Lüders *et al.* 2000). Pathophysiological conditions however give rise to an increased cellular level of BAG3 protein, thereby turning on BAG3-mediated selective autophagy. This mechanism also referred to as the "BAG1 – BAG3 Switch" allows a cell to adapt to and react to cellular stress (Gamerdinger *et al.* 2009). BAG3 has been reported to sequester ubiquitinated proteasomal clients to cytoplasmic punctae upon proteasome inhibition. These punctae can be co-labeled for LC3, a marker for autophagosomes (Minoia *et al.* 2014). Furthermore BAG3 is actively involved in the formation of perinuclear compartments called aggresomes (Gamerdinger *et al.* 2011). Aggresomes can be referred to as a kind of collecting point for proteins marked for degradation by autophagy (reviewed by Kopito, 2000). Aggresome targeting of client proteins is achieved by an interaction of BAG3 with the microtubule-motor protein dynein, thereby selectively directing HSP70 bound substrates to the motor and subsequently to the aggresome (Gamerdinger *et al.* 2011). An example for this BAG3 mediated transport is mutated SOD1 (Superoxide Dismutase 1), a protein linked to amyotrophic-lateral-sklerosis (ALS) and an established HSP70 substrate (Wang et al 2009). SOD1 is specifically directed to aggresomes through BAG3 mediated coupling of SOD1 to the dynein motor (Gamerdinger *et al.* 2011). In support of these findings isoforms of 14-3-3 protein, which have been previously described to play a role in aggresome formation (Waelter *et al.* 2001, Omi *et al.* 2008, Wang *et al.* 2009), were shown to act as adaptor for dynein – BAG3 interaction and to recruit motor cargo for transport to the aggresome (Xu *et al.* 2013).

1.7 The actin cytoskeleton

Also important for cellular integrity is the cytoskeleton. It generally consists of three main components which are actin-filaments, microtubules and intermediate filaments. Together they are responsible for many essential functions of the cell such as spatial organization of cellular content, connecting the cell to the extracellular matrix and generation of force to enable cellular movement and changes of shape (reviewed by

Fletcher and Mullis, 2010). Next to these fundamental processes, the actin cytoskeleton has been described in many important cellular functions such as endocytosis (Morel *et al.* 2009), autophagy (Mi *et al.* 2015, reviewed by Coutts and La Thangue, 2016) and intracellular transport (reviewed by Khaitlina, 2014). Therefore, it is not surprising that actin is a highly conserved protein and one of the most abundantly expressed proteins in eukaryotic cells (reviewed by Dominguez and Holmes, 2011). Via dynamic remodeling and the interplay of the actin cytoskeleton with an ever growing number of actin-binding proteins (ABPs) the diverse and highly complex cellular activities mentioned above can be accomplished. Actin exists in two forms namely the monomeric / globular G-actin and the filamentous F-actin. Being an ATPase, actin can switch between its two forms in an ATP dependent manner, tightly regulated by ABPs. As indicated by their respective names, G-actin is monomeric and not incorporated into actin filaments, whereas F-actin is the major component of actin filaments. Generally actin filaments are asymmetric with a barbed end (or + end), which is the growing site of an actin filament and the pointed end (or – end) of the filament at which de-polymerization occurs. Continuous polymerization and de-polymerization is referred to as actin treadmiling (reviewed by Carlier and Shekhar, 2017). In addition to treadmilling, generation and maintenance of an intact and dynamic actin cytoskeleton requires constant nucleation of new filaments, branching, crosslinking, severing and capping, mediated with the help of ABPs. Some of the most important actin regulating ABPs are the Rho family GTPases Rho, Rac and Cdc42. They control the assembly of stress fibers (Rho), lamellipodia (Rac) and filopodia (Cdc42), in response to extra – and intracellular signals (Asanuma *et al.* 2006, Krugman *et al.* 2001, reviewed by Raftopoulou and Hall, 2004). Lamellipodia consist of highly branched actin filaments at the leading edge of a migrating cell. Via actin treadmilling, force is generated to move the cell forward. Filopodia are cellular protrusions reaching beyond the leading edge, sensing the environment whereas stress fibers span the cell and link it to the extracellular matrix via focal adhesions and adherens junctions (reviewed by Le Clainche and Carlier, 2008). It becomes apparent, that dynamic actin cytoskeleton rearrangement is essential for cellular function. But how is actin polymerization initiated? Actin filament polymerization occurs in three phases: nucleation, elongation and steady state. Formins mediate *de novo* nucleation of unbranched actin filaments such as stress fibers and filopodia by promoting the interaction between two actin monomers (reviewed by Lee and Dominguez, 2010). For nucleation of actin monomers from existing filaments the Arp2/3 (actin related proteins 2/3) complex comes into play as an inductor of branched actin filaments like lamellipodia (Wu *et al.* 2012, Rogers *et al.* 2003, Mejillano *et al.* 2004). Nucleation is followed by elongation of the actin filament by incorporation of G-actin into the filament via ATP

hydrolysis. This is facilitated by ABPs such as profilin which can bind directly to the FH1 domain of formins (Romero *et al.* 2004). The steady state of actin filament polymerization describes the state of actin treadmilling described above in which new G-actin is integrated at the barbed end and F-actin dissociates from the pointed end of the actin filament. In their review, Fletcher and Mullins (2010) nicely compare cytoskeletal building blocks to the popular toy LEGO, as both consist of multiple copies of key pieces which can be put together to form larger structures which can be disassembled and reassembled for specific function according to cellular needs.

A role of BAG3 in cellular migration and adhesion could be established as homozygous BAG3 deficient mouse embryonic fibroblasts show delayed filopodia and focal adhesion formation and reduced motility (Iwasaki *et al.* 2007). In muscle cells BAG3 has been shown to interact with and stabilize the actin capping protein CapZ in order to maintain myofibrillar integrity (Hishiya *et al.* 2010). In striated muscles the BAG3 interacting protein SYNPO2 localizes together with BAG3 at Z-disks which are actin anchoring structures. Through CASA, BAG3 and SYNPO2 are involved in Z-disk maintenance via filamin degradation (as described above) (Ulbricht *et al.* 2013). A common feature of the SYNPO family proteins is their ability to bind to actin, this includes the family member and novel BAG3 interactor Synaptopodin (SYNPO), which will be discussed in the following chapter.

1.8 The actin-binding protein Synaptopodin (SYNPO)

SYNPO2 which was, as mentioned above, identified to bind to BAG3 in CASA, belongs to the SYNPO family of proteins defined by sequence homology and their ability to bind to actin (Chalovich abd Schroeter 2010). The peptide screen for interaction partners of the BAG3 WW-domain which lead to the identification of SYNPO2 as binding partner of BAG3 also detected SYNPO as a possible BAG3 WW-domain interactor (PhD thesis Ulbricht 2013, unpublished data). The SYNPO family comprises at least four members being Synaptopodin (SYNPO), SYNPO2 (also termed Myopodin), SYNPO2-like protein and Fesselin (Weins *et al.* 2001, Schroeter *et al.* 2008). SYNPO, the founding member and eponym of the SYNPO family, was first identified in 1991 as a protein of 44 kDa in size, which is expressed in podocytes of rat kidney glomeruli (Mundel *et al.* 1991). Later on it was shown that the originally identified 44 kDa SYNPO is a proteolytic fragment of full length SYNPO, which can be detected in Western Blot experiments at 100 kDa (rat

forebrain) or 110 kDa (rat kidney) (Mundel *et al.* 1997). Furthermore SYNPO was shown to localize in punctae, which co-localize with the actin cytoskeleton in immunofluorescence experiments, and was also detected in focal contacts (Mundel *et al.* 1997). SYNPO is involved in the bundling and elongation of actin filaments by interaction with the actin crosslinker α-actinin and is therefore a dual actin / α-actinin binding protein (Kremerskothen *et al.* 2005). Knockout of SYNPO in murine podocytes results in a significant delay in reformation of actin stress fibers after treatment with the actin depolymerizing agent cytochalasin D (Asanuma *et al.* 2005). Actin stress fibers are specific for non-muscle cells and are composed of actin and non-muscle myosin II. In addition they interact with various crosslinkers such as α-actinin-4. They are important for cell adhesion, morphogenesis, migration and mechanotransduction as they can produce force by movement of myosin II motor domains along the actin filaments (figure 1.6) (reviewed by Tojkander *et al.* 2012).

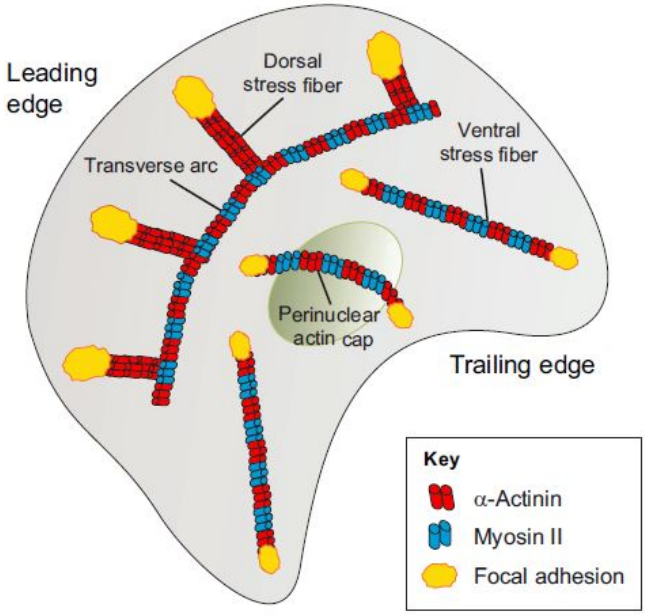

Figure 1.6: Schematic representation of stress fibers and their orientation and components. Four types of stress fibers are distinguished from each other by their cellular localization, orientation, composition and association with focal adhesions. The most important components of actin stress fibers are α-actinin and non-muscle myosin II as indicated in red and blue. Figure is taken from Tojkander *et al.* (2012).

Besides other functions mentioned above, stress fibers are associated with wound healing. It could be shown that SYNPO expression is up-regulated under laminar shear stress in endothelial cells and that SYNPO plays a role in endothelial wound healing. It is hypothesized that SYNPO participates in wound healing because of its ability to remodel

the actin cytoskeleton, which promotes cellular migration and wound closure (Mun *et al.* 2014). The effect of SYNPO on cellular migration has also been described by Asanuma *et al.* (2006), who could show that podocyte migration is impaired upon gene disruption of SYNPO. Furthermore, they were able to link SYNPO to RhoA in stress fiber formation. RhoA belongs to the Rho family of small GTPases and promotes stress fiber formation *in vivo* (reviewed by Ridley, 1997). The role of SYNPO in stress fiber formation is to block (by competitive binding) Smurf-1-mediated ubiquitylation of RhoA and thereby preventing its degradation via the proteasome (Asanuma *et al.* 2006). This shows that SYNPO is not only a component of stress fibers but also a modulator of their formation. In podocytes, SYNPO has been shown to interact with 14-3-3β and 14-3-3η, chaperone-like phospho-serine / thereonine-binding proteins, in a phosphorylation dependent manner. 14-3-3β interaction protects SYNPO from Cathepsin-L mediated cleavage and thereby preserves SYNPO induced stress fiber formation (Faul *et al.* 2008). Homozygous knockout mice for SYNPO have been reported to lack spine apparatuses in excitatory neurons and show deficits in spatial learning (Deller *et al.* 2003). Together these data indicate various roles of SYNPO in cytoskeletal integrity and neuronal function and give first hints on an involvement of SYNPO in mechanotransduction.

1.9 Aim of the work

The precise regulation of chaperone assisted selective autophagy is crucial for protein homeostasis and muscular maintenance. Together with SYNPO2, the co-chaperone BAG3 is indispensable for the degradation and synthesis of filamin under mechanical strain (Ulbricht *et al.* 2013).

This work was conducted in order to identify and characterize further components interacting with BAG3 and their potential involvement in CASA. Here the actin binding protein SYNPO, identified in the same peptide screen which originally identified SYNPO2 as BAG3 binding partner, was chosen as a prominent candidate protein for BAG3 interaction and CASA function. With its bundling and elongation activity of actin filaments, its ability to bind to α-actinin, the PDZ-domain containing protein MAGI-1 and its association with actin stress fiber formation (Kreemerskothen *et al.* 2005, Yanagida-Asanuma *et al.* 2007, Faul *et al.* 2008), SYNPO displays characteristics similar to those described for SYNPO2 in muscle cells (Linnemann *et al.* 2010, Ulbricht *et al.* 2013). It

was of interest whether SYNPO carries out similar functions as SYNPO2 in cells which do not express SYNPO2.

In addition, SYNPO in general was subject for further molecular characterization, as there is not much known about SYNPO beyond its roles in podocytes and in neuronal context.

2. Materials and Methods

2.1 Material

2.1.1 Appliances

Appliance	Supplier
Autoclave	Tuttnauer Systec
Biofuge fresco	Heraeus
Biofuge pico	Heraeus
Blot-system (mighty small transfer)	Amersham
Cooling centrifuge 5415R	Eppendorf
Cooling centrifuge 5810R	Eppendorf
Developing machine CURIX 60	AGFA
Electrophoresis Power supply	Amersham
Electrophoresis-system HE33	Hoefer
Extraction system	HLC Biotech
Freezer (-80°C)	Forma Scientific

Freezer (-20°C)	Liebherr / Siemens
Fridge	Siemens
Gel-documentation-system Gel Doc	Biorad
Heating block	Eppendorf
Ice machine MF22	Scotsman
Incubator	Heraeus / Binder
Laminar flow hood	Nalge Nunc Industries
Light microscope ID03	Zeiss
LSM Axiovert 100M	Zeiss
Magnetic stirrer MR2002	Heildolph
Mastercycler	Eppendorf
Mastercycler epgradient S	Eppendorf
Microwave	Bosch
Milli-Q-Plus Water purifier	Millipore
pH-meter	Mettler Toledo
Photometer	Eppendorf
Pipettes	Eppendorf
qPCR-Cycler CFX96 Touch	Biorad
Rotating wheel	Renner
SDS-Page-system (mighty small II)	Amersham
Rocking platform	Stuart
Scale	KernKB
Special accuracy scale SI-234	Denver Instruments
Tabletop centrifuge 400R	Heraeus
Thermo-block	HLC Biotech QBT
Thermocycler T3000	Biometra
Thermo-shaker	Medline Scientific
Ultrasonicator UP100H	Hielscher Ultrasound Technology
Vortex-Genie 2	Scientific Industries
Waterbath A100	Lauda

2.1.2 Consumables

Material	Supplier
Cell culture dishes	Sarstedt
Common laboratory demand	Faust, Meckenheim
Fuji X-Ray Film Super RX	Fuji
Reaction tubes	Eppendorf
Plasticware	Roth

2.1.3 Kits, enzymes and standards

Kit	Supplier
CalPhos-Transfection Kit	Clonetech
ECL Blot detection	Thermo Fisher Scientific
iScript cDNA Synthesis Kit	Biorad
JetPRIME Transfection Kit	Peqlab
NucleoBond® Xtra Maxi	Macherey-Nagel
NucleoSpin® Gel and PCR Clean-up	Macherey-Nagel
NucleoSpin® Plasmid	Macherey-Nagel
SsoFast™ EvaGreen® Supermix	Biorad

Standard	Supplier
Gene Ruler DNA Ladder Mix 1 kb	Fermentas
Prestained Protein Standard Plus	Biorad

Enzyme	Supplier
Alkaline Phosphatase	Thermo Scientific
Complete Protease-Inhibitor Cocktail	Roche
KOD-Polymerase	Millipore
Lambda Protein Phosphatase	New England Biolabs
PCR nucleotide mix	Roche
Restrictionendonucleases	Fermentas

RNase A	Segentic
T4-DNA-Ligase	Thermo Scientific

2.1.4 Chemicals

Chemical	Supplier
2-Propanol (Isopropanol)	Roth
Acetic acid	Roth
Acrylamide (30%)/bis-Acrylamide	Roth
Agar	Roth
Agarose	Roth
Ampicillin	Roth
ATP (adenosine triphosphate)	Sigma Aldrich
Bacto-Yeast extract	Roth
Bacto-Trypton	Roth
Bafilomycin A1	LC Labs
$CaCl_2$ (Calciumchloride)	Roth
Coomassie Brilliant Blue R250	Sigma Aldrich
DMSO (Dimethylsulfoxide)	Roth
DTT (Dithiothreitol)	Sigma Aldrich
EDTA (Ethylenediaminetetraacetate)	Roth
Ethanol (absolute)	Roth
Glucose	Roth
Glutamine	Life Technology
Glycerine	Roth
Glycine	Roth
HCl	Roth
HEPES	Roth
Imidazole	Roth
K_2HPO_4	Roth
Kanamycine	Roth
KCl	Roth

KH_2PO_4	Roth
KOH	Roth
Mercaptoethanole	Roth
Methanol	Roth
MG132	Peptanova
$MgCl_2$	Roth
$MgSO_4$	Roth
MOPS	Roth
MOWIOL®	Calbiochem
Na_2HPO_4	Roth
NaCl	Roth
NaOH	Roth
Nonidet p-40	Sigma Aldrich
Penicillin	Life Technology
Ponceau S	Roth
Protein-G sepharose	GE Healthcare
Puromycine	Calbiochem
SDS	Roth
Streptomycin	Life Technology
TCA	Roth
TEMED	Roth
Tris	Roth
Triton X100	Roth
Tween-20	Sigma Aldrich

2.1.5 Antibodies

2.1.5.1 Primary Antibodies

Antigen	Species	Supplier
β-actin	mouse	Abcam
BAG3	rabbit	Proteintech
EEA1	goat	Santa Cruz

FLAG (M2)	mouse	Sigma Aldrich
γ-Tubulin	goat	Santa Cruz
LAMP1	mouse	Abcam
S6-P	rabbit	New England Biolabs
SYNPO	rabbit	Synaptic Systems
SYNPO2	rabbit	Prof. Fürst / Uni Bonn
Ubiquitin (FK2)	mouse	Biomol

2.1.5.2 Secondary Antibodies

Antigen	Species	Supplier
Clean Blot	diverse	Thermo Scientific
Goat IgG + PO	rabbit	Sigma Aldrich
Goat IgG Alexa Fluor 488	donkey	Abcam
Mouse IgG	/	Santa Cruz
Mouse IgG Alexa Fluor 488 nm	goat	Invitrogen
Mouse IgG + PO	goat	Sigma Aldrich
Rabbit IgG	/	Santa Cruz
Rabbit IgG Alexa Fluor 488 nm	goat	Invitrogen
Rabbit IgG Alexa Fluor 546 nm	goat	Invitrogen
Rabbit IgG Alexa Fluor 633 nm	goat	Invitrogen
Rabbit IgG + PO	goat	Sigma Aldrich
True Blot	rat	Rockland

2.1.6 Plasmids

Plasmid	Comment
pcDNA 3.1(+) w/o t	Expression of proteins in mammalian cells tag. Under control of a viral promoter.
pcDNA-BAG3	AG Höhfeld
pCMV-Tag2B-empty	Expression of proteins in mammalian cells with N-terminal FLAG-tag. Under control of a CMV-promoter (Invitrogen).

pCMV-Tag2b-ANXA2	Cloned from human cDNA transcript
pCMV-Tag2B-BAG3	AG Höhfeld
pCMV-Tag2B-BAG3-WAWA	AG Höhfeld
pCMV-Tag2b-SYNPOc	Cloned from human cDNA transcript
pCMV-Tag2b-SYNPOb	Cloned from human cDNA transcript
pCMV-Tag2b-SYNPOc-PAAY1st	Cloned from pCMV-Tag2b-SYNPOc with specific primers containing the desired mutations.
pCMV-Tag2b-SYNPOc-PAAY2nd	Cloned from pCMV-Tag2b-SYNPOc with specific primers containing the desired mutations.
pCMV-Tag2b-SYNPOc-PPXYdouble	Cloned from pCMV-Tag2b-SYNPOc with specific primers containing the desired mutations.
pCMV-Tag2b-Vim	Cloned from human cDNA transcript
pTraffic-LC3	AG Höhfeld
pTraffic-p62	AG Höhfeld
pEGFP-BAG3	AG Höhfeld
pEYFP-Vim	AG Höhfeld

2.1.7 Oligonucleotides

OligonucleotideSequence (5'→3')

Annexin-FW-BamHI	CGCTTTGGATCCATGTCTACTGTTCACGAAATCC
Annexin2-Rev-XhoI	CGCTTTCTCGAGTCAGTCATCTCCACCACACAG
qPCR B2M FW	GTGATCTTTCTGGTGCTTGTC
qPCR B2M RV	AAGTTGGGCTTCCCATTCTC
qPCR GAPDH FW	GAGAAACCTGCCAAGTATGATGAC
qPCR GAPDH RV	ATCGAAGGTGGAAGAGTGGG
SY-Long-FW-HindIII	GCGTTTAAGCTTATGCTGGGTCCTCACCTCCCAC
SY-Long-Rev-XhoI	GCAAGCCTCGAGTTACTTGAAGCAGAAGGAAGGCTTC
SY-Long-qPCR-Hu-FW	ACACCGCAGCTGCCCAAAGC
SY-Long-qPCR-Hu-RV	TGAAGAGCTGGACGCCACGG
SYNPO-qPCR-Hu-FW	CGTGGAGAAGCCCAAGGTGACC
SYNPO-qPCR-Hu-RV	GCTCCCTTCCCAGAGGCCTC

SYNPO-PT610AA-FW	ACTTCACTGCACCCGCCGCCTACACTGAGACC
SYNPO-PT610AA-RV	GGTCTCAGTGTAGGCGGCGGGTGCAGTGAAGT
SYNPO-PS629AA-FW	CTGGGTGAGGTCTCCTGCCGCATATTCTGTCCTGTA
SYNPO-PS629AA-RV	TACAGGACAGAATATGCGGCAGGAGACCTCACCCAG
Vimentin-FW-BamHI	GCGTTTGGATCCATGTCCACCAGGTCCGTGTC
Vimentin-Rev-HindIII	GCAAGCAAGCTTTTATTCAAGGTCATCGTGATGC

2.1.8 siRNA

Gene	siRNA	Species	Supplier
BAG3	Hs_BAG3_5	human	Qiagen
BAG3	Hs_BAG3_6	human	Qiagen
SYNPO	GS11346 for SYNPO	human	Qiagen

2.1.9 Bacterial strains, mammalian cell lines

Strain / Cell line	Comment
E. Coli TG1	Stratagene
A7r5	embryonal smooth muscle cells from aorta (rattus norvegicus)
Hek-293	embryonic kidney cells (*homo sapiens*)
HeLa	Cervical cancer cells (*homo sapiens*)
MEF	Embryonic fibroblasts (*mus musculus*)
SH-SY5Y	Neuroblasts from neural tissue (*homo sapiens*)

2.2 Methods

2.2.1 Handling of the prokaryote *E. Coli*

2.2.1.1 Cultivation

LB.Medium (with Amp/Kan):	1 % Bacto-Trypton
	0,5 Bacto-Yeast extract
	0,5 % Nacl
	pH7,5 → autoclave
	(1:10000 Amp [200 mg/ml] / Kan [50 mg/ml])
LB-Agar (mit Amp/Kan):	1 % Bacto-Trypton
	0,5 Bacto-Yeast extract
	0,5 % NaCl
	1,5 % Bacro-Agar
	pH7,5 → autoclave
	(1:10000 Amp [200 mg/ml] / Kan [50 mg/ml])

In this work *Escherichia Coli* (*E. coli*) was used as an amplification system for cloned plasmids. For this purpose *E. coli* were transformed by heat shock and incubated overnight on LB-agar plates containing either ampicillin or kanamycin for positive selection of bacteria carrying the desired plasmid. This was followed by overnight incubation at 37°C of a positively transformed single *E. coli* colony in 3 to 5 mL of antibiotic containing LB medium at 200 rpm. The obtained cells were centrifuged and further processed in plasmid isolation.

2.2.1.2 Competent cells

For successful transformation of bacteria via heat shock they need to be “made competent” for receiving DNA. This was done by inoculating LB-medium with the *E. coli* strain TG1 and over night incubation at 37°C and 130 rpm. 1 mL of the overnight culture

was used for inoculation of 100 mL LB-medium containing ampicillin. This was incubated at 37°C and 130 rpm until an optical denisity of 0.5 (measured at 600 nm (OD_{600})) was reached. The bacteria were then centrifuged for 10 min at 4000 rpm and 4°C after which the supernatant was discarded. The remaining pellet was re-suspended in ice cold 80 mM $CaCl_2$-solution which induces the chemical competence. After that the bacteria were incubated for 30 min on ice, followed by centrifugation for 10 min at 4°C and 4000 rpm. The supernatant was discarded again and the pellet re-suspended in 100 mM CaCl2-solution containing 20% glycerin. For storage aliquots of 100 µL were frozen at -80°C.

2.2.1.3 Transformation of *E. coli* via heat shock

Competent bacteria (see above) are capable of taking up plasmids from their environment. For this 12 µL of a ligation or 0.5 µg purified plasmid is pipetted on 100 µL competent TG1 cells and incubated for 30 min on ice. This was followed by a 50 sec heat shock at 42°C with subsequent addition of 1 mL LB-medium. The transformed bacteria were incubated for 1 h at 37°C and roughly 350 rpm. For positive selection the bacterial suspension was plated on LB-agar plates containing either ampicillin or kanamycin and incubated over night at 37°C. Successfully transformed cells were now able to create colonies by cell division. These plasmid containing colonies were then further amplified with subsequent purification of the plasmid DNA.

2.2.2 Handling of eukaryotic cell lines

2.2.2.1 Cultivation

Cell Culture Medium **A7r5**: Dulbecco's Modified Eagle Medium
10 % FCS
100 IU/mL Penicillin
100 IU/mL Streptomycin
4 mM L-Glutamine

Cell Culture Medium **Hek-293**: Dulbecco's Modified Eagle Medium
10 % FCS

100 IU/mL Penicillin
100 IU/mL Streptomycin
2 mM L-Glutamine
Pyruvate
Non-essential amino acids

Cell Culture Medium **HeLa**: Dulbecco's Modified Eagle Medium
10 % FCS
100 IU/mL Penicillin
100 IU/mL Streptomycin

Cell Culture Medium **MEF**: Dulbecco's Modified Eagle Medium
10 % FCS
100 IU/mL Penicillin
100 IU/mL Streptomycin

Cell Culture Medium **SH-SY$_5$Y**: Dulbecco's Modified Eagle Medium
15 % FCS
100 IU/mL Penicillin
100 IU/mL Streptomycin
2 mM L-Glutamine
Pyruvate
Non-essential amino acids

PBS:
137 mM NaCl
2.7 mM KCl
8 mM Na_2HPO_4
1.4 mM KH_2PO_4
pH 7.4 → autoclave

Trypsin-Solution: 0.05 % Trypsin / EDTA

All cell lines were cultivated at 37°C, 5% CO_2 content and 95 % humidity. Before reaching confluence, cells were split into new cell culture dishes. Here culturing medium was discarded and cells were washed with PBS once, followed by the addition of 1 mL Trypsin-Solution. The following incubation times at 37°C were applied until cells were successfully detached from the surface of the cell culture plate: A7r5 – 5-10 min; Hek-293 – 5 min; HeLa – 3 min; MEF – 3 min and SH-SY_5Y – 10 min. The detached cell suspension was resuspended in the respective pre-warmed medium and split in the following ratios: A7r5 – 1:3; Hek-293 – 1:6; HeLa – 1:10; MEF – 1:10 and SY_5Y – 1:5.

2.2.2.2 Transfection of HeLa cells with Calcium Phosphate

2x HBS:	1.6 g NaCl
	0.74 g KCl
	0.0027 g Na_2HPO_4
	0.2 g Glucose
	1.19 g HEPES
	pH 7.05
	ad 100 mL with aqua bidest. → sterile filtration
$CaCl_2$-Solution:	2.5 M $CaCl_2$ → sterile filtration

The cells were split one day before transfection so that a ~ 40 – 60 % confluence was reached. Cell culture medium was exchanged with fresh medium prior to transfection. For transfection of cells grown in 10 cm cell culture dishes the following transfection reaction was prepared:

20 µg Plasmid-DNA
86.8 µL $CaCl_2$-Solution
ad. 700 µL H_2O

Plasmid-DNA was first diluted in the respective volume of sterile H_2O and shortly vortexed after the addition of the $CaCl_2$-solution. Whilst slightly vortexing the same volume (700 µL for 10 cm dishes) 2x HBS was added drop by drop to the prepared Plasmid-DNA containing solution. This was followed by a 5 min incubation at RT for the development of calcium phosphate precipitates. The reaction mix was then pipetted drop

by drop onto the prepared cells. After incubation of the transfected cells for 8 h, cell culture medium containing the transfection reaction mix was discarded, cells were washed once with PBS and fresh, pre-warmed culturing medium was given onto the cells. After 48 h incubation cells were harvested for following experiments. For the transfection of cells cultured in cell culture dishes of differing volumes, the transfection reaction mix is adjusted to the growth area of the respective dish.

2.2.2.3 Liposome mediated transfection of HeLa cells

For transfection of HeLa cells with siRNA or Plasmid-DNA the JetPrime-Kit from Peqlab was used. Here cells were split the day before transfection to grow to a confluence of about 25 – 40 %. Cells were transfected according to the manufacturers' protocol with 4 µg DNA (10 cm dishes) or 100 – 200 pmol siRNA (6 cm dishes). Medium was replaced by fresh, pre-warmed cell culture medium after 8 h. After 48 h incubation time cells were either re-transfected with siRNA or harvested for further use.

2.2.2.4 Treatment of HeLa cells with inhibitors

For the inhibition of the proteasome or autophagy, HeLa cells were treated with the following inhibitors at a confluence of 80 % for 16 h overnight, followed by harvest of the cells for experimental use.

MG132:	final concentration: 10 µM
Bafilomycin A1:	final concentration: 200 nM
E64d:	final concentration: 20 µM

2.2.3 Methods in molecular biology

2.2.3.1 Plasmid preparation (MAXI/Mini)

For purifying plasmid-DNA from *E. coli*, the NucleoSpin® Plasmid Kit from Macherey-Nagel (bacterial culture volume of 3 – 4 mL) or the NucleoBond® Xtra Maxi Kit also from

Macherey-Nagel (bacterial culture volume of 300 mL) were used. Plasmid preparation was performed according to the instructions given by the manufacturers.

2.2.3.2 Polymerase Chain Reaction (PCR)

Polymerase Chain Reaction (PCR) is used to specifically amplify nucleotide sequences. A PCR generally consist of three phases which are repeated for about 30 times to exponentially amplify the desired genetic sequence. The four phases of a PCR are the following: DNA denaturation at 95°C, annealing of oligonucleotide primers to the template sequence (temperature is dependent on the primer pair used) and elongation of the aligned oligonucleotides by the DNA polymerase (temperature for elongation depends on the polymerase used). Here DNA sequences for cloning were amplified using the KOD DNA polymerase with proofreading function. The following reaction mix for optimal performance of the polymerase was applied (all reagents were pipetted on ice):

DNA-template:	1 µg
dNTP-solution each 10 mM:	2 µL
5’ oligonucleotide:	20 pm
3’ oligonucleotide:	20 pm
5x KOD Buffer:	10 µL
DMSO:	1 µL
KOD-Polymerase:	1 µL
Aqua bidest:	ad 50 µL

The following thermal cycler program was used for amplification of the template DNA:

1. initial denaturation:	95°C	3 min.
2. denaturation:	95°C	45 sec.
3. annealing:	40-65°C	45 sec.
4. elongation:	72°C	1-2 min.
5. repeat step 2 – 4 for 30 times		
6. final elongation:	72°C	10 min.
7. cooling:	4°C	infinite

2.2.3.3 Agarose gel electrophoresis

Agarose gel electrophoresis is an electrophoretic method for the separation of DNA fragments of differing lengths. DNA fragments are separated due to their negative charge and their size, as smaller pieces of DNA can migrate faster through the porous gel towards the anode than larger ones. Visualization of the DNA is enabled by the DNA intercalating dye SYBR® Safe DNA gel stain by Invitrogen™, which is detectable under ultraviolet light. The agarose gel was cast using 1 % agarose in 1x TAE Buffer. The suspension was boiled until the agarose was completely resolved and poured into the casting chamber with the addition of 1 µL SYBR® Safe DNA gel stain. DNA samples were mixed with 6x sample buffer obtained from Thermo Scientific prior to loading to the gel. The DNA size marker 1kb GeneRuler™ DNA Ladder Mix from Thermo Scientific was used and agarose gels were run via application of 120 V for about 50 min.

2.2.3.4 Restriction digest

In order to clone a genetic sequence into a plasmid, insert DNA and plasmid need to be digested with the same restriction endonucleases. These enzymes create DNA overhangs which facilitate annealing of the insert DNA with the plasmid. By using two different restriction endonucleases on insert and plasmid, the right orientation of the insert in the finished plasmid is ensured. Cutting sites for the restriction endonucleases were integrated into the insert DNA via the oligonucleotides used in the PCR reaction to amplify the desired insert DNA. The digest of insert DNA and plasmid DNA was performed using the FastDigest restriction enzymes from Fermentas according to the protocol given by the manufacturer. The restriction digest reaction of plasmid DNA was additionally supplied with alkaline phosphatase which prevents religation of the plasmid DNA to itself. After the restriction digest, the obtained DNA fragments were purified via agarose gel extraction and their DNA concentration was measured with the NanoPhotometer®.

2.2.3.5 Agarose Gel Extraction

In order to extract DNA fragments previously separated by agarose gel electrophoresis for further processing, the agarose gel containing the separated samples was laid on a

UV-light table to visualize DNA. Desired DNA fragments were cut from the gel and transferred to reaction tubes followed by dissolving of the gel and purification of the DNA with the help of the NucleoSpin® Gel and PCR Clean-up Kit by Macherey-Nagel according to the manufacturers' instructions.

2.2.3.6 Ligation

After digesting insert DNA and the plasmid backbone with the respective restriction enzymes, the generated fragments were ligated. For optimal ligation conditions, the ratio of insert to plasmid molar mass was 3:1. For exact calculation of the required amount of insert and plasmid DNA the following formula was applied: insert mass in ng = 3 x (bp insert / bp plasmid) x vector mass in ng. Next to the addition of insert and plasmid DNA, ligation reactions were supplied with T4-Ligase-Buffer and T4-Ligase obtained from Thermo Scientific according to the manufacturers protocol. Ligation reactions were pipetted on ice and incubated overnight at 16°C and slight shaking. After incubation, 12 µL of the ligation reaction were given onto competent TG1 E. coli for transformation as described above.

2.2.3.7 DNA Sequencing

Sequence analysis of all cloned DNA constructs was performed by the company GATC Biotech AG.

2.2.3.8 Quantitative real-time PCR (q-PCR)

For quantification of protein transcripts via qRT-PCR, RNA was isolated from HeLa cells using the InviTrap® Spin Universal RNA Mini Kit from Stratec. With the NanoPhotometer® isolated RNA was analyzed for purity and the obtained concentration was determined. To prepare cDNA from RNA the iScript cDNA Synthesis-Kit from BioRad was used according to the manufacturers' instructions. Here 0.5 µg of RNA were used per sample. For amplification and detection of PCR products during q-PCR the DNA intercalting dye EvaGreen-Kit was used according to the guidelines given by the manufacturer. As reference genes B2M and GAPDH were used. The qPCR was performed as follows:

cDNA-Synthesis:

Reagent	Amount
Isolated RNA	0.5 µg
5’ Oligonucleotide	20 pm
3’ Oligonucleotide	20 pm
10 x iScript-Buffer	2 µL
iScript-Polymerase	1 µL
A. bidest	Ad 20 µL

→ cDNA was synthesized at 42°C for 45 min

qPCR:

Reagent	Amount
cDNA	1 µL
H2O	6.5 µL
5’ Oligonucleotide	5 pm
3’ oligonucleotide	5 pm
EvaGreen Dye	6.5 µL
A. bidest	15 µL

qPCR programm:

Phase	Temp.	Time
1. Initial denaturation	97°C	3 min
2. Denaturation	94°C	45 sec
3. Annealing	68°C	30 sec
4. Elongation	72°C	2 min
5. Repeat phase 1. – 5 for 30 x		
6. Final elongation	72°C	7 min
7. Denaturation	97°C	3 min
8. Cooling	4°C	infinite

2.2.4 Methods in protein biochemistry

2.2.4.1 Generation of crude extracts

Lysis buffer RIPA (+SDS):	25 mM Tris, pH 8
	150 mM NaCl
	0.1 % SDS
	0.5 % Sodiumdeoxycholate
	1 % Nonidet P-40
	10 % Glycerol
	2 mM EDTA
	1 x “Complete” Protease inhibitor cocktail
SDS sample buffer (3x):	0.2 M Tris/HCl, pH 6.8
	6 % SDS
	30 % Glycerol
	0.03 % Bromophenol blue
	15 % β-Mercaptoethanol

For analysis of cellular protein composition cells needed to be harvested and lysed. Cells were washed with PBS once prior to harvest. Cells were rubbed of the cell culture dish and suspended in PBS for transfer into a reaction tube. The cell suspension was centrifuged at 3500 rpm for 3 min and the supernatant was discarded. Depending on the cell pellet size, cells were resuspended in an appropriate amount of RIPA lysis buffer (ranging from 20 – 80 µL per cell pellet). The resuspended cells were incubated for 20 min on ice to ensure sufficient lysis and centrifuged for 1 min at 10.000 rpm at 4°C to pellet residual cellular complexes. The supernatant containing the proteins for analysis was transferred into a new reaction tube and protein concentration was determined via Bradford test. Extracted protein solutions were adjusted to a working concentration of 4 mg/mL via the addition of lysis buffer and three times concentrated SDS-sample buffer. For treatment with lambda phosphatase crude extracts were generated as described above. Lambda phosphatase was however added prior to adjustment of protein

concentration via the addition of 3x SDS-sample buffer. A detailed description of the lambda phosphatase assay is described below.

2.2.4.2 Lambda Phosphatase assay

For de-phosphorylation of proteins the lambda phosphatase from New England Biolabs was used. Here crude extracts were diluted with RIPA lysis buffer without the protease inhibitor cocktail to a working concentration of 6 µg / µL. 40 µL of crude extract were incubated with 5 µL 10x Phosphatase Buffer, 5 µL MnCl2 (10 mM) and 300 units lambda-phosphatase, for 30 min at 30°C. The reaction was stopped by the addition of 25 µL 3x SDS-sample buffer with subsequent boiling of samples at 95°C for 5 min. Samples were analyzed via SDS-Gel electrophoresis and Western Blot.

2.2.4.3 Discontinuous SDS-Page

running buffer: 25 mM Tris
190 mM Glycin
1 % SDS

Separation Gel:

Gel concentration	7.5 %	10 %	12.5 %	15 %
1.5 M Tris/HCl, pH 8.8:	1.52 mL	1.52 mL	1.52 mL	1.52 mL
30 % Acrylamide (0.8 % BisAa.)	1.51 mL	20 mL	2.52 mL	3.02 mL
dH_2O	2.89 mL	24 mL	1.87 mL	1.37 mL
10 % SDS	89 µL	89 µL	89 µL	89 µL
10 % APS	39 µL	39 µL	39 µL	39 µL
TEMED	4 µL	4 µL	4 µL	4 µL

Stacking Gel:

1 M Tris/HCl, pH 6.5	400 µL
30 % Acrylamide (0.8 % BisAa.)	266 µL
dH2O	882 µL
10 % SDS	48 µL

10 % APS	16 µL
TEMED	1.6 µL

SDS-Page (Sodium Dodecyl Sulfate Polyacrylamide gel electrophoresis) is an electrophoretic method to separate and visualize protein monomers according to their molecular weight. Proteins are denatured by heat in the presence of sodium dodecyl sulfate (SDS) which attaches to the resulting protein monomers, supplying them with a negative charge. Thereby the characteristic charge of each protein is overlayed. Once loaded to an SDS containing polyacrylamide gel the negatively charged protein monomers migrate through the gel by applying electricity. Their speed of migration is given by the molecular weight of the individual protein monomers. 30 – 50 µg of total protein per lane were loaded on SDS-Page gels and run at 20 mA for about 1.5 hours. Acrylamide percentage of the respective gel used and running time were dependent on the molecular weight of the protein to be analyzed.

2.2.4.4 Coomassie staining

Coomassie solution:	50 % Methanol
	10 % Acidic acid
	0.125 % Coomassie Brillant Blue R 250
Destaining solution:	50 % Methanol
	10 % Acidic acid

For unspecific staining of proteins separated on an SDS-Page gel Coomassie Brillant Blue G-250 was used. The gel was incubated overnight in Coomassie solution at room temperature on a rocking platform. Background stain was removed via incubation of the gel in destaining solution twice for 30 min until only the stained protein bands were visible.

2.2.4.5 Western Blot

Transfer Buffer:	20 mM Tris
	144 mM Glycine
	20 % Methanol
	0.01 % SDS
TBST-Buffer:	20 mM Tris/HCl pH 7.6
	137 mM NaCl
	0.006 % Triton X-100
Ponceau S solution:	5 % Albumin Fraction V/TBST
	0.1 % Ponceau S
	5 % Acidic acid
Blocking solution:	2% skim milk powder in TBST buffer

The principle of Western Blots is based upon the transfer of proteins from a polyacrylamide gel onto a nitrocellulose membrane in an electric field. On this membrane the proteins of interest can be visualized with the help of protein specific antibodies. For the transfer an SDS-Page gel was placed onto a nitrocellulose membrane and embedded in Whatman™ paper and sponges on each side. Blots were placed into a transfer buffer containing chamber and run at 300 mA for 90 min. The procedure was followed by staining of the nitrocellulose membrane with Panceau S solution to assess blotting efficiency. Membranes were washed with dH2O to remove the Panceau S stain and incubated for 30 min in 2 % skim milk containing TBST-Buffer (blocking solution) at room temperature.

2.2.4.6 Immunodetection

After blocking of the nitrocellulose membrane obtained from Western Blot (see above), primary antibody, specific for the protein to be analyzed, was added to the membrane. Antibodies used were previously diluted in blocking solution in a ratio of 1:250 up to 1:2000, depending on the antibody used. The membrane was incubated with the primary antibody at 4°C overnight on a rocking platform. This was followed by three washing steps with TBST to remove residual primary antibody unbound to the membrane. After washing, the secondary, peroxidase coupled antibody was given onto the membrane at a 1:10000 dilution for 1 h at room temperature. The secondary antibody which was

applied was dependent on the species the primary antibody is derived from. After three additional TBST washing steps the bound antibodies were detected via a peroxidase mediated chemoluminescence reaction. This was achieved by the use of ECL-solution applied according to the instructions given by the manufacturer. In a dark room X-ray films were laid on top of the membrane for exposure of differing lengths (depending on the efficacy of the primary antibody and abundance of the protein to be detected). X-ray films were developed in an automated developing machine.

2.2.4.7 Bradford protein assay

For determination of protein concentration the Bradford protein assay was applied. With Coomassie Brilliant Blue G-250 proteins from complexes which can be measured in a photometer. Under normal conditions Coomassie Brilliant Blue G-250 has an absorption maximum at 470 nm. In complex with proteins this absorption maximum is shifted to 595 nm which can be used as basis for measurement. Prior to measurement of protein sample concentration, the photometer was calibrated with a γ-Globuline standard. For the measurement 1 µL of protein sample was given to 1 mL Bradford solution and mixed thoroughly. After 10 min incubation at room temperature the Bradford-sample mix was given into a plastic cuvette for measurement. 1 mL of Bradford-solution was taken as blank.

2.2.4.8 TCA protein precipitation

For concnetration of protein samples they were precipitated using trichloroacetic acid (TCA). Samples were treated with a final TCA concentration of 12.5 % and incubated for at least 1 h on ice, followed by 30 min centrifugation at 20.000 g and 4°C. The TCA containing supernatant was completely removed from the sample and the precipitated protein pellet was resusupended in SDS sample buffer. If necessary, acidic pH was neutralized via the addition of 1 – 2 µL 1 M Tris pH 9.0 prior to boiling the sample at 95°C for 5 min.

2.2.4.9 Immunoprecipitation

RIPA Lysis buffer (without SDS):	25 mM Tris, pH 8.0
	150 mM NaCl
	0.5 % Sodiumdeoxycholate
	1 % Nonidet P-40
	10 % Glycerol
	2 mM EDTA
	1 x “Complete” Protease inhibitor cocktail
MOPS/KCl washing buffer:	20 mM MOPS, pH 7.2
	100 mM KCl
Elution buffer:	0.1 M Glycine / HCl, pH 3.5

Immunoprecipitation is used for isolation of protein complexes bound to a protein of interest. 4 x 10 cm cell culture dishes of HeLa cells were harvested and lysed with RIPA lysis buffer (without SDS) for 30 min on ice. After that, crude extracts were shortly ultrasonicated (2 x 10 sec) followed by 20 min centrifugation at 16.000 g and 4°C. The supernatant containing the proteins was diluted to a working concentration of 8 µg / µL with MOPS/KCl buffer. For immunoprecipitation of overexpressed proteins containing a FLAG-tag M2 sepharose was used, to which the FLAG.tag can bind directly. For immunoprecipitation under endogenous conditions protein-G sepharose, together with a specific antibody for the protein to be analyzed was used. Here the antibody heavy chain can bind to the protein-G covered beads. M2 sepharose and protein-G sepharose were equilibrated with 3 RIPA washing steps before usage in immunoprecipitation. Protein extracts for analysis were incubated with M2 sepharose or protein-G sepharose and antibody for 3 h at 4°C on a rotating wheel. After incubation the samples were washed 3 x with 1 mL RIPA washing buffer (without SDS) and 3 x with 1 mL MOPS/KCl buffer. Then bound protein complexes were eluted from the sepharose beads via the addition of 1 mL elution buffer and 12 min incubation on ice. The eluted protein complexes were precipitated by the addition of TCA as described above. Isolated protein complexes were analyzed via SDS-Page and Western Blot.

2.2.4.10 Mass Spectrometry

For identification of novel interaction partners of SYNPO mass spectrometry via MALDI-TOF (matrix assisited laser desorption ionization – time of flight) was performed by the Proteomics Facility of the Center for Molecular Medicine Cologne (http://cecad.uni-koeln.de/Services.274.0.html). For sample preparation an immunoprecipitation experiment was performed as described above with an additional elution step using ATP. Obtained protein complexes were separated using a 12.5 % acrylamide gel in SDS-Page followed by Coomassie staining of the gel. Prominent bands visualized via Coomassie staining were cut from the gel, transferred into a reaction tube and sent to Cologne. Peptide data obtained from mass spectrometry was aligned to the UniProt database.

2.2.5 Methods in Cell biology

2.2.5.1 Immunofluorescence

PBS: 137 mM NaCl
2.7 mM KCl
8 mM Na_2HPO_4
1.4 mM KH_2PO_4
pH 7.4

Quenching-Solution 50 mM NH_4Cl

Blocking Solution 3 % BSA in PBS

HeLa cells were seeded out in 24 well plates equipped with round glass cover slips. For immunofluorescent staining cells were washed twice with PBS and fixed with 4 % paraformaldehyde in PBS for 12 min at room temperature. After three washing steps with PBS cells were permeabilzed via addition of 0.2 % Triton-X 100 in PBS for 12 min at room temperature. After additional three washing steps quenching-solution was applied for 30 min only for cells that were used for EEA1 staining. For all other antibodies used

for staining, cells were directly blocked with blocking solution for 1 h after washing with PBS. Antibodies were diluted according to manufacturers' guidelines in blocking solution and cells were incubated with the respective antibody for at least 1 h at room temperature. For EEA1 staining the antibody solution was incubated with the cells in a humidity chamber at 4°C overnight. Incubation with the primary antibody was followed by three subsequent PBS washing steps before the secondary antibody could be applied. Secondary antibodies were diluted 1:400 in blocking solution and incubated with the cells for 1 up to 4 h. Cells were again washed three times with PBS and shortly dipped in A. bidest to remove residual salts from PBS before mounting with MOWIOL®. Samples were left at a dark place at room temperature overnight for the mounting medium to dry before analysis with the microscope.

2.2.6 Statistics

Significance was calculated using the students T-Test in Excel. Each experiment was performed independently for at least three times (n). Western Blots were quantified using the software ImageJ. For immunofluorescence the LSM image browser was used. Strategies for cloning of plasmids were tested with the software GENtle.

3. Results

3.1 SYNPO2 is not expressed in HeLa cells

Previously published findings link BAG3 to the SYNPO family of proteins via an interaction of BAG3 with SYNPO2 in the context of mechanotransduction in muscle and immune cells (Ulbricht *et al.* 2013). Besides SYNPO2, a peptide screen consisting of proline-rich peptides, performed to identify novel interactors of the BAG3 WW-domain, also identified SYNPO as a binding partner of BAG3 (PhD thesis Ulbricht 2013, unpublished data). As SYNPO2 expression shows tissue specificity to muscle cells, the immune system, prostate, colon and small intestine (Lin *et al.* 2001), the closely related protein SYNPO was hypothesized to take on a comparable role to SYNPO2 function in CASA in cells that do not express SYNPO2. In order to find a cell line which lacks SYNPO2 but expresses SYNPO, crude extracts of five different cell lines were tested for SYNPO2 and SYNPO expression. As can be seen in figure 3.1 (A) SYNPO2 is expressed in A7r5 (*Rattus norvegicus*, smooth muscle) and SH-SY5Y (*Homo sapiens*, neuroblasts from neural tissue) cells lines. SYNPO expression can be detected in all cell lines tested namely A7r5, Hek-293 (*Homo sapiens*, embryonic kidney), HeLa (*Homo sapiens*, cervical cancer), MEF (*Mus musculus*, embryonic fibroblasts) and SH-SY5Y (figure 3.1 (B)). HeLa cells were chosen for the analysis of SYNPO in the context of CASA, as they do not express SYNPO2 but show SYNPO expression.

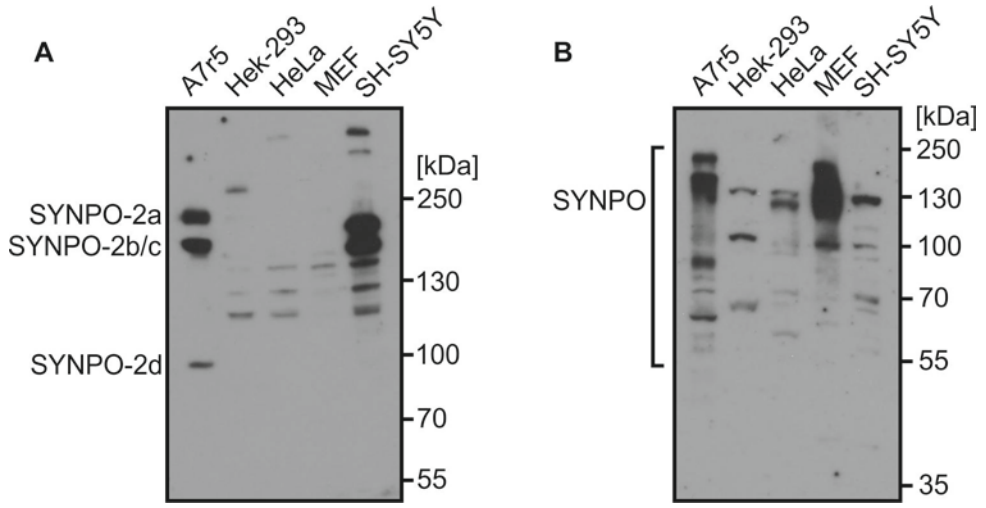

Figure 3.1: Expression of SYNPO2 and SYNPO in various cell lines of mammalian origin. SYNPO2 is detectable in A7r5 and SH-SY5Y cells (A) whereas SYNPO expression can be detected in crude extracts of all cell lines tested. The most prominent band detected by the antibody against SYNPO manifests itself at a size of 130 kDa. 40 µg of protein were loaded for each lane.

3.2 SYNPO is a novel interactor of BAG3

SYNPO2 and SYNPO share a 35 % sequence homology using the Basic Local Alignment Search Tool (BLAST) (https://blast.ncbi.nlm.nih.gov/Blast.cgi). Additionally both proteins could be identified as interactors of the BAG3 WW-domain in a peptide screen (PhD thesis Ulbricht 2013, unpublished data), and both proteins contain at least one centrally located PPXY motif (Ulbricht *et al.* 2013) (figure 3.2). To test for a potential interaction of endogenously expressed BAG3 and SYNPO, co-immunoprecipitation experiments were performed using HeLa cells, showing that indeed BAG3 can co-precipitate in a complex with the 130 kDa isoform(s) of SYNPO (SYNPOa/c) (figure 3.2).

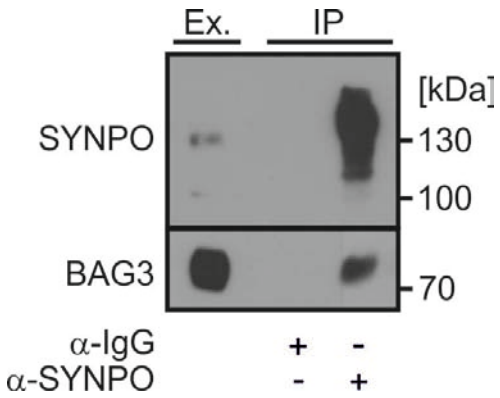

Figure 3.2: SYNPO interacts with BAG3. SYNPO complexes were pulled down with an antibody specific for SYNPO. Western blot analysis shows the presence of BAG3 in these SYNPO complexes isolated from HeLa crude extracts. 32 µg protein were loaded of the extract (left lane). 1/3 of total eluate was loaded for the IgG controls and the specific IPs respectively.

3.3 SYNPO in *Homo sapiens*

The human gene for SYNPO is located on chromosome 5, q33.1, has a size of 58.140 bp and comprises, depending on the isoform, three exons (two coding exons) and two introns. Three different genetic isoforms of SYNPO can be expressed, giving rise to three different isoforms of the translated protein (figure 3.3). The three isoforms of SYNPO are identical in their central sequence but differ in their respective N- or C-termini and in their predicted molecular weights which lie at 74 kDa for the shortest SYNPO isoform: SYNPOb, 96 kDa for the intermediate isoform: SYNPOa and 99 kDa for the longest SYNPO isoform: SYNPOc.

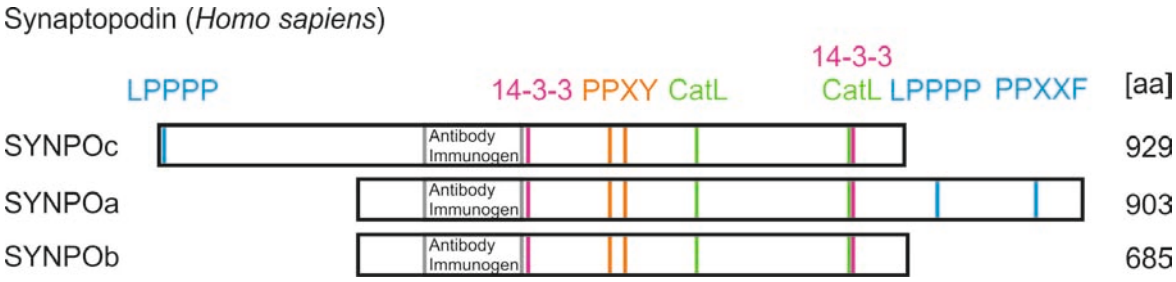

Figure 3.3: Schematic representation of the three isoforms of human SYNPO protein. Motifs and binding sites are marked in color. Furthermore the immunogen of the antibody used in this work is marked as a grey box. All three isoforms contain two subsequent PPXY motifs located in the center of the protein. Additionally two CatL cleavage sites (marked in green) and two binding sites for 14-3-3 protein can be found in each isoform. SYNPOc has an LPPPP motif at its N-terminus whereas SYNPOa. contains a C-terminally located LPPPP and PPXXF motif.

3.4 Analysis of SYNPO in HeLa cells

A general overview of SYNPO expression in five different mammalian cell lines could already be seen in figure 3.1. A clear discrepancy in the size of the detected bands by the SYNPO antibody (prominent band at 130 kDa) and the predicted molecular weight between 74 to 99 kDa (figure 3.3) can be observed. In order to verify that the detected bands in figure 3.1 are indeed SYNPO isoforms, FLAG-Tag expression constructs have been cloned for overexpression of SYNPOb and SYNPOc. Overexpression of the short isoform of SYNPO could be detected at 100 kDa (figure 3.4 (A)). The distinctive band seen in figure 3.3 at approximately 130 kDa could be identified as SYNPOc as shown in figure 3.4 (B). A functional overexpression construct for SYNPOa could not be generated in the course of this work. This leaves the question of the molecular weight and migration behavior of SYNPOa in HeLa cells unanswered. Importantly, due to only slight differences in amino acid number between SYNPOa (903 aa) and SYNPOc (929 aa), it cannot be excluded, that SYNPOa might run at roughly the same height as SYNPOc (130 kDa) in an SDS-page gel. Therefore the 130 kDa SYNPO band is designated as SYNPOa/c if not stated otherwise.

Next to SYNPO isoform characterization, the impact of SYNPOb / SYNPOc overexpression on the cellular concentration of BAG3 was investigated, revealing no changes in BAG3 protein levels for SYNPOb overexpression but a significant increase of BAG3 upon SYNPOc overexpression.

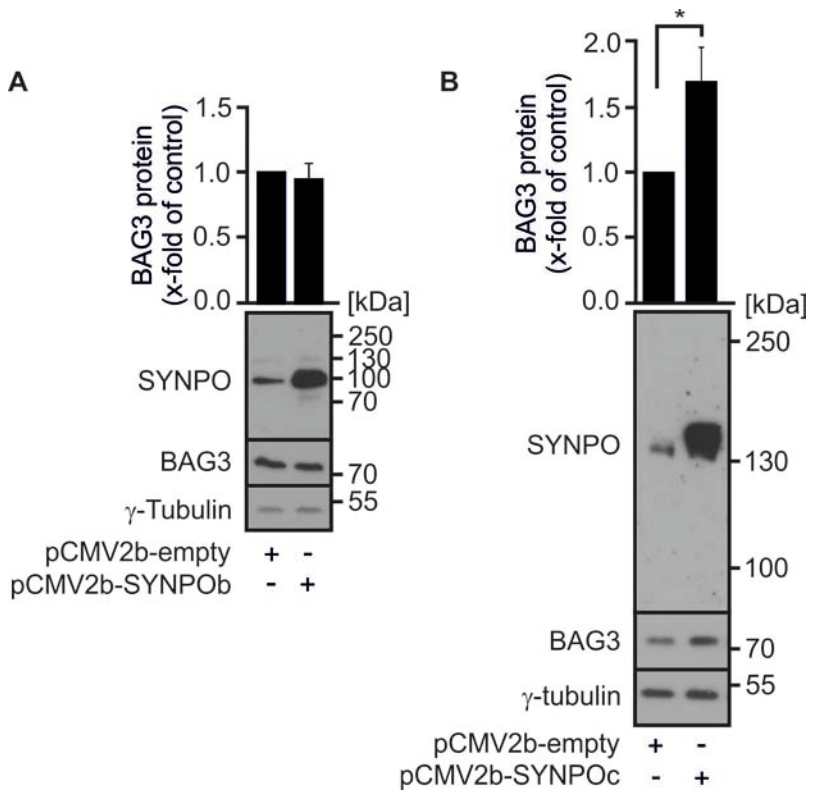

Figure 3.4: Overexpression of SYNPOb and SYNPOc. HeLa cells were transfected with the expression constructs pCMV2b-SYNPOb (A) and pCMV2b-SYNPOc (B) respectively and incubated for 48 h. Crude extracts were analyzed by Western blot, showing that SYNPOb appears at a size of 100 kDa (A) whereas SYNPOc runs slightly above 130 kDa (B). Overexpression of SYNPOb leaves detectable BAG3 unaffected (A) whereas BAG3 protein levels are increased upon overexpression of SYNPOc (B). Each lane was loaded with 40 µg of total protein.

Furthermore, it was investigated whether depletion of the SYNPO isoforms by using specific siRNAs can abrogate the detected SYNPO signals at 130 and 100 kDa. This was indeed the case, confirming the specificity of the used antibody. It was also investigated whether this depletion of SYNPO affects BAG3 protein levels. As depicted in figure 3.5 simultaneous knockdown of SYNPO isoforms did not affect BAG3 protein levels.

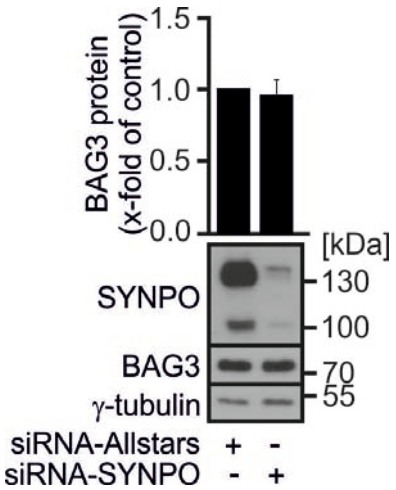

Figure 3.5: Knockdown of SYNPO isoforms by specific siRNAs. HeLa cells were transfected with specific siRNA against SYNPO for 48 h prior to harvest. It can be observed that detectable SYNPO signals at 130 and 100 kDa are highly diminished, whereas BAG3 remains unchanged upon depletion of SYNPO in HeLa cells. 40 µg of protein were loaded for each lane.

A previous report by Faul *et al.* (2008) shows that SYNPO contains two prominent CatL cleavage sites indicated in green in figure 3.2. Indeed the authors could show that SYNPO is cleaved by CatL in podocytes resulting in a 44 kDa SYNPO fragment. To test whether SYNPO is also cleaved by CatL in HeLa cells, E64d, a specific inhibitor of CatL was employed. Administration of E64d did not alter SYNPO protein levels in HeLa cells (quantified for SYNPOa/c) (figure 3.6). Furthermore it is of note that the 44 kDa SYNPO fragment resulting from proteolytic cleavage by CatL could not be detected in any experiments performed for this work.

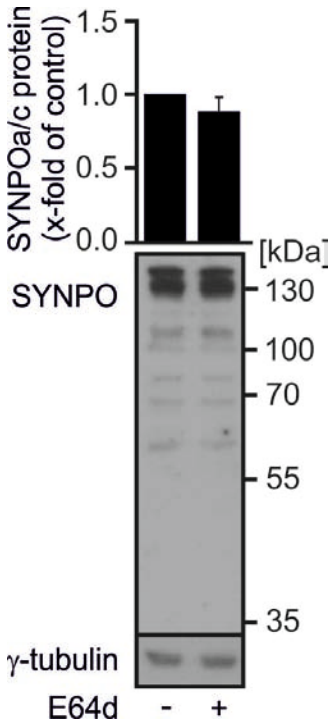

Figure 3.6: SYNPO is not cleaved by CatL in HeLa cells. HeLa cells were treated with E64d for 16 h overnight prior to cell lysis. SYNPOa/c protein levels remain unaffected by E64d treatment visualized by the diagram. Weak signals for SYNPOb at approximately 100 kDa and no band at 44 kDa could be observed (44 kDa is the expected cleavage product of SYNPO in podocytes (Faul *et al.* 2008)). 40 µg of protein were loaded for each lane.

3.5 SYNPOa/c shows an upward shift in Western blots upon proteasome inhibition

Because SYNPO2 is degraded quickly via autophagy upon mechanical strain, it should be assessed whether inhibition of the proteasome (induction of autophagy), by MG132 treatment, or the inhibition of the autophagy-lysosomal pathway (induction of proteasomal degradation of proteins), by BafA1 treatment, has any effect on SYNPO. As shown in figure 3.7 treatment of HeLa cells with the respective inhibitors does not show a significant change of SYNPOb levels (figure 3.7 A). For SYNPOa/c there is a shift in size upon proteasomal inhibition via MG132, which is quantified in the upper right (upper band) and lower right (lower band) panel (figure 3.7 B). In regards of degradation or stabilization the inhibitors do not show an effect on SYNPOa/c.

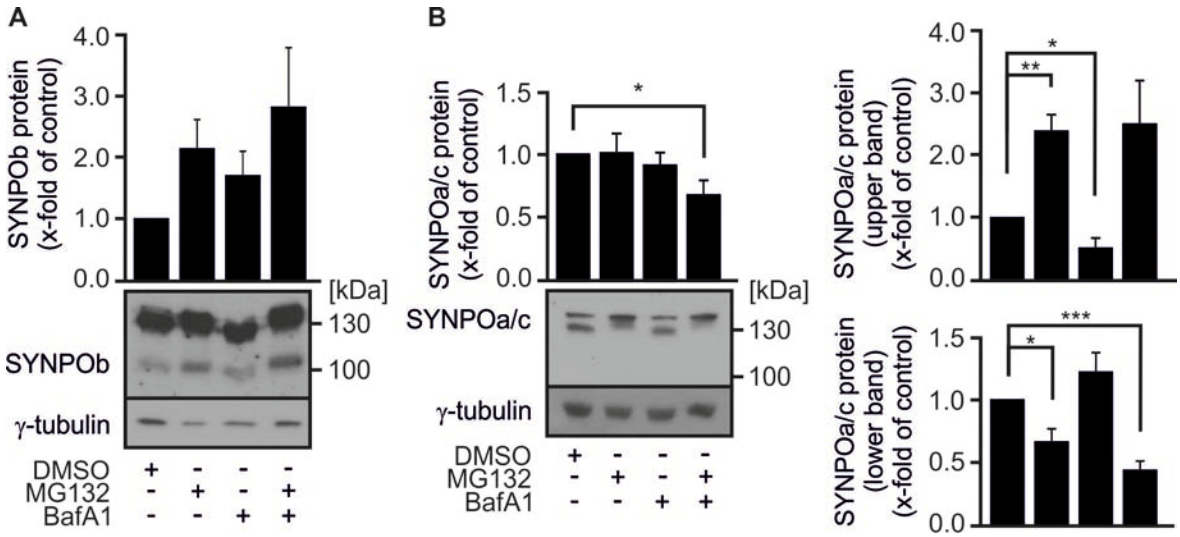

Figure 3.7: Inhibition of protein degradation pathways and shift in size of SYNPOa/c. HeLa cells were treated, for 16 h prior to harvest, with either DMSO as control, MG132 (proteasome inhibition) or BafA1 (inhibitor of autophagy). SYNPOb shows great variation in protein stability upon treatment with the respective inhibitors (A). SYNPOa/c protein neither gets stabilized nor degraded by the application of either of the two inhibitors. However a shift to a higher molecular weight band of SYNPOa/c can be observed when treating cells with MG132 or a combination of MG132 and BafA1 (B). Separate quantification of the two SYNPOa/c bands observed is shown in the two diagrams on the right. 40 µg of protein were loaded for each lane.

3.6 SYNPOa/c is phosphorylated *in vivo*

When regarding the long isoform of SYNPO in HeLa cells, two distinct bands can be observed at approximately 130 kDa in height, as shown above in figure 3.3. Additionally a shift to the upper band of SYNPOa/c can be induced by MG132 treatment of the cells (figure 3.7). This phenomenon gives rise to the question whether SYNPOa/c is post-translationally modified and therefore shows a second band of slightly higher molecular weight in Western Blot experiments. To elucidate the nature of the upper SYNPOa/c band, a Lambda Protein Phosphatase (λPP) assay was performed. The data demonstrate that SYNPOa/c is phosphorylated *in vivo* (figure 3.8). Overnight treatment of HeLa cells with MG132 shows the previously observed effect of a shift of the SYNPOa/c band to a higher molecular weight with no effect on the total SYNPOa/c protein level (figure 3.7). λPP treatment efficiently diminished the upper band signal of SYNPOa/c also for the MG132 treated samples (figure 3.8).

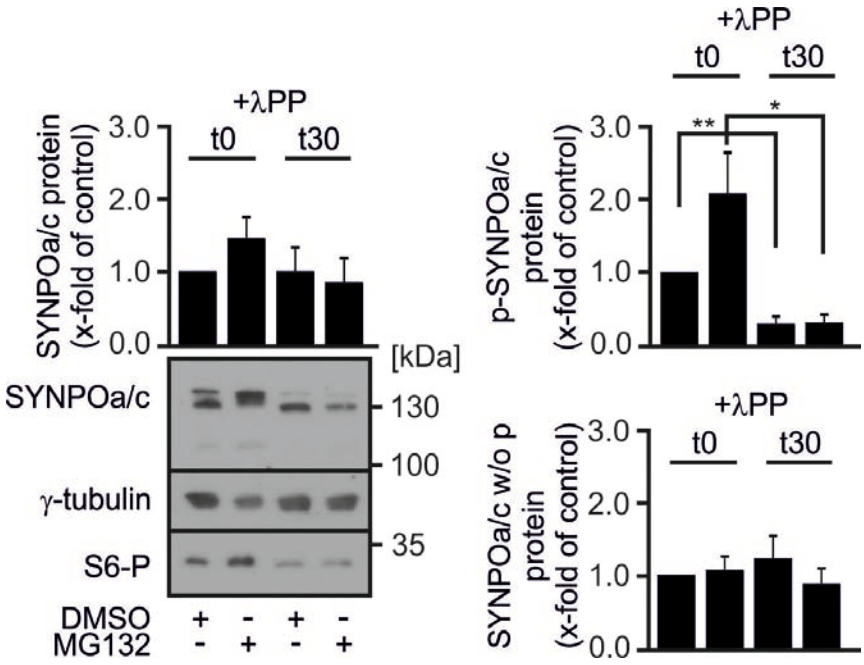

Figure 3.8: 130 kDa SYNPOa/c is phosphorylated. HeLa cells were treated with DMSO or MG132 for 16 h prior to harvest. Crude extracts were subjected to incubation with Lambda Protein Phosphatase (λPP) for 0 min (control, t0) and 30 min (t30) at 30°C. S6-P, an antibody detecting solely the phosphorylated form of S6 protein serves as a control for protein dephosphorylation. The shift of the SYNPOa/c band upon MG132 treatment can be clearly observed, whereas total protein amount remains constant, regardless of the treatment (left panel). Incubation with λPP attenuates the Western Blot signal for the phosphorylated form of SYNPOa/c, quantified in the upper right panel. λPP treatment has no effect on the amount of native, unphosphorylated SYNPOa/c (SYNPOa/c w/o p), (lower right panel). 40 µg of protein were loaded for each lane.

3.7 BAG3 as an effector of SYNPO

It was further assessed whether altered BAG3 protein expression has any impact on SYNPO protein levels. This was monitored by either overexpression or siRNA mediated knockdown of BAG3 in HeLa cells. Overexpression of BAG3 shows a stabilizing effect on SYNPO (figure 3.9 A), whereas BAG3 depletion has the no significant effect on SYNPO protein levels (figure 3.9 B).

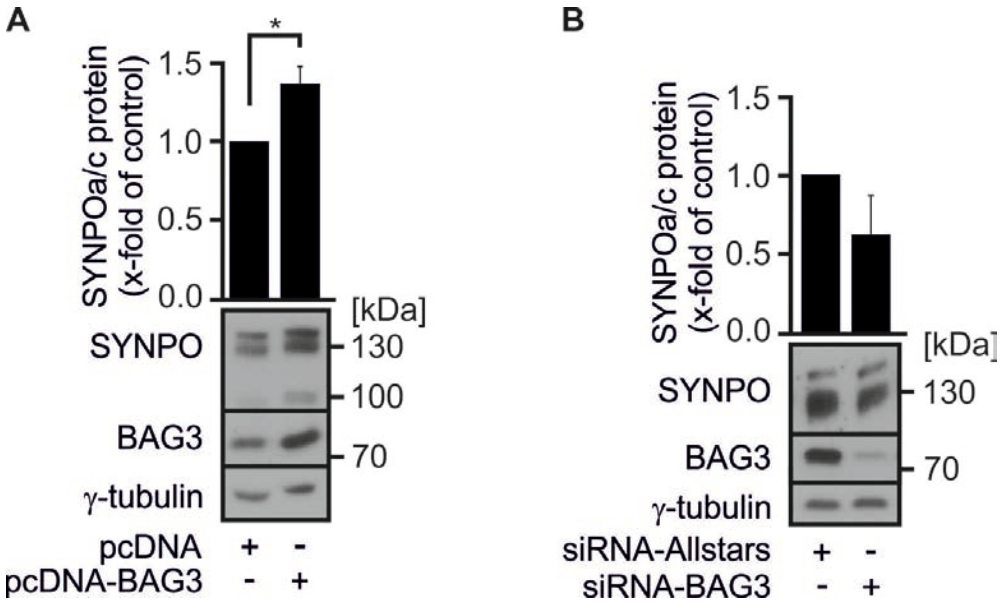

Figure 3.9: SYNPOa/c protein levels upon alterations in BAG3 expression. (A) HeLa cells were transfected with pcDNA-BAG3 and the respective control plasmid pcDNA-empty (48 h). A clear stabilization of SYNPOa/c protein can be observed when increasing BAG3 expression. (B) HeLa cells were transfected with siRNA against BAG3 for 24 h, then a re-transfection was performed for additional 48 h. Depletion of BAG3 shows a minor, but not significant, decrease in SYNPOa/c protein levels. 40 µg of protein were loaded for each lane. It is of note, that SYNPOb appears to be stabilized by BAG3 overexpression as well (A) but was not quantified in the context of this work.

3.8 BAG3 – SYNPOc interaction depends on BAG3 WW-domain and SYNPOc PPXY motifs

As could be established in the beginning endogenous BAG3 and SYNPOa/c can be co-immunoprecipitated (figure 3.1). In order to confirm whether this interaction is mediated via an interaction of SYNPO PPXY-motifs with the WW-domain of BAG3 (as it is for BAG3 and SYNPO2 (Ulbricht *et al.* 2013)), mutant forms of SYNPOc and BAG3, equipped with a FLAG-Tag, were used. In detail, the BAG3 mutant used (pCMV2b-BAG3-WAWA, W26A, W48A) contains a non-functional WW-domain. In addition three different SYNPOc mutants were employed. The first SYNPOc mutant has a double amino acid substitution in the first PPXY motif: P610A and T611A further designated as pCMV2b-SYNPOc-PAAY^{1st}. The second mutant contains a double mutation within the second PPXY-motif of SYNPOc (P629A, S630A), titled pCMV2b-SYNPOc-PAAY^{2nd}. The third and last SYNPOc mutant is a double mutant of both PPXY motifs simultaneously, pCMV2b-SYNPOc-PAAY^{double}. It could be shown that the interaction of SYNPO and BAG3 is clearly dependent on a functional WW-domain of BAG3 and intact PPXY motifs

on the side of SYNPOc (figure 3.10). pCMV2b-SYNPOc-PAAY^{1st} is still fully able to bind BAG3, as bound BAG3 amounts are comparable to the wildtype control. For pCMV2b-SYNPOc-PAAY^{2nd} binding of BAG3 is highly diminished whereas pCMV2b-SYNPOc-PAAY^{double} shows only very slight residual binding of BAG3 (figure 3.10 A). Vice versa it can be observed that SYNPO – BAG3 interaction is abrogated by employing FLAG-BAG3-WAWA in an IP experiment. In addition it can be observed that overexpressed BAG3 wildtype is able to bind to SYNPOa/c w/o p, p-SYNPOa/c as well as to SYNPOb (figure 3.10).

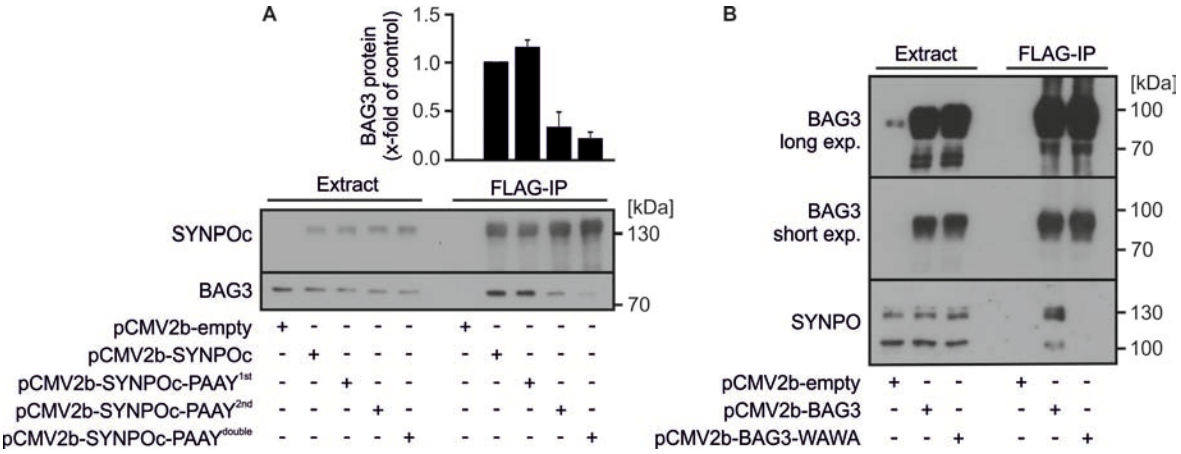

Figure 3.10: SYNPOc – BAG3 interaction is dependent on SYNPOc PPXY motifs and BAG3 WW-domain. HeLa cells were transfected with FLAG-tagged mutant forms of SYNPOc (A) or mutant BAG3 (B) for 48 h prior to harvest. Cell extracts were subjected to IP directed against the FLAG-epitope of the overexpressed constructs. Mutation of SYNPOc-PPXY motifs abrogates BAG3 binding to SYNPOc (A). Additionally SYNPOc – BAG3 interaction is abolished upon mutation of BAG3 WW-domain (B). Furthermore BAG3 wildtype shows binding to SYNPOa/c w/o p, p-SYNPOa/c and SYNPOb (B). 32 µg of protein was loaded per lane for all extract samples. 1/3 of the total eluate from the FLAG-IPs was applied per lane.

Immunofluorescence experiments were performed to analyze the localization of SYNPO and the impact of BAG3 on this. Additionally, the binding of SYNPOc and BAG3 and the dependency on SYNPOc PPXY motifs should be confirmed using a different experimental approach. As expected co-localization of SYNPOc and BAG3 is no longer detectable when co-expressing pCMV2b-SYNPOc-^{PAAYdouble} together with pEGFP-BAG3. Interestingly overexpressed SYNPOc wildtype as well as pCMV2b-SYNPOc-PAAY^{double} localize into punctate structures (figure 3.11). This punctate pattern of SYNPO has been described previously (Mundel *et al.* 1997), however the molecular characteristics of these SYNPO punctae have thus far not been elucidated. Next to the loss of SYNPOc – BAG3 co-localization upon overexpression of pCMV2b-SYNPOc-PAAY^{double} it is of

interest, that BAG3 overexpression alone (figure 3.11, left panel) is not sufficient to show a punctate pattern of BAG3 protein. Only in combination with SYNPOc overexpression does BAG3 co-localize to the SYNPOc punctae which suggests an active recruitment of BAG3 by SYNPOc to these punctae (figure 3.11 3rd panel).

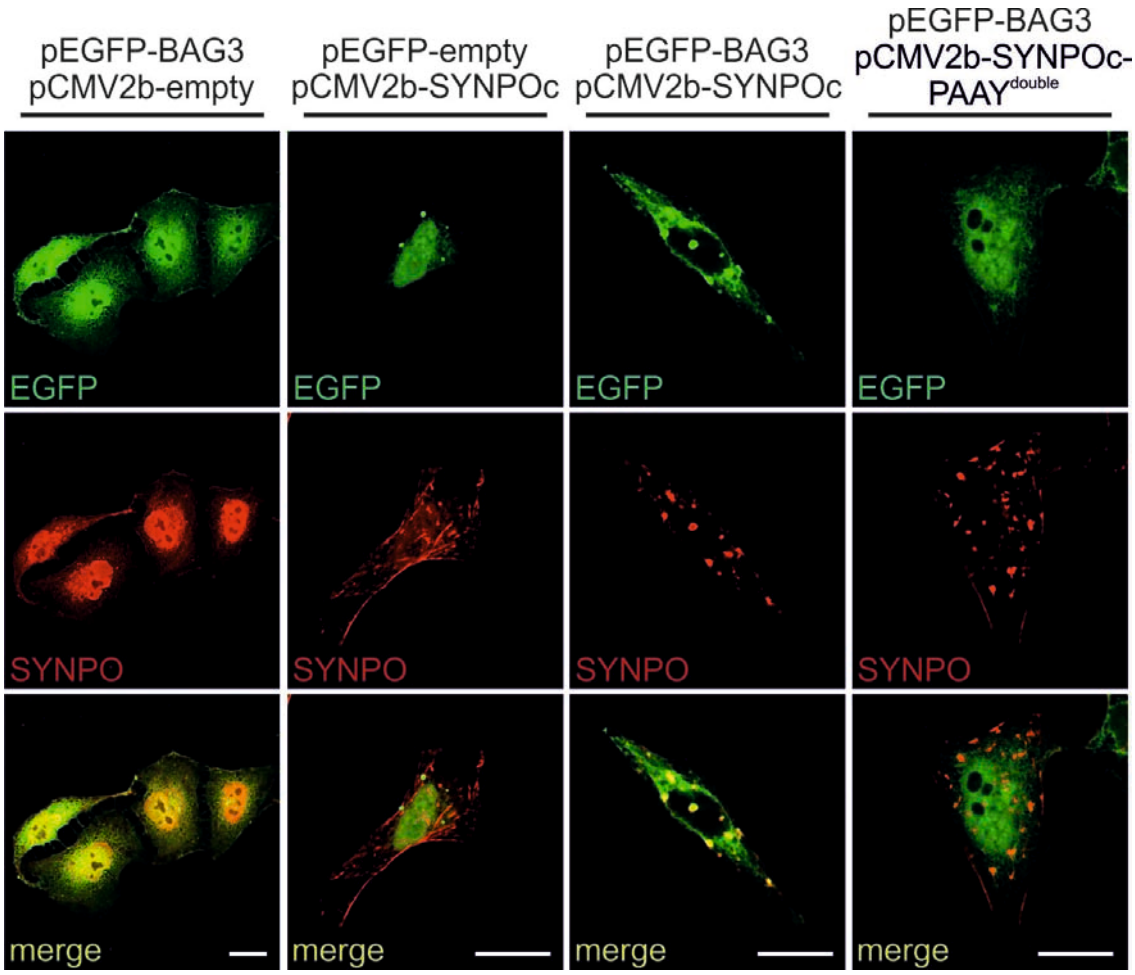

Figure 3.11: SYNPOc PPXY motifs are crucial for SYNPOc – BAG3 co-localization. HeLa cells were transfected with either pEGFP-empty, pEGFP-BAG3, pCMV2b-SYNPOc or pCMV2b-SYNPOc-PAAY^{double} for 48 h. SYNPOc – BAG3 co-localization is lost upon overexpression of pCMV2b-SYNPOc-PAAY^{double}. SYNPOc wildtype as well as SYNPOc-PAAY^{double} appear in punctate structures. White bars correspond to 20 µm.

3.9 General assessment of SYNPOc punctae

Accumulation of SYNPOc in dot-like structures directly evokes the question of the molecular character of these SYNPOc punctae. As described above the punctate pattern of SYNPO has been observed previously and could be shown to co-localize to actin

(Mundel at al. 1997). However further characteristics of these SYNPO punctae remain to be elucidated. Asanuma *et al.* (2005) describe SYNPO punctae in podocytes to be amorphous, cytoplasmic, phalloidin-positive aggregates. In HeLa cells (used in this work) overexpression of SYNPOc results in similar punctae morphology, however the punctae observed appear to be rather round with a large proportion of them showing small pointed protrusions (figure 3.12).

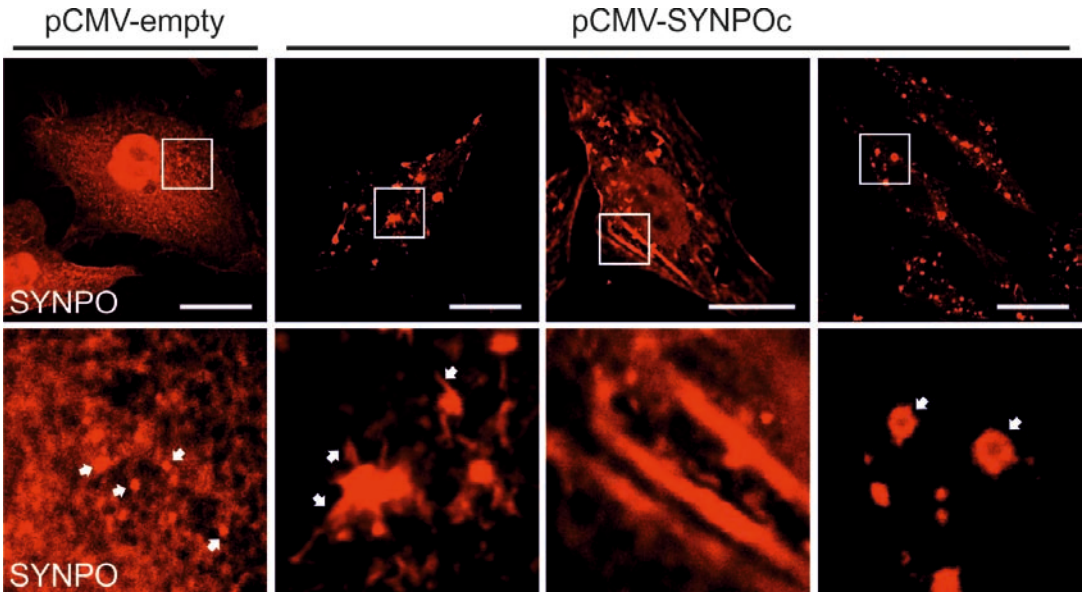

Figure 3.12: SYNPOc punctae in HeLa cells. HeLa cells were transfected with pCMV-empty (control) or pCMV-SYNPOc for 48 hours prior to immunostaining procedure. Endogenous SYNPO is evenly distributed throughout the cytoplasm in control cells forming few small punctae indicated by white arrows (1st panel from the left). Upon overexpression, SYNPOc accumulates in large punctae which are distributed throughout the cytoplasm (panels 2, 3 and 4) Many punctae show small pointed protrusions marked by white arrows (2nd panel). Some cells overexpressing SYNPOc show, next to SYNPOc punctae, thick stress fibers (3rd panel). Additionally ring like SYNPOc punctae can be frequently observed (4th panel). Bottom pictures represent a 5x magnification of the area marked by the white box in the upper panel. The white bars equal 20 µm.

To shed light into the potential function of SYNPOc punctae, several markers of different cellular pathways and structures were employed. Markers for autophagy (p62 and LC3), lysosomes (LAMP-1), aggresomes (vimentin), ubiquitin (FK2) and the cytoskeleton (actin and tubulin) have been subjected to immunofluorescent staining of HeLa cells transfected with pCMV2b-SYNPOc as shown in figure 3.13. It can be seen, that the SYNPOc punctae show neither co-staining for p62, LC3, LAMP-1, vimentin (VIM), FK2 nor tubulin. Staining of the actin cytoskeleton via phalloidin however confirms the previously described (Mundel *et al.* 1997) co-localization of F-actin with SYNPO punctae.

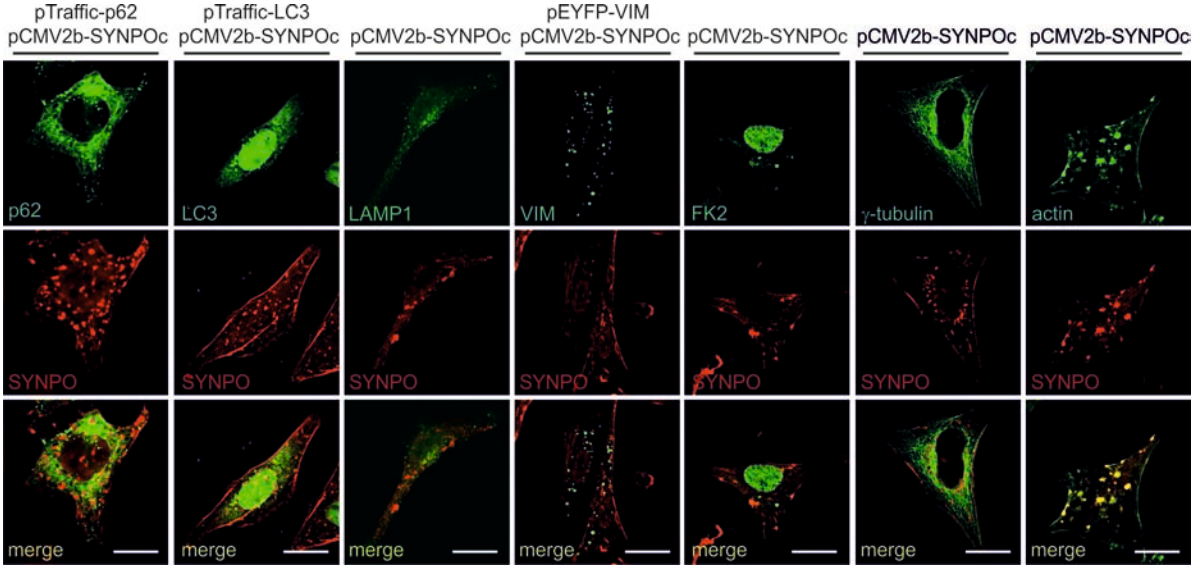

Figure 3.13: SYNPOc punctae in combination with various molecular markers. HeLa cells have been transfected with pCMV2b-SYNPOc and other plasmids as indicated above the respective panels for 48 h. SYNPOc punctae do not associate with p62 and LC3 (autophagy), LAMP-1 (lysosomes), vimentin (aggresomes), FK2 (ubiquitin) nor γ-tubulin. A co-localization of SYNPOc punctae can solely be observed with the actin cytoskeleton as shown in the right most panel. White bars equal 20 µm.

In addition to immunofluorescence experiments (figure 3.13) co-immunoprecipitation was performed in order to confirm the previously described binding of SYNPO to actin. As expected β-actin co-precipitates with SYNPO as depicted in figure 3.14.

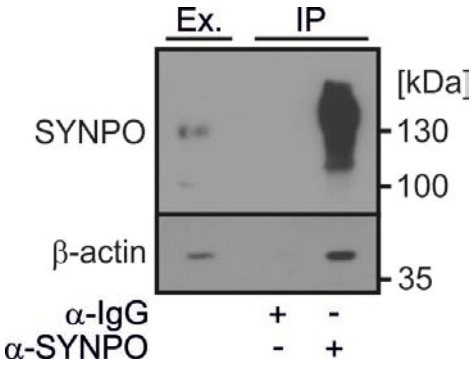

Figure 3.14: IP of SYNPO validating its interaction with actin. SYNPO complexes were pulled down from HeLa cell crude extracts using a specific antibody against SYNPO. It can be seen that β-actin co-precipitates with SYNPO as shown by a specific band for β-actin in the Western blot. 32 µg protein were loaded of the extract (left lane). 1/3 of total eluate was loaded for the IgG controls and the specific IP respectively.

3.10 SYNPOc punctae co-localize with the endosomal marker EEA1

As shown above in figure 3.13, SYNPOc punctae fail to co-localize with molecular markers for autophagosomes, lysosomes, aggresomes and microtubule. As established in figure 3.12, SYNPOc punctae were observed to form ring like structures. Fratti *et al.* (2001) show that the endosomal marker Early Endosome Antigen 1 (EEA1) also appears in ring-like structures upon immunofluorescent staining in murine macrophages. Therefore EEA1 was tested for co-localization to SYNPOc punctae. As depicted in figure 3.15 SYNPOc punctae co-localize with early endosomes under endogenous conditions (left panels) as well as upon overexpression of SYNPOc (right panels).

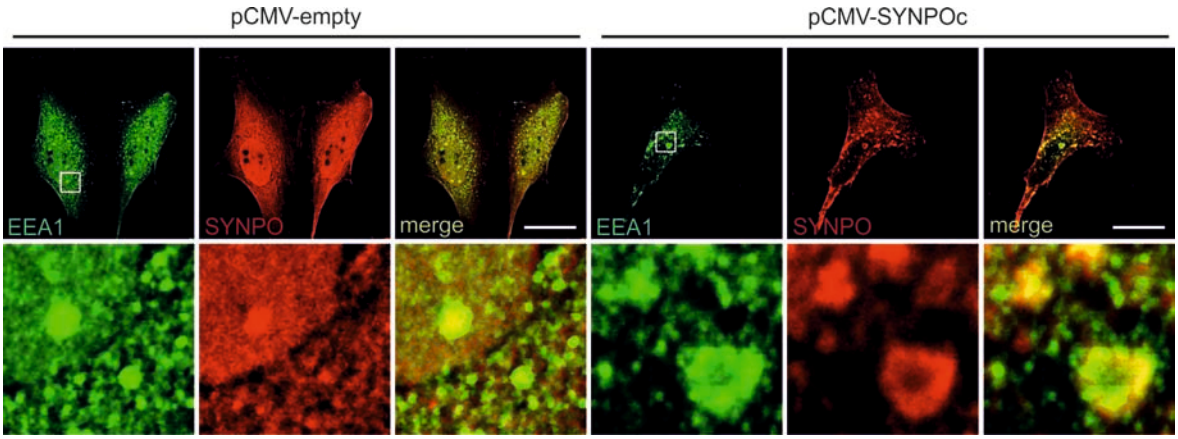

Figure 3.15: SYNPO punctae co-localize with EEA1. HeLa cells have been transfected with pCMV-empty (panels 1-3) and pCMV-SYNPOc (panels 4-6). The endosomal marker protein EEA1 co-localizes with SYNPO punctae under endogenous conditions (panel 1-3) and upon overexpression of SYNPOc (panel 4-6). SYNPOc ring like structures are positive for EEA1. Lower panels represent a 5x magnification of the area marked by the white box. White bars equal 20 µm.

3.11 Identification of novel SYNPO binding partners via mass spectrometry

For further elucidation of the molecular function of SYNPO and in order to identify binding partners aiding the characterization of SYNPOc punctae, IP for SYNPO with subsequent peptide analysis via mass spectrometry was performed. Proteins which co-precipitated with SYNPO were either eluted via addition of glycine buffer or incubation with ATP. Total eluates were separated via SDS-gel electrophoresis and stained by

Coomassie brilliant blue. Prominent bands, as depicted in figure 3.16 were cut from the gel and sent to analysis via mass spectrometry. Obtained peptide data was run against the protein database UniProt and a total of 100 potential binding partners of SYNPO could be identified. These have been further narrowed down by their score parameter and their relevance for cytoskeletal dynamics or connection to cellular vesicles or BAG3 (table 3.1).

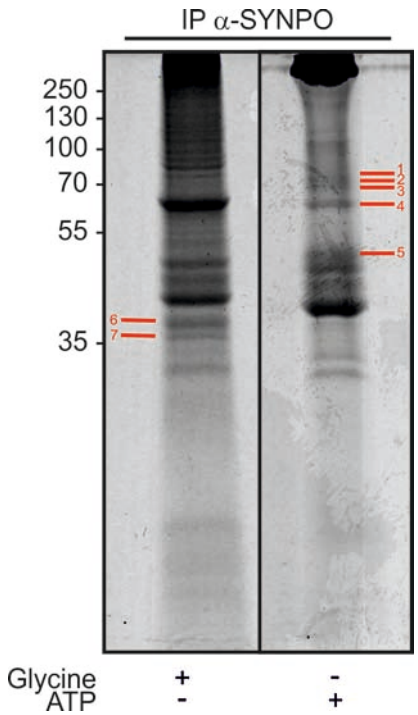

Figure 3.16: SDS-gels of SYNPO IP for mass spectrometry. HeLa cell crude extract was subjected to IP of SYNPO. Elution was either performed by addition of glycine (left panel) or ATP (right panel). Red bars point out bands which were cut from the gel for analysis via mass spectrometry. For identification each band was assigned a number, also given in red, next to the bars.

Table 3.1: Potential SYNPO binding partners identified via mass spectrometry: From total data obtained by mass spectrometry this list of potential SYNPO binding partners was generated. Parameters were the protein score and a link to cytoskeletal functions / dynamics, cellular vesicles or BAG3. It is of note that roughly 25 % of the identified potential SYNPO binding partners are associated with mRNA processing according to literature (data not included in the table).

Abbreviation	Full name	Score	kDa	band #
Actb	Actin, cytoplasmic 1	1017,5	42	5
Actg1	Actin, cytoplasmic 2	872,35	42	5
Aldoa	Fructose-biphosphate aldolase A	303,95	39	6
ANXA1	Annexin A1	516,38	39	7
ANXA2	Annexin A2	792,4	39	7
ANXA3	Annexin A3	298,87	36	7
ANXA5	Annexin A5	588,34	36	7
Capza1	F-actin-capping protein subunit alpha-1	174,6	33	6
Capza2	F-actin-capping protein subunit alpha-2	149,21	33	7
Chmp4b	Charged multivesicular body protein	114,38	25	7
Fscn1	Fascin	169,61	55	4
Gapdh	Glyceraldehyde-3-phosphate dehydrogenase	422,28	36	6
Hspa8	Heat shock cognate 71 kDa protein	1043,03	71	1
Hspa9	Stress-70 protein, mitochondrial	564,31	73	1
Pdlim1	PDZ and LIM domain protein 1	351,92	36	6
Tpm1	Tropomyosin alpha-1 chain	1551,2	33	7
VIM	Vimentin	1937,18	54	4

3.12 Validation of potential SYNPO binding partners obtained via mass spectrometry

As expected, various components of the actin cytoskeleton were identified as potential binding partners of SYNPO in mass spectrometry (table 3.1). Especially Annexin A2 (ANXA2) was of interest as it has been previously described to function in vesicle formation and autophagy (Moreau *et al.* 2015, Morozova *et al.* 2015). Surprisingly vimentin (VIM) was also identified as a putative binding partner of SYNPO by mass spectrometry (table 3.1) opposing the data obtained from immunofluorescence experiments shown above in figure 3.13 in which co-localization of SYNPOc with vimentin could not be observed. For clarification a FLAG-tagged overexpression construct of vimentin (pCMV2b-Vim) was generated and used in an IP directed against the FLAG-epitope of overexpressed vimentin. The same experiment was performed using an overexpression construct for Annexin A2 (pCMV2b-ANXA2). Both, Annexin A2 and vimentin were able to co-precipitate SYNPOa/c. Additionally BAG3 could be detected in the precipitate of ANXA2 complexes (figure 3.17).

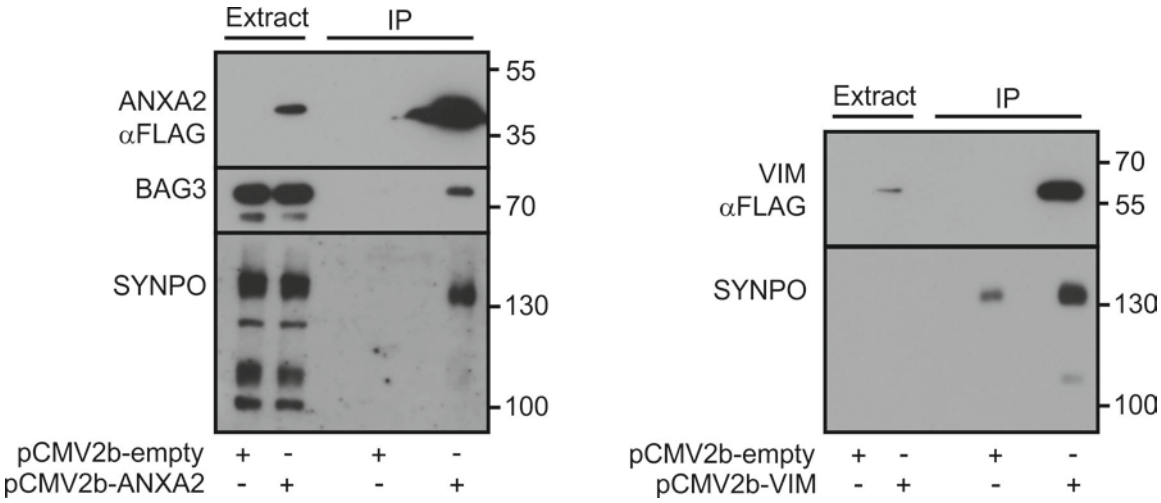

Figure 3.17: Annexin A2 and vimentin bind SYNPO. HeLa cells were transfected with either pCMV2b-ANXA2 or pCMV2b-VIM for 48 h. IP was directed against the FLAG-epitope of the overexpressed proteins. Annexin A2 as well as vimentin are able to co-precipitate SYNPO. Annexin A2 additionally co-precipitates BAG3. 32 µg protein was loaded of the extract (left lanes). 1/3 of total eluate was loaded for the negative controls and the specific IPs respectively.

4. Discussion

The co-chaperone BAG3 has been shown to be involved in essential cellular processes such as apoptosis (Lee *at al.* 1999, Zhang *et al.* 2012), cell migration, actin cytoskeleton dynamics (Iwasaki *et al.* 2007), autophagy (Arndt *et al.* 2010, Ulbricht *et al.* 2013), proteostasis and transcriptional processes (Ulbricht *et al.* 2013). Being such a versatile protein, it will be important to elucidate the BAG3 interactome and its various functions depending on cell type and context. This is also of pathological relevance as mutations in the human BAG3 gene are associated with severe myopathies (Villard *et al.* 2011, Kostera-Pruszczyk *et al.* 2015). In this work the actin binding protein SYNPO could be identified as a novel binding partner of BAG3. Whereas the SYNPO family member SYNPO2 cooperates with BAG3 during autophagy in muscle and immune cells (Ulbricht *et al.* 2013), SYNPO does apparently not fulfill degradative functions in HeLa cells under the experimental conditions used. SYNPOc localizes to punctate, actin-containing assemblies to which BAG3 is recruited. It could be shown in HeLa cells that SYNPOc co-localizes with early endosomes, implicating a possible involvement of SYNPOc in the transport or processing of endocytic vesicles. In addition, many new putative binding partners of the SYNPO – BAG3 complex could be identified in the context of this work, of which Annexin A2 could be shown to interact with BAG3 and SYNPO *in vivo.* Due to its role in endosomal transport (Mayran *et al.* 2003, Morel *et al.* 2009), identification of Annexin A2 supports the possible involvement of SYNPOc and BAG3 in endosomal transport or processing.

4.1 SYNPO, a novel BAG3 binding partner

The actin binding protein SYNPO could be identified as a novel interactor of BAG3 in HeLa cells (figure 3.2). Thus far most of the published data concerning SYNPO is derived from experiments on kidney podocytes and neuronal cells (Mundel *et al.* 1991 and 1997, Deller *et al.* 2003, Schiewek *et al.* 2004, Asanuma *et al.* 2006). For a more general assessment of SYNPO expression crude extracts derived from several human and murine cell lines were tested for the presence of SYNPO. In kidney podocytes Mundel *et al.* (1991 and 1997) observed a SYNPO band with the size of 110 kDa with an additional proteolytic fragment of 44 kDa. In extracts from rat forebrain SYNPO is detectable at 100 kDa (Mundel *et al.* 1997). In this work all cell lines tested show most prominent SYNPO bands at a size of approximately 130 kDa. Additionally a band at 100 kDa can be observed for all five cell lines. Next to unique bands at various heights for the respective cell lines no band can be seen at 44 kDa (figure 3.1). This is surprising as one would expect a band at 110 kDa especially for the Hek-293 extract as this cell line is derived from human embryonic kidney cells. However, the cell extracts revealing a band at 110 kDa and the proteolytic cleavage product at 44 kDa described by Mundel *et al.* (1991 and 1997) are derived from kidney podocytes which is a highly specialized cell type exclusive to the glomeruli of the kidney (reviewed by Pavenstädt, 2000). This specialization might explain the difference in the detected bands for SYNPO, as podocyte SYNPO might undergo different posttranslational processing than in other cell types, or even more likely SYNPO isoforms may be differentially expressed depending on the cell type. Research of the NCBI and UniProt database (https://www.ncbi.nlm.nih.gov, http://www.uniprot.org/) revealed a total of three SYNPO isoforms, SYNPOc, SYNPOa and SYNPOb (figure 3.3). Overexpression constructs were cloned for SYNPOb and SYNPOc and transfected to HeLa cells, revealing that the band observed at 130 kDa corresponds to SYNPOc whereas SYNPOb was identified to be the band at 100 kDa (figure 3.4). The 110 kDa SYNPO band which seems to be podocyte specific is therefore most likely the SYNPOa isoform which is in compliance with the literature concerning the number of amino acids SYNPOa is composed of (Asanuma *et al.* 2005). In order to avoid confusion, it is of note that in many publications SYNPOa is referred to as SYNPO long. Migration behavior of SYNPO in HeLa cells differs from the predicted molecular mass by the Uniprot database, and cannot be directly compared to previously published data from podocytes (Mundel *et al.* 1997, Asanuma *et al.* 2005). Therefore it cannot be conclusively said that SYNPOa has a size of 110 kDa in HeLa

cells as it has in podocytes. SYNPOa is only 26 amino acids shorter than SYNPOc (figure 3.3) and therefore might also migrate at 130 kDa like SYNPOc in SDS-gels of HeLa crude extracts. Thus, the endogenous 130 kDa SYNPO band was designated as SYNPOa/c in this work.

siRNA mediated knockdown of SYNPO in HeLa cells led to a loss of detectable signal for SYNPOa/c (130 kDa) and SYNPOb (100 kDa) (figure 3.5). In the context of the experiments to validate the observed SYNPO signals BAG3 protein was also analyzed. The siRNA mediated knockdown of SYNPO does not show any obvious effects on BAG3 protein levels (figure 3.5). Additionally SYNPOb overexpression in HeLa cells renders detectable BAG3 protein levels unchanged in comparison to the control. However, there is a stabilization of BAG3 protein upon overexpression of SYNPOc (figure 3.4). Here it would be of interest whether this stabilization is due to an increase of BAG3 transcription, a stabilizing effect of SYNPOc on native BAG3 protein, or a consequence of an inhibitory effect of SYNPOc on BAG3 degradation. A transcriptional effect of SYNPOc on BAG3 would be rather interesting in regards of a cellular stress response, as BAG3 is up-regulated under cellular stress such as oxidative or mechanical stress (Bonelli *et al.* 2004, Ulbricht *et al.* 2015). Upon administration of the proteasome inhibiting and autophagy inducing agent MG132, BAG3 is known to be up-regulated on the transcriptional level (Wang *et al.* 2008). A qPCR experiment with oligonucleotides specific for BAG3 gene products could give insight whether SYNPOc has an effect on BAG3 expression and thereby is a potential inducer of a cellular stress response via BAG3.

Concerning SYNPO turnover in podocytes, it is cleaved by the lysosomal endopeptidase Cathepsin L (CatL). Binding to 14-3-3 protects SYNPO from this proteolytic cleavage (Faul *et al.* 2008). Treatment of HeLa cells with E64d, a specific inhibitor of CatL, did not show any effect on SYNPOc expression as shown in figure 3.6. Again no band at 44 kDa could be observed for the DMSO treated control and full length SYNPOa/c levels remain unchanged upon treatment with E64d. This shows that CatL mediated cleavage is likely to be a podocyte specific mechanism, which emphasizes, that expression and processing of SYNPO is highly dependent on the cell type or on the specific extracellular environment the cells have to face. Podocytes for example mark the outermost cover of the glomerular basement membrane, where they are constantly exposed to fluid shear stress and tensile forces arising from intravascular pressure (Vasmant *et al.* 1984; Suleiman *et al.* 2017).

To further analyze SYNPO degradation, HeLa cells were treated with either MG132, a proteasome inhibitor known to induce autophagy (Ding *et al.* 2007, Lan *et al.* 2014), BafA1 (an inhibitor of autophagy by prevention of autophagosome – lysosome fusion (Mauvezin *et al.* 2015) or with both inhibitors, followed by quantification of SYNPO protein via Western Blot (figure 3.7). Degradation, or a possible involvement of SYNPO in the proteasomal degradation pathway or autophagy would manifest itself in a stabilization of SYNPO upon inhibition of the respective pathway. After treatment with the inhibitors there is neither a stabilization nor a decrease in SYNPO protein levels observable (figure 3.7). Except when both inhibitors are applied SYNPOa/c levels are slightly diminished. This however might be due to extreme cellular stress evoked by the combination of both inhibitors which might induce apoptosis.

In summary, these data demonstrate that SYNPO is stable in HeLa cells. It might be possible that degraded SYNPO is rapidly replaced by newly synthesized SYNPO. An experimental setup using the inhibitors MG132 and BafA1 in addition to an agent which inhibits protein translation (e.g. cyclohexamide) could give further insight into SYNPO turnover.

Even though SYNPO levels remain stable upon MG132 treatment of HeLa cells, there is a prominent change in 130 kDa SYNPO (SYNPOa/c) upon MG132 treatment observable (figure 3.8). The lower band of the usual double band of 130 kDa SYNPO undergoes an upward shift resulting in enrichment of the upper SYNPO band. Since total amounts of detectable SYNPOa/c remain the same (figure 3.8) the lower band of SYNPOa/c is not degraded but changed in its size. Variations in migration behaviour are commonly a sign of post-translational modifications of a protein such as phosphorylation (Wegener *et al.* 1984; Ishida *et al.* 2000), glycosylation (Nielsen *et al.* 2004) ubiquitination (Elsasser *et al.* 2012) and others (Carruthers *et al.* 2015). Furthermore SYNPOb has been previously reported to be phosphorylated *in vivo* (Faul *et al.* 2008). To test whether 130 kDa SYNPO is also phosphorylated, HeLa cell crude extracts were subjected to lambda-phosphatase treatment resulting in vast reduction of the upper 130 kDa SYNPO band in the DMSO treated control extract as well as in the MG132 treated one (figure 3.8). To assess the functionality of the phosphatase treatment a specific antibody against the phosphorylated form of the translational regulator S6 kinase 1 (S6) was used as a control. As for the upper band of 130 kDa SYNPO, phosphorylated S6 is largely reduced upon lambda-phosphatase treatment. Faul *et al.* (2008) identified two phosphorylation sites in human SYNPOb, T216 and S619. As SYNPOb shares its complete sequence with SYNPOa and SYNPOc (figure 3.3), SYNPOa and c contain the same potential phosphorylation sites. It would be of interest, whether SYNPOa and c are phosphorylated

at the same amino acids as SYNPOb (which would be T460 and S863 for SYNPOc respectively). Alanine substitution of the potential phosphor-acceptor sites of a SYNPOc overexpression construct would abrogate 130 kDa SYNPO phosphorylation if indeed the same amino acids as reported for SYNPOb are phosphorylated in SYNPOc.

4.2 The interplay of BAG3 and SYNPO

SYNPOa/c are the most abundantly expressed SYNPO isoforms in HeLa cells (figure 3.3). Furthermore SYNPOa/c are the only SYNPO isoforms which co-precipitate with BAG3 under endogenous conditions (figure 3.1). Using an overexpression construct of BAG3 including a FLAG-Tag for immunoprecipitation experiments, SYNPOb can be observed to co-precipitate with BAG3, however to a far lesser extent than SYNPOa/c (figure 3.10). Additionally overexpression of SYNPOc did show a stabilizing effect on BAG3 (figure 3.4) and it could be shown that 130 kDa SYNPO (SYNPOa/c) is phosphorylated *in vivo* (figure 3.8). Hence, this work focussed on the further investigation of SYNPOc and its role as an interactor of BAG3.

Overexpression of BAG3 in HeLa cells could stabilize SYNPOa/c protein levels (figure 3.9, A). As described for overexpression of SYNPOc (see above) it remains unclear, whether this stabilization of SYNPOa/c occurs due to a translational effect or because BAG3 prevents SYNPOa/c degradation. As siRNA mediated knockdown of BAG3 did not show a significant reduction nor stabilization of SYNPOa/c protein levels (figure 3.9, B) a translational effect of BAG3 on SYNPOa/c seems to be favorable in this context. A qRT-PCR experiment using specific oligonucleotides for SYNPOc mRNA would give insight into SYNPOc transcription upon BAG3 overexpression. Such an experiment was indeed performed, however primer design specific for SYNPOc mRNA and the other SYNPO isoforms turned out to be quite challenging as SYNPO contains, depending on the isoform, only one or two coding exons (data obtained from the ensemble database (http://www.ensembl.org)) limiting the possibilities to design oligonucleotides greatly. The oligonucleotides designed for this work failed to amplify the SYNPOc gene product and could therefore not be used.

4.3 BAG3 and SYNPO in CASA

As established in figure 3.1 130 kDa SYNPO (SYNPOa/c) is a novel interactor of the co-chaperone BAG3. The SYNPO family member SYNPO2 was previously shown to bind to the BAG3 WW-domain via its PPXY motif (Ulbricht *et al.* 2013). SYNPOc protein with mutant PPXY motifs was overexpressed in HeLa cells and used in immunoprecipitation experiments. The same was done for a WW-domain mutant of BAG3. Mutated SYNPOc (both PPXY motifs) as well as mutated BAG3 failed to co-precipitate BAG3 or SYNPO respectively, confirming that this interaction is mediated via the WW-domain of BAG3 and SYNPO PPXY motifs (figure 3.10 and 3.11). Here the second of the two SYNPOc PPXY motifs seems to be of higher importance for binding BAG3 as mutation of only the first PPXY motif does not show any influence on BAG3 binding whereas mutation of only the second PPXY motif shows a vast reduction of co-precipitated BAG3. However only a double mutation of both PPXY motifs almost completely abrogates BAG3 binding (figure 3.10). These data coincide with the peptide screen preformed for the identification of novel binding partners of the BAG3 WW-domain. Besides showing an interaction with SYNPO and SYNPO2 the peptide screen could narrow down the consensus binding motif of the BAG3 WW-domain to PP P/S Y (PhD thesis Ulbricht, 2013). The first PPXY motif of SYNPO contains the amino acids PPTY whereas the second motif consists of the amino acids PPSY.

Previous studies have linked SYNPO2 to the BAG3 and HSC70 mediated autophagic degradation process of filamin in muscle and immune cells (CASA) (figure 1.5) (Ulbricht *et al*. 2013). Belonging to the same protein family and both having the ability to bind to BAG3, SYNPO might have similar functions as SYNPO2 in CASA but a different tissue specificity. However, as discussed above, treatment of HeLa cells with MG132 or BafA1 did not show stabilization nor degradation of SYNPO (figure 3.7). This indicates that SYNPO behaves differently than SYNPO2, which is rapidly degraded after treatment of A7r5 cells with MG132 and roughly 4-fold stabilized by administration of BafA1 (Ulbricht *et al.* 2013). To further elucidate a potential link to autophagic degradation, immunofluorescent co-staining experiments were performed in HeLa cells using specific antibodies against p62 and LC3, which are both established markers for autophagosomes (Bjorkoy *et al.* 2009, Tanida *et al.* 2008), and LAMP1 a lysosomal marker (reviewed by Saftig and Klumperman, 2009; Eskelinen, 2006). If SYNPO were to be degraded via the autophagy lysosomal pathway a partial co-localization of SYNPO with these markers is expected. However all three marker proteins failed to show a co-localization with SYNPOc punctae (figure 3.13). Together these data lead to the conclusion, that in regards of an involvement in CASA, SYNPO fails to conduct a similar

function in HeLa cells, under the experimental conditions used, as SYNPO2 does in muscle cells. However, as BAG3 expression is induced under cellular stress conditions, degradation pathways involving BAG3, like CASA, are also in dependency of cellular stress. For filamin degradation cellular stress is induced by mechanical strain (Ulbricht *et al.* 2013). Another protein which involves BAG3 for its degradation is the microtubule-associated protein tau, which is primarily expressed in neurons. Tau is especially known for its pathological relevance in Alzheimer disease (Iqbal *et al.* 2010). Under stressful conditions, such as proteasome inhibition, BAG3 was shown to facilitate the clearance of soluble tau (Lei *et al.* 2015). In addition, BAG3 has been described to promote degradation of mutant huntingtin, associating BAG3 with polyQ diseases such as Huntington disease (Carra *et al.* 2008). Furthermore, Crippa *et al.* (2010) and Gamerdinger *et al.* (2011) describe BAG3 in degradation of amytrophic-lateral-sclerosis (ALS) linked mutant SOD1. It might be possible, that the chosen growth conditions for HeLa cells in this work do not create a cellular stress situation in which BAG3 mediated protein degradation is needed. Challenging of the cells by e.g. overexpressing polyQ constructs or starvation would generate a context in which BAG3 mediated degradation is “switched on”, possibly showing an effect on SYNPO behavior in HeLa cells. Here it would be of interest to compare SYNPO behavior to SYNPO2 in order to draw definite conclusions about a role of SYNPO – BAG3 interaction in autophagic degradation.

An upstream involvement of SYNPO in CASA can also not be excluded. Due to its ability to bind to BAG3, SYNPO might be involved in recruitment of BAG3 to the actin cytoskeleton. Indeed, overexpression of SYNPOc in HeLa cells leads to the accumulation of BAG3 in almost the same punctate pattern as SYNPOc (figure 3.11) allowing for the postulation of a recruitment of BAG3 into those SYNPOc punctae and thereby to the actin cytoskeleton. The actin cytoskeleton has been shown to be critical for autophagosome formation. Upon actin depolymerization via for example cytochalasin D, autophagosome formation is inhibited, showing that the actin cytoskeleton is an important factor in autophagy (Aplin *et al.* 1992, Aguilera *et al.* 2012). It could be shown that actin filaments co-localize with early omegasomes prior to their association with LC3 (Aguilera *et al.* 2012). Omegasomes are membrane protrusions that eventually develop into phagophors or isolation membranes (Axe *et al.* 2008). Even though the actin cytoskeleton is involved in the formation of autophagosomes beyond this initial step (reviewed by Kruppa *et al.* 2016), the early omegasome stage represents a possible timeframe in which BAG3 could be recruited by SYNPO. This is because the early omegasome is not yet associated with LC3, which is important because SYNPOc did not

co-localize with LC3 in immunofluorescence experiments (figure 3.13), making an involvement of SYNPO in later stages of autophagosome formation unlikely.

4.4 SYNPO punctae: Hubs for actin polymerization?

SYNPO has been repeatedly confirmed to be an actin binding protein (Mundel *et al.* 1997, Kreemerskothen *et al.* 2005, Asanuma *et al.* 2005). Overexpression of SYNPOc in HeLa cells shows the previously in neuronal and kidney cells described punctate pattern of SYNPO in immunofluorescence experiments (figure 3.12) (Mundel *et al.* 1997, Asanuma *et al.* 2005). In this work a co-localization of SYNPOc punctae with phalloidin, a marker for the actin cytoskeleton could be observed (figure 3.13) in agreement with published data (Mundel *et al*. 1997, Asanuma et al 2005, Kremerskothen *et al.* 2005, Faul *et al.* 2008). In contrast to Asanuma *et al.* (2005) describing SYNPO punctae in podocytes as amorphous, cytoplasmic, phalloidin-positive aggregates, in this work SYNPOc punctae induced by overexpression of SYNPOc in HeLa cells appear to be round in shape with many of them showing small pointed protrusions rather resembling α-actinin-4 staining as shown by Asanuma *et al.* (2005) as sites of short branched actin filaments (figure 3.12). Furthermore, Asanuma *et al.* (2005) could show that co-expression of SYNPOb and α-actinin-4 abrogates SYNPOb punctae and results in long parallel and unbranched actin bundles. This gives rise to the hypothesis that SYNPOc punctae might serve as a hub for actin polymerization in HeLa cells. This is supported by the ability of SYNPO to interact with BAG3. Findings by Fontanella *et al.* (2010) associate BAG3 with the eukaryotic chaperonin CCT / TRiC (cytosolic chaperonin containing TCP-1 / TCP-1 ring complex) suggesting a role of BAG3 in CCT substrate folding. This is of interest, because CCT is mandatory for the folding of actin und tubulin into their respective three dimensional structures (Sternlicht *et al.* 1993, Llorca *et al.* 2000). Knockdown of CCT results in reduction of the availability of native G-actin, growth arrest and changes in cellular shape and motility due to alterations in tubulin and actin cytoskeleton integrity (Grantham *et al.* 2006). In the context of SYNPOc punctae and their potential role in actin polymerization, it might be possible that through the interaction of SYNPOc and BAG3, also CCT is recruited to the SYNPOc punctae creating a source of newly synthesized G-actin in close proximity to the polymerizing actin filaments. Furthermore CCT has been implicated not only in the folding of actin but also in regulating actin polymerization kinetics. Here CCT subunits have been shown to reduce

actin filament elongation *in vitro* suggesting a role of CCT subunits in quality control of the newly synthesized actin filament. However, it is more likely that CCT subunits protect the growing end of the actin filament as hydrophobic surfaces of the actin monomers building the filament are transiently exposed in the process of integration of new actin monomers for elongation (Grantham *et al.* 2002). Co-staining of SYNPOc and CCT in immunofluorescence experiments could give first hints on a possible connection of SYNPOc and BAG3 regulated actin dynamics with CCT.

Upon overexpression of SYNPOc many rather large BAG3 positive SYNPOc punctae are detectable, which all might be possible sites for actin polymerization (figure 3.11). That few stress fibers are observable upon SYNPOc overexpression might be due to the excess of SYNPOc created by overexpression (figure 3.11, 3.12 and 3.13). As described by Asanuma *et al.* (2005) only co-expression of α-actinin-4 induced the formation of long parallel actin fibers in podocytes. Maybe the increased amount of SYNPOc can't be compensated for by the endogenous α-actinin-4 levels, leaving sites of accumulated SYNPOc and BAG3 ready for actin polymerization but lacking an equal amount of required co-factors for this process.

4.5 SYNPO interactors: hints for intracellular transport

Via immunoprecipitation with subsequent SDS-Page, SYNPO protein complexes could be isolated for analysis via mass spectrometry. Many interesting potential SYNPO binding partners could be identified, of which many are actin cytoskeleton associated proteins (table 3.1). One of the binding partners identified is Annexin A2 (ANXA2). A FLAG-tagged overexpression construct of ANXA2 could successfully co-precipitate 130 kDa SYNPOa/c in immunoprecipitation (figure 3.17), validating the results gained from mass spectrometry. Interestingly BAG3 could also be identified to co-precipitate in a complex with ANXA2 (figure 3.17). ANXA2 belongs to the large family (more than 160 family members) of Annexins which are known to bind to phospholipids in a Ca^{2+} dependent manner (reviewed by Gerke and Moss, 2002). ANXA2 is specifically of interest as an interactor of the BAG3 – SYNPO complex as it has been described to be able to bind F-actin (Filipenko and Waisman, 2001). However it is reported, that ANXA2 does not localize to stress fibers but is associated with the organization of membrane associated actin, especially in membrane regions enriched in sphingolipids and cholesterol, termed lipid rafts (Harder *et al.* 1997; Babiychuk and Draeger, 2000).

Furthermore ANXA2 is implicated in endosome biogenesis as it associates with early endosomal membranes and is involved in early-to-late endosomal transport via selective actin nucleation and polymerization (Emans *et al.* 1993; Mayran *et al.* 2003; Morel *et al.* 2009). Indeed the actin cytoskeleton is, next to the microtubule cytoskeleton, a major player in intracellular transport of diverse cargo e.g. secretory vesicles, cellular organelles or protein complexes (reviewed by Ross *et al.* 2008). Transport is either mediated via polarized actin polymerization on the surface of organelles (e.g. micropinocytotic vesicles or pathogenic bacteria) propelling the respective cargo forward on so called actin comet tails (Theriot *et al.* 1992; Christien *et al.* 1999, Merrifield *et al.* 2001; Orth *et al.* 2001). Or by motor protein dependent actin transport via proteins of the myosin family, which can move along actin filaments in an ATP dependent manner (reviewed by Hammer and Sellers (2011), Maravillas-Montero and Santos-Argumedo (2012)). Even more intriguingly, cargo transported on actin cytoskeletal tracks can be handed over to dynein or kinesin (which are the microtubule associated motor proteins) for further transport via the microtubule cytoskeleton and vice versa (Kural *et al.* 2007, Watanabe and Higuchi 2007). Additionally, the transported cargo can be switched from one actin filament to another at filament intersections (Snider *et al.* 2004). As SYNPO has been shown to be able to bind myosin II (Kannan *et al.* 2015) it might also be able to bind other myosin family members like myosin V, VI or X, which are associated with cargo transport (reviewed by Ross *et al.* 2008).

BAG3 has also been reported to be involved in intracellular transport as a factor in aggresome formation via the microtubule cytoskeleton (Gamerdinger *et al.* 2011). Aggresomes are defined as microtubule-dependent, cytoplasmic inclusion bodies serving as a site for accumulation and sequestration of misfolded / aggregated proteins which can be cleared via autophagy (Johnston *et al.* 1998, García-Mata 1999). The intermediate filament protein vimentin (Herrmann and Aebi 2000) could be established as a marker for aggresomes as it forms a cage like structure around these perinuclear compartments whereas in the absence of an aggresome it is evenly distributed in the cytoplasm (Johnston *et al.* 1998). It is of note, that vimentin could also be identified as an interactor of SYNPO via mass spectrometry (table 3.1). Even though immunofluorescent staining did not show a co-localization of SYNPOc and vimentin (figure 3.13), the binding of the two proteins could be confirmed by immunoprecipitation (figure 3.17).

In the context of cellular transport, BAG3 mediates loading of misfolded cargo proteins to the microtubule motor protein dynein through a direct interaction. The dynein – BAG3 – cargo complex is then transported to the aggresome (Gamerdinger *et al.* 2011). BAG3 mediated cargo loading is facilitated by 14-3-3 protein which recruits BAG3 – cargo

complexes to the motor (Xu *et al.* 2013). Additionally, BAG3 mediated aggresome targeting of the mutant protein SOD1 via dynein is an ubiquitin independent process (Gamerdinger *et al.* 2011) in contrast to the ubiquitin-dependent mechanisms of aggresome targeting via dynein and Histone Deacetylase 6 (HDAC6) (Kawaguchi *et al.* 2003, Ouyang *et al.* 2012).

Here a potential interplay of ANXA2 with SYNPO and BAG3 could come into play by mediating intracellular transport along actin filaments ultimately handing over cargo to the microtubule network via BAG3. Through the interaction of ANXA2 – BAG3 – SYNPO – myosin and the actin cytoskeleton a transport machinery for e.g. endosomes may be generated. Here ANXA2 could mediate binding to the endosomal membrane anchoring it to the actin cytoskeleton via SYNPO. SYNPO in turn binds to the myosin motor and recruits BAG3 into the complex. For further transport along the microtubule cytoskeleton BAG3 could potentially mediate the switch to the dynein motor as it can bind directly to it and thereby releasing SYNPO, as SYNPOc does not associate with microtubuli (figure 3.13). ANXA2 possibly remains in the BAG3 – dynein complex to mediate continued binding to the transported endosome.

Indeed a co-localization of SYNPOc punctae with the early endosome marker EEA1 could be observed in immunofluorescence (figure 3.15), underscoring a potential involvement of SYNPO, BAG3 and ANXA2 in endosomal trafficking. An additional immunofluorescence experiment using a marker for late endosomal compartments like Rab7 (McCaffrey *et al.* 2001) could further confirm the hypothesis, that SYNPO is only involved in trafficking of early endosomes, whereas BAG3 mediates further transport to late endosomal compartments. Whether the co-localization of SYNPOc with early endosomes indeed serves the purpose of endosomal transport could be monitored via life cell imaging using fluorescently labeled dextran which is taken up by endosomes and can thus be monitored under the microscope in combination with overexpression of fluorescently labeled SYNPOc. Furthermore it has to be established whether SYNPO can interact with the myosin motors as it can with myosin II (Kannan *et al.* 2015) to make transport along the actin cytoskeleton possible.

Another quite exciting hypothesis in the context of early endosome transport potentially mediated by an interplay of BAG3 – SYNPO – ANXA2 is the delivery of membranes for autophagosome formation via transport of ATG9A (autophagy related 9A) positive endosomes. Multiple compartments are thought to serve as a resource of membranes for autophagosome formation such as the endoplasmic reticulum, the Golgi, the plasma membrane, mitochondria or early and recycling endosomes. (Ylä-Anttila *et al.* 2009, Yen

et al. 2010, Hailey *et al.* 2010, Ravikumar *et al.* 2010, Longatti and Tooze 2012, Ge *et al.* 2013) ANXA2 has been associated with sorting of the transmembrane protein ATG9A from endosomes. Here ATG9A is taken up from the plasma membrane by endocytosis and is delivered to the recycling endosome via early endosomal compartments in an ANXA2 dependent manner (Puri *et al.* 2013 and 2014, Moreau *et al.* 2015). Eventually, ATG9A containing vesicles are incorporated into the autophagosomal outer membrane (Yamamoto *et al.* 2012). Upon starvation induced autophagy ANXA2 levels were observed to be upregulated which resulted in an increase in ATG9A vesicle movement and an increase in autophagosome formation (Moreau *et al.* 2015). Via interacting with ANXA2 (figure 3.17) and SYNPO association to early endosomes (figure 3.15) the BAG3 – SYNPO complex might also be involved in this process of ATG9A containing membrane delivivery to autophagic structures.

The last interesting hypothesis which needs to be taken into account is endosomal movement by actin comet tails potentially generated by an interplay of SYNPO, BAG3 and ANXA2. Here co-localization of SYNPOc to endosomes and the potential role of SYNPO and BAG3 as a hub for actin polymerization (as described above) come into play together with ANXA2. It has been described, that ANXA2 plays an essential role in actin-based rocketing of macropinosomes, which are endosomal vesicles specific for the uptake of extracellular fluid (Merrifield *et al.* 2001). Co-transfection of fluorescently labeled SYNPOc with Lifeact, a marker to visualize F-actin (Riedl *et al.* 2008) and addition of fluorescent dextran would allow for monitoring of endosomal trafficking and its dependence on actin and SYNPOc.

Another interactor of SYNPO identified via mass spectrometry is Tropomyosin 1 (TPM1) (Table 3.1). Tropomyosins make up a family which is involved in actin dynamics, cellular migration and suppression of tumorigenesis (Ono and Ono, 2002; Bryce *et al.* 2003; reviewed by Gunning *et al.* 2008). TPM1 is, next to other tropomyosins, necessary for stress fiber formation via a stabilizing function, whereas another tropomyosin family member, TPM4, has been described to recruit myosin II to stress fibers (Tojkander *et al.* 2011). Furthermore it could be shown that SYNPO can rescue Tropomyosin deficiency in the model organism *Drosophila melanogaster* and human cancer cells (Wong *et al.* 2012). This interaction of SYNPO with TPM1 indicates that SYNPO does not only mediate stress fiber formation in podocytes but also in epithelial cells. Whether BAG3 is also found in a complex with SYNPO and TPM1 as could be shown for ANXA2 (see above) remains to be analyzed.

3.6 BAG3 and SYNPO in mechanotransduction

There are several reports revealing that BAG3 as well as SYNPO are mechanosensitive proteins (Ulbricht *et al.* 2013 and 2015, Mun *et al.* 2014, Kannan *et al.* 2015). This means they can be stimulated by, and are involved in the reaction to mechanic impulses, turning a mechanical signal into a biochemical one. Thus far many proteins have been identified to contribute to mechanotransduction, such as integrins which are components of focal adhesions connecting a cell to the extracellular matrix (ECM) (reviewed by Juliano *et al.* 2004) or cadherins being essential for cell-cell contacts (adherens junctions) (reviewed by Meng and Takeichi, 2009) as well as myosin motors which are components of actin stress fibers (reviewed by Vincente-Manzanares *et al.* 2009) and many more (reviewed by Ingber, 2006). In the context of mechanotransduction BAG3 was not only shown to be essential for the degradation of denatured filamin upon tension induced mechanical strain (CASA) but is also involved in regulating transcription of new filamin via inhibition of Large Tumor Suppressor Kinase 1 (LATS1) and Angiomotin Like 1 (AMOTL1), which in turn release the Hippo pathway transcription factors Yes Associated Protein 1 (YAP) and WW Domain Containing Transcription Regulator 1 (WWTR1 or TAZ) for nuclear translocation (Ulbricht *et al.* 2013). Connecting BAG3 to the Hippo pathway is quite intriguing as it is one of the major signaling pathways associated with mechanotransduction (Dupont *et al.* 2011, Aragona *et al.* 2013). Next to its involvement in filamin turnover under mechanical stress, BAG3 has been described to be involved in cell migration and adhesion via interaction with the guanine nucleotide exchange factor PDZGEF2 (PDZ domain containing Guanine Nucleotide Exchange Factor 2) which induces activation of Rap1 (Iwasaki *et al.* 2010). All this suggests that BAG3 is a major player in mechanotransduction and potentially has additional roles in this complex cellular response to mechanic stimuli, besides its fundamental role in filamin turnover.

SYNPO has first been implicated to be a mechanosensitive protein by its involvement in endothelial wound healing induced by laminar shear stress (Mun *et al.* 2014). Furthermore, SYNPO has been described to protect the small GTPase RhoA from degradation and thereby is involved in stress fiber formation (Asanuma *et al.* 2006). It can be reasoned that SYNPO is indirectly involved in YAP/TAZ signaling via RhoA, because RhoA and intact stress fibers are required to maintain nuclear YAP/TAZ localization in response to mechanical stress (Dupont *et al.* 2011). Additionally, recent work by Kannan *et al.* (2015) shows SYNPO to be an important factor in maturation of adherens junctions under mechanical stress. Here SYNPO is recruited to the maturing adherens junction, where in turn it is involved in the recruitment of α-actinin-4 and

Vinculin. While the molecular mechanism by which SYNPO is relocated to the developing junction remains to be elucidated, the authors could show that SYNPO and α-actinin-4 accumulation can be experimentally induced by applying cyclic strain to the cells (Kannan *et al.* 2015). Recruitment of SYNPO to adherens junctions may potentially be mediated by the membrane associated protein MAGI-1 (Membrane Associated Guanylate Kinase Inverted 1), a junctional protein which can bind to SYNPO, β-catenin (a major component of adherens juctions) as well as α-actinin-4 (Dobrosotskaya and James 2000, Patrie *et al.* 2002, Stetak and Hajnal 2011). In addition to these findings associating SYNPO with adherens junctions, SYNPO was reported to bind to the junction stabilizing factor CD2 associated protein (CD2AP) (Schiwek *et al.* 2004, Huber *et al.* 2006, Tang and Brieher, 2013). CD2AP is a scaffolding protein and a regulator of the actin cytoskeleton. Recent findings identify CD2AP as a linker protein of cellular junctions to the actin cytoskeleton (Welsch *et al.* 2001, Tang and Brieher 2013). These multiple interactions highly suggest a role of SYNPO in cellular adhesion under mechanical stress. Kannan *et al.* (2015) propose that SYNPO is able to establish a physical link between adherens junctions (via binding to α-actinin-4 and MAGI-1) and actin stress fibers potentially via CD2AP or myosin II, which could both be established as binding partners of SYNPO *in vivo* (Schiwek *et al.* 2004; Huber *et al.* 2006; Kannan *et al.* 2015).

As mentioned above, SYNPO is involved in stress fiber formation via RhoA (Asanuma *et al.* 2006). Additionally it could be shown in podocytes, that binding of SYNPOb to 14-3-3β in a phosphorylation dependent manner protects it from proteolytic cleavage by CatL, which in turn maintains stress fiber formation and integrity via RhoA (Faul *et al.* 2008). Interestingly, Kannan *et al.* (2015) report an upward shift of SYNPO in Western blots upon administration of mechanical force to the cells which closely resembles the shift in size observed for SYNPOa/c upon MG132 treatment in this work. As proteolytic cleavage of SYNPOa/c by CatL could not be observed in HeLa cells (figure 3.6) MG132 induced phosphorylation of SYNPOa/c might resemble SYNPO modification upon mechanical stimuli. How proteasomal inhibition and mechanotransduction might be connected via phosphorylated SYNPO remains elusive. Few data linking the proteasome and the actin cytoskeleton are available. In dendritic spines association of the proteasome with the actin cytoskeleton could be shown. The authors suggest that this association is involved in spatial sequestration of the proteasome to allow for local remodeling of the protein composition (Bingol and Schuman, 2006). Furthermore, administration of MG132 to *Saccharomyces cerevisiae* was demonstrated to result in defects in cell morphology and actin organization (Haarer *et al.* 2011). However, this effect is not surprising, as many factors involved in cytoskeleton dynamics are degraded by the proteasome e.g. the actin

capping protein CapZ (Hishiya *et al.* 2010), RhoA (Asanuma *et al.* 2006), β-catenin (Aberle *et al.* 1997), or the small GTPase Rac1 in its GTP bound (active) state (Lynch *et al.* 2006). In regards of adherens junctions MG132 has been reported to be able to block cadherin (the main adhesion molecule in adherens junctions) endocytosis for degradation or recycling by a thus far unknown mechanism (Xiao *et al.* 2003, cadherin turnover reviewed by Nanes and Kowalczyk, 2012). As BAG3 is transcriptionally upregulated upon MG132 treatment (Wang *et al.* 2008) and has been implicated to be a regulator of cellular adhesion and migration (Iwasaki *et al.* 2007 and 2010), it might be involved in modulating adhesive strength via interaction with SYNPO. However data on BAG3 involvement in cellular adhesion and migration is limited to focal adhesions rather than adherens junctions and no direct co-localization of BAG3 with focal adhesion plaques could thus far be observed (Iwasaki *et al.* 2007). SYNPO however, has been observed to localize to sites of focal adhesions (Mundel *et al.* 1997, Asanuma *et al.* 2006) which indicates that the SYNPOc punctae which are also positive for BAG3 (figure 3.11) are unlikely to be sites of focal adhesion. Therefore it is plausible, that SYNPO needs to be released of its BAG3 bound state in order to localize to sites of maturing adherens junctions. Additionally, the phosphorylation of SYNPOa/c in HeLa cells observed in this work (figure 3.8) and the reported upward shift of SYNPO in MDCK cells by Kannan *et al.* (2015) might be functionally distinct from each other as SYNPO might conduct different roles in differing cell types. Furthermore, Kannan *et al.* (2015) did not further investigate the nature of the observed SYNPO upward shift. It might actually be an effect due to another post-translational modification other than phosphorylation.

4.7 Outlook

In this work, the broad interactome of BAG3 could be further expanded by SYNPO. Whereas the exact consequence of BAG3 – SYNPO interaction remains elusive, the many newly identified SYNPO binding partners give hints on possible scenarios like intracellular transport or mechanotransduction. Especially the prospect of an involvement in intracellular transport could be further underlined by showing that SYNPOc punctae co-localize with early endosomes. The molecular function behind this co-localization and whether BAG3 is involved as well remains to be established.

The question of similar functions between SYNPO and SYNPO2 in the context of BAG3 mediated protein degradation could not be completely answered. First data point to a

generally different role of SYNPO than SYNPO2. However follow-up experiments are needed, challenging the HeLa cells with stressful stimuli to further enhance BAG3 mediated degradation.

In addition, SYNPO could be further characterized on a molecular level, showing that in HeLa cells SYNPO is a stable protein under the chosen experimental conditions. Furthermore, SYNPO could be shown to be phosphorylated. It would be especially interesting to elucidate whether SYNPO – BAG3 interaction is disrupted by phosphorylation of SYNPO, providing a molecular switch for this interaction. Identification and mutation of SYNPO phosphorylation sites is indispensable in order to answer many open questions on the nature of SYNPO in epithelial cells and its role as an interactor of BAG3.

Taken together, this work lays a fundament for the study of BAG3 – SYNPO interaction in epithelial cells, providing general information about SYNPO behavior in HeLa cells and giving ideas on how BAG3 and SYNPO might function together in the constant effort of a cell to adapt to its ever changing surroundings.

List of Abbreviations

°C	Degree Centigrate
µ	Micro
aa	amino acid
ABP	actin binding protein
AMOTL1	Angiomotin Like 1
Amp	Ampicillin
ANXA2	Annexin A2
BAG	Bcl-2 associated athanogene
BSA	Bovine serum albumin
CASA	chaperone assisted selective autophagy
CCT	cytosolic chaperonin containing TCP-1
CD2AP	CD2 associated protein
DMSO	Dimethylsulfoxide
DNA	Desoxyribonucleic acid
dNTP	Desoxyribonucleoside triphosphate
E. Coli	*Escherichia Coli*
ECL	enhanced chemiluminescence
EDTA	Ethylendiamine-N,N,N',N'-Tetraacetate
EEA1	Early endosome antigen 1
EM	extracellular matrix
et al.	*et aliter*
exp.	exposure
F-actin	filamentous actin
g	Gramm
g	gravitational constant
G-actin	globular / monomeric actin
GAPDH	Glycerine-aldehyde-3-phosphate-dehydrogenase
h	hour
HCl	acetic acid
HDAC6	Histone Deacetylase 6
HSP70	Heat Shock 70 kDa Protein
HSPB8	Heat Shock Protein Family B member 8
IF	Immunofluorescence
IP	Immunoprecipitation
kb	kilo bases
kDa	kilo Dalton
L	liter
LATS1	Large Tumor Suppressor Kinase 1
LB	Luria-Bertani-Medium
LC3	Microtubule-associated protein 1A/1B-light chain 3
M	Molar (mol/L)
m	Milli
MAGI-1	Membrane Associated Guanylate Kinase Inverted 1
min	minute
mRNA	messenger RNA
n	nano
OD	optical density
p	pico
p62	protein 62 kDa / Sequestosome 1
PBS	phosphate buffered saline

PCR	polymerase chain reaction
RNase	Ribonuclease
RNA	Ribonucleic acid
RT	room temperature
SDS	sodium dodecyl sulfate
sec	second
SYNPO	Synaptopodin
SYNPOc	long isoform of Synaptopodin 929 aa
SYNPOb	short isoform of Synaptopodin 685 aa
TAZ	WW Domain Containing Transcription Regulator 1 (WWTR1)
TBS	Tris-bufferd saline
TEMED	N,N,N',N#-Tetramethylenediamine
TRiC	TCP-1 ring complex)
Tris	Tris (hydroxymethyl) aminomethane
U	units
UV	ultraviolet
rpm	rounds per minute
VIM	Vimentin
YAP	Yes Associated Protein 1)
w/o	without
wt	wild type

List of Figures

References

Aberle H, Bauer A, Stappert J, *et al.* (1997) β-catenin is a target for the ubiquitin-proteasome pathway. EMBO Journal 16(13):3797-804

Aguilera AO, Berón W, Colombo MI (2012) The actin cytoskeleton participates in the eraly events of autophagosome formation upon starvation induced autophagy. Autophagy 8(11):1590-1603

Aplin A, Jasionowski T, Tuttle DL, *et al.* (1992) Cytoskeletal Elements Are Required for the Formation and Maturation of Autophagic Vacuoles. J Cell Phys 152:458-66

Aragona M, Panciera T, Manfrin A, *et al.* (2013) A Mechanical Checkpoint Controls Multicellular Growth through YAP/TAZ Regulation by Actin-Processing Factors. Cell 154:1047-59

Arndt V, Dick N, Tawo R (2010) Chaperone-Assisted Selective Autophagy is Essential for Muscle Maintenance. Curr Biol. 20:143-48

Asanuma K, Kim K, Oh J, *et al.* (2005) Synaptopodin regulats the actin-bundling activity of α-actinin in an isoform-specific manner. J Clin Invest. 115(5):1188-98

Asanuma K, Yanagida-Asanuma E, Faul C, *et al.* (2006) Synaptopodin orchestrates actin organization and cell motility via regulation of RhoA signalling. Nat Cell Biol. 8(5):485-91

Axe EL, Walker SA, Manifava M, *et al.* (2008) Autophagosome formation from membrane compartments enriched in phosphatidylinositol 3-phosphate and dynamically connected to the endoplasmic reticulum. J Cell Biol. 182(4):685-701

Babiychuk EB, Draeger A (2000) Annexins in Cell Membrane Dynamics: Ca2+-regulated Association of Lipid Microdomains. J Cell Biol. 150(5):1113-23

Bates GP, Dorsey R, Gusella JF *et al.* (2015) Huntington disease. Nat Rev Dis Primers 1:15005

Behl C (2016) Breaking BAG: The Co-Chaperone in Health and Disease. Trends in Pharmacol Sci. 37(8):672-88

Bento CF, Renna M, Ghislat G, *et al.* (2016) Mammalian Autophagy: How Does It Work? Ann Rev. Biochem. 85:685-713

Bingol B, Schuman EM (2006) Activity-dependent dynamics and sequestration of proteasomes in dendritic spines. Nature 44:1144-48

Bjorkoy G, Lamark T, Pankiv S, *et al.* (2009) Monitoring autophagic degradation of p62/SQSTM1. Methods Enzymol. 452:181-197

Bonelli P, Petrella A, Rosati A, *et al.* (2004) BAG3 protein regulates stress-induced apoptosis in normal and neoplastic leukocytes. Leukemia 18:358-60

Bruno AP, Festa M, Dal Piaz F, *et al.* (2008) Identification of a synaptosome-associated form of BAG3 protein. Cell Cycle 7(19):3104-5

Bryce NS, Schevzov G, Ferguson V, *et al.* (2003) Specification of Actin Filament Function and Molecular Composition by Tropomyosin Isoforms. Mol Biol Cell. 14:1002-16

Caplan AJ (2003) What is a co-chaperone? Cell Stress & Chaperones 8(2):105-7

Carlier MF, Shekhar S (2017) Global treadmilling coordinates actin turnover and controls the size of actin networks. Nat Rev Mol Cell Biol. 18(6):389-401

Carra S, Seguin AJ, Lambert H, Landry J (2008) HspB8 Chaperone Activity toward Poly(Q)-containing Proteins Depends on Its Association with Bag3, a Stimulator of Macroautophagy. J Biol Chem. 283(3):1437-44

Carruthers NJ, Parker GC, Gratsch T, et al. (2015) Protein Mobility Shifts Contribute to Gel Electrophoresis Liquid Chromatography Analysis. J Biomol Tech. 26:103-12

Chalovich JM, Schroeter MM (2010) Synaptopodin family of natively unfolded, actin binding proteins: physical properties and potential biological functions. Biophys Rev. 2:181-89

Chen Y, Yang LN, Cheng L, et al. (2013) BAG3 Interactome Ananlysis Reveals a New Role in Modulating Proteasome Activity. Mol Cell Prot. M112.025882

Chia PZC, Gleeson PA (2014) Membrane tethering. F1000 Prime Rep. 6:74

Choi JS, Lee JH, Kim HY *et al.* (2006) Developmental expression of Bis protein in the cerebral cortex and hippocampus of rats. Brain Res. 1092:69-78

Christien J, Merrifield, Stephen E, et al. (1999) Endocytic vesicles move at the tips of actin tails in cultured mast cells. Nat Cell Biol. 1:72-74

Coulson M, Robert S, Saint R (2005) Drosophila starving Encodes a Tissue-Specific BAG-Domain Protein Required for Larval Food Uptake. Genetics 171:1799-812

Coutts AS, La Thangue NB (2016) Regulation of actin nucleation and autophagosome formation. Cell Mol Life Sci. 73:3249-63

Crippa V, Sau D, Rusmini P, et al. (2010) The small heat shock protein B8 (HspB8) promotes autophagic removal of misfolded proteins involved in amyotrophic lateral sclerosis (ALS). Human Mol Gen. 19(17):3440-56

Cuervo AM, Wong E (2014) Chaperone-mediated autophagy: roles in disease and aging. Cell Res. 24:92-104

Deller T, Korte M, Chabanis S, *et al.* (2003) Synaptopodin-deficient mice lack spine apparatus and show deficits in synaptic plasticity. PNAS 100(18):10494-99

De Marco M, Turco MC, Rosati A (2011) BAG3 protein is induced during cardiomyoblast differentiation and modulates myogenin expression. Cell Cycle 10(5):850-52

Ding WX, Ni HM, Gao W, *et al.* (2007) Linking of Autophagy to Ubiquitin-Proteasome System Is Important for the Regulation of Endoplasmic Reticulum Stress and Cell Viability. Am J Pathol. 171(2):513-24

Dobrosotskaya I.Y, G.L. James. (2000) MAGI-1 interacts with β -catenin and is associated with cell–cell adhesion structures. Biochem. Biophys. Res. Commun. 270:903–909.

Dominguez R, Holmes KC (2011) Actin Structure and Function. Annu Rev Biophys. 40:169-86

Dupont S, Morsut L, Aragona M, *et al.* (2011) Role of YAP/TAZ in mechanotransduction. Nature 474:179-85

Edkins AL (2015) CHIP: a co-chaperone for degradation by the proteasome. Subcell Biochem. 78:219-42

Elsasser S, Shi Y, Finley D (2012) Binding of Ubiquitin Conjugates to Proteasomes as Visualized with Native Gels. Methods Mol Biol. 832:403-22

Emans N, Gorvel JP, Walter C, *et al.* (1993) Annexin II Is a Major Component of Fusogenic Endosomal Vesicles. J Cell Biol. 120(6):1357-69

Eskelinen EL, (2006) Roles of LAMP-1 and LAMP-2 in lysosome biogenesis and autophagy. Mol Aspects Med. 27:495-502

Fan CY, Lee S, Cyr DM (2003) Mechanisms for regulation of Hsp70 function by Hsp40. Cell Stress & Chaperones 8(4):309-16

Faul C, Donnelly M, Merscher-Gomez S, *et al.* (2008) The actin cytoskeleton of kidney podocytes is a direct target of the antiproteinuric effect of cyclosporine A. Nat Med. 14(9):931-8

Feng Y, He D, Yao Z, Klionsky DJ (2014) The machinery of macroautophagy. Cell Res 24:24-41

Filipenko NR, Waisman DM (2001) The C Terminus of Annexin II Mediates Binding to F-actin. J Biol Chem. 276(7):5310-15

Fletcher DA, Mullins RD (2010) Cell mechanics and the cytoskeleton. Nature 463:485-92

Fontanella B, Birolo L, Infusini G, *et al.* (2010) The co-chaperone BAG3 interacts with the cytosolic chaperonin CCT: new hints for actin folding. Int J Biochem Cell Biol. 42: 641–650

Franaszczyk A, Bilinska Z, Sobieszczanska-Malek M, *et al.* (2014) The BAG3 gene variants in Polish patients with dilated cardiomyopathy: four novel mutations and a genotype-phenotype correlation. J Transl Med. 12:192

Fratti RA, Backer JM, Gruenberg J *et al.* (2001) Role of phosphotidylinositol 3-kinase and Rab5 effectors in phagosomal biogenesis and mycobacterial phagosome maturation arrest. J Cell Biol 154(3):631-44

Fuchs M, Poirier DJ, Seguin S, *et al.* (2010) Identification of the key structural motifs involved in HspB8/HspB6-Bag3 interaction. Biochem J. 425:245-55

Gamerdinger M, Hajieva P, Kaya AM, *et al.* (2009) Protein quality control during aging involves recruitment of the macroautophagy pathway by BAG3. EMBO Journal 28:889-901

Gamerdinger M, Kaya aM, Wolfrum U, *et al.* (2011) BAG3 mediates chaperone-based aggresome-targeting and selective autophagy of misfolded proteins. EMBO reports 12:149-56

García-Mata R, Bebök Z, Sorscher EJ, Sztul ES (1999) Characterization and Dynamics of Aggresome Formation by a Cytosolic GFP-Chimera. J Cell Biol. 146(6):1239-54

Ge L, Melville D, Zhang M, Schekman R (2013) The ER-Golgi intermediate compartment is a key membrane source for the LC3 lipidation step of autophagosome biogenesis. eLife 2:e00947

Gerke V, Moss SE (2002) Annexins: From Structure to Function. Physiol Rev. 82:331-71

Glick D, Barth S, Macleod KY (2010) Autophagy: cellular and molecular mechanisms. J Pathol 221(1):3-12

Grantham J, Ruddock LW, Roobol A, Carden M (2002) Eukaryotic chaperonin containing Tcomplex polypeptide 1 interacts with filamentous actin and reduces the initial rate of actin polymerization in vitro. Cell Stress & Chaperones 7(3):235-42

Grantham J, Brackley K, Willison KR (2006) Substantial CCT activity is required for cell cycle progression and cytoskeletal organization in mammalian cells. Exp Cell Res 312:2309-24

Gunning P, O'Neill G, Hardeman E (2008) Tropomyosin-Based Regulation of the Actin Cytoskeleton in Time and Space. Physiol Rev. 88:1-35

Haarer B, Aggeli D, Viggiano S, *et al.* (2011) Novel Interactions between Actin and the Proteasome Revealed by Complex Haploinsufficiency. PLoS Genet 7(9):e1002288

Hailey DW, Kim PK, Satpute-Krishnan P, *et al.* (2010) Mitochondria supply membranes for autophagosome biogenesis during starvation. Cell 141(4):656-67

Hammer JA 3rd, Sellers JR (2011) Walking to work: roles for class V myosins as cargo transporters. Nat Rev Mol Cell Biol. 13(1):13-26

Harder T, Kellner R, Parton RG, Gruenberg J (1997) Specific Release of Membrane-bound Annexin II and Cortical Cytoskeletal Elements by Sequestration of Membrane Cholesterol. Mol Biol Cell. 8:533-45

Hartl FU, Bracher A, Hayer-Hartl M (2011) Molecular chaperones in protein folding and proteostasis. Nature 475:324-32

Herrmann H, Aebi U (2000) Intermediate filaments and their associates: multi-talented structural elements specifying cytoarchitecture and cytodynamics. Curr Opin Cell Biol. 12:79-90

Hishiya A, Kitazawa T, Takayama S (2010) BAG3 and Hsc70 Interact With Actin Capping Protein CapZ to Maintain Myofibrillar Integrity Under Mechanical Stress. Circ Res. 107(10):1220-31

Homma S, Iwasaki M, Shelton GD, *et al.* (2006) BAG3 Deficiency Results in Fulminant Myopathy and Early Lethality. Am J Pathol. 169(3):761-73

Huber TB, Kwoh C, Wu H, *et al.* (2006) Bigenic mouse models of focal segmental glomerulosclerosis involving pairwise interaction of CD2AP, Fyn, and synaptopodin. J Clin Invest. 116(5):1337-45

Ingber DE (2006) Cellular mechanotransduction: putting all the pieces together again. FASEB J. 20:811-27

Iqbal K, Liu F, Gong CX, Grundke-Iqbal I (2010) Tau in Alzheimer Disease and Related Tauopathies. Curr Alzheimer Res. 7(8):656-64

Ishida N, Kitagawa M, Hatakeyama S, Nakayama K (2000) Phosphorylation at Serine 10, a Major Phosphorylation Site of $p27^{Kip1}$, Increases Its Protein Stability. J Biol Chem 275(33):25146-54

Iwasaki M, Homma S, Hishiya A, *et al.* (2007) BAG3 Regulates Motility and Adhesion of Epithelial Cancer Cells. Cancer Res. 67(21)

Iwasaki M, Tanaka R, Hishiya A, *et al.* (2010) BAG3 directly associates with guanine nucleotide exchange factor of Rap1, PDZGEF2, and regulates cell adhesion. Biochem Biophys Res Commun. 400(3):413-18

Johnston JA, Ward CL, Kopito RR (1998) Aggresomes: A Cellular Response to Misfolded Proteins. J Cell Biol 143(7):1883-98

Juliano RL, Reddig S, Alahari S, *et al.* (2004) Integrin regulation of cell signaling and motility. Biochem Societey Transact. 32:3
Khaitlina SY (2014) Intracellular Transport Based on Actin Polymerization. Biochemistry (Moscow) 79(9):917-27

Kannan N, Tang VW (2015) Synaptopodin couples epithelial contractility to α-actinin-4-dependent junction maturation. J Cell Biol. 211(2):407-34

Kathage B, Gehlert S, Ulbricht A, *et al.* (2017) The cochaperone BAG3 coordinates protein synthesis and autophagy under mechanical strain through spatial regulation of mTORC1. Biochem Biophys Acta 1864(1):62-75

Kawaguchi Y, Kovacs JJ, McLaurin A, *et al.* (2003) The Deacetylase HDAC6 Regulates Aggresome Formation and Cell Viability in Response to Misfolded Protein Stress. Cell 115:727-38

Kopito RR (2000) Aggresomes, inclusion bodies and protein aggregation. Trends Cell Biol 10

Kostera-Pruszczyk A, Suszek M, Ploski R, *et al.* (2015) BAG3-related myopathy, polyneuropathy and cardiomyopathy with long QT syndrome. J Muscle Res Cell Motil. 36:423-32

Kremerskothen J, Plaas C, Kindler S, *et al.* (2005) Synaptopodin, a molecule involved in the formation of the dendritic spine apparatus, is a dual actin/α-actinin binding protein. J Neurochem. 10:597-606

Krugman S, Jordens I, Gevaert K, *et al.* (2001) Cdc42 induces filopodia by promoting the formation of an IRSp53:Mena complex. Curr Biol. 11:1645-55

Kruppa AJ, Kendrick-Jones J, Buss F (2016) Myosins, Actin and Autophagy. Tarffic 17:878-890

Kumar A, Singh A, Ekavali (2015) A review on Alzheimer's disease pathophysiology and its management: an update. Pharmacol Rep. 67(2):195-203

Kural C, Serpinskaya AS, Chou YH, *et al.* (2007) Tracking melanosomes inside a cell to study molecular motors and their interaction. PNAS. 104(13):5378-82

Lan D, Wang W, Zhuang J, Zhao Z (2014) Proteasome inhibitor-induced autophagy in PC12 cells overexpressing A53T mutant α-synuclein. Mol Med Reports 11:1655-60

Le Clainche C, Carlier AF (2008) Regulation of Actin Assembly Associated With Protrusion and Adhesion in Cell Migration. Physiol Rev. 88:489-513

Lee SH, Dominguez R (2010) Regulation of Actin Cytoskeleton Dynamics in Cells. Mol Cells. 29(4):311-25

Lee JH, Takahashi T, Yasuhara N, *et al.* (1999) Bis, a Bcl-2-binding protein that synergizes with Bcl-2 in preventing cell death. Oncogene 18:6183-90

Lei Z, Brizzee C, Johnson GVW (2015) BAG3 facilitates the clearance of endogenous tau in primary neurons. Neurobiol Aging 36(1):241-8

Li WW, Li J, Bao JK (2012) Microautophagy: lesser-known self-eating. Cell Mol Life Sci. 69(7):1125-36

Lin F, Yu YP, Woods J, *et al.* (2001) Myopodin, a Synaptopodin Homologue, Is Frequently Deleted in Invasive Prostate Cancers. Am J Pathol. 159(5):1603-12

Linnemann A, van der Ven PF, Vakeel P, *et al.* (2010): The sarcomeric Z-disc component myopodin is a multiadapter protein that interacts with filamin and alpha-actinin. Eur J Cell Biol. 89(9):681-92

Llorca O, Martín-Benito J, Ritco-Vonsovici M, *et al.* (2000) Eukaryotic chaperonin CCT stabilizes actin and tubulin folding intermediates in open quasi-native conformations. EMBO Journal 19(22):5971-79

Longatti A, Tooze SA (2012) Recycling endosomes contribute to autophagosome formation. Autophagy 8(11):1682-83

Lüders J, Demand J, Höhfeld J (2000) The ubiquitin-related BAG-1 provides a link between the molecular chaperones Hsc70/Hsp70 and the proteasome. J Biol Chem 275:4613–4617

Lynch EA, Stall J, Schmidt G, *et al.* (2006) Proteasome-mediated Degradation of Rac1-GTP during Epithelial Cell Scattering. Mol Biol Cell. 17:2236-42

Maravillas-Montero JL, Santos-Argumedo L (2012) The myosin family: unconventional roles of actin-dependent molecular motors in immune cells. J Leukoc Biol. 91(1):35-46

Mauvezin C, Nagy P, Juhász G, Neufeld TP (2015) Autophagosome-lysosome fusion is independent of V-ATPase-mediated acidification. Nat Commun. 6:7007

Mayer, MP (2010) Gymnastics of molecular chaperones. Mol. Cell 39:321−331

Mayran N, Parton RG, Gruenberg J (2003) Annexin II regulates multivesicular endosome biogenesis in the degradation pathway of animal cells. EMBO Journal 22(13):3242-53

McCaffrey MW, Bielli A, Cantalupo G, *et al.* (2001) Rab4 affects both recycling and degradative endosomal trafficking. FEBS Letters 495:21-30

Mejillano MR, Kojima S, Applewhite DA, *et al.* (2004) Lamellipodial Versus Filopodial Mode of the Actin Nanomachinery: Pivotal Role of the Filament Barbed End. Cell 118:363-73

Meng W, Takeichi M (2009) Adherens Junction: Molecular Architecture and Regulation. Cold Spring Harb Perspect Biol. 1:a002899

Merabova N, Sariyer IK, Saribas AS, *et al.* (2015) WW domain of BAG3 is required for the induction of autophagy in glioma cells. J Cell Physiol 230(4):831-41

Merrifield CJ, Rescher U, Almers W, *et al.* (2001) Annexin 2 has an essential role in actin-based macropinocytic rocketing. Curr Biol. 11:1136-41

Mi N, Chen Y, Wang S, *et al.* (2015) CapZ regulates autophagosomal membrane shaping by promoting actin assembly inside the isolation membrane. Nat Cell Biol. 17(9):1112-25

Minoia M, Boncoraglio A, Vinet J, *et al.* (2014) BAG3 induces the sequestration of proteasomal clients into cytoplasmic puncta. Autophagy 10(9):1603-21

Moreau K, Ghislat G, Hochfeld W, *et al.* (2015) Transcriptional regulation of Annexin A2 promotes starvation-induced autophagy. Nat Commun. 6:8045

Morel E, Parton RG, Gruenberg J (2009) Annexin A2-Dependent Polymerization of Actin Mediates Endosome Biogenesis. Develop. Cell 16:445-57

Morozova K, Sridhar S, Zolla V, *et al.* (2015) Annexin A2 promotes phagophore assembly by enhancing Atg16L+ vesicle biogenesis and homotypic fusion. Natur Commun. 6:5856

Mullock BM, Smith CW, Ihrke G, *et al.* (2000) Syntaxin 7 Is Localized to Late Endosome Compartments, Associates with Vamp 8, and Is Required for Late Endosome-Lysosome Fusion. Mol Biol Cell 11:3137-53

Mun GI, Park S, Kremerskothen J, Boo YC (2014) Expression of synaptopodin in endothelial cells exposed to laminar shear stress and its role in endothelial wound healing. FEBS Letters 588:1024-30

Mundel P, Gilbert P, Kriz W (1991) Podocytes in Glomerulus of Rat Kidney Express a CHarcteristic 44 KD Protein. J Histochem Cytochem. 39(8):1047-56

Mundel P, Heid HW, Mundel TM, *et al.* (1997) Synaptopodin: An Actin-associated Protein in Telencephalic Dendrites and Renal Podocytes. J Cell Biol. 139(1):193-204

Murata S, Minami Y, Minami M, Chiba T, Tanaka K (2001) CHIP is a chaperone-dependent E3 ligase that ubiquitylates unfolded protein. EMBO Rep. 2:1133–1138

Murphy ME (2013) The HSP70 family and cancer. Carcinogenesis 34(6):1181-88

Nakamura F, Stossel TP, Hartwig JH (2011) The filamins Organizers of cell structure and function. Cell Adhesion & Migration 5(2):160-9

Nanes BA, Kowalczyk AP (2012) Adherens junction turnover: regulating adhesion through cadherin endocytosis, degradation, and recycling. Subcell Biochem. 60:197-222

Navarro-Yepes J, Burns M, Anandhan A, *et al.* (2014) Oxidative Stress, Redox Signaling, and Autophagy: Cell Death Versus Survival. Antiox Redox Signal. 21(1):66-85

Nielsen D, Gyllberg H, Östlund P, *et al.* (2004) Increased levels of insulin and insulin-like growth factor-1 hybrid receptors and decreased glycosylation of the insulin receptor α- and β-subunits in scrapie-infected neuroblastoma N2a cells.- Biochem J. 380:571-9

Norton N, Li D, Riedler MJ, *et al.* (2011) Genome-wide Studies of Copy Number Variation and Exome Sequencing Identify Rare Variants in BAG3 as a Cause of Dilated Cardiomyopathy. Am J Hu Gen. 88:273-82

Omi K, Hachiya NS, Tanaka M, *et al.* (2008) 14-3-3zeta is indispensable for aggregate formation of polyglutamine-expanded huntingtin protein. Neurosci Letters. 431:45-50

Ono S, Ono K (2002) Tropomyosin inhibits ADF/cofilin-dependent actin filament dynamics. J Cell Biol. 156(6):1065-76

Orth JD, Cao KH, McNiven MA (2001) The larger GTPase dynamin regulates actin comet formation and movement in living cells. PNAS. 99(1):167-72

Ouyang H, Ali YO, Ravichandran M, *et al.* (2012) Protein Aggregates Are Recruited to Aggresome by Histone Deacetylase 6 via Unanchored Ubiquitin C Termini. J Biol Chem. 287(4):2317-27

Patrie KM, Drescher AJ, Welihinda A, *et al.* (2002) Interaction of Two Actin-binding Proteins, Synaptopodin and α-Actinin-4, with the Tight Junction Protein MAGI-1. J Biol Chem. 277(33):30183-90

Pavenstädt H (2000) Roles of the podocyte glomerular function. Am J Physiol Renal Physiol. 278:F173-9

Puri C, Renna M, Bento CF, *et al.* (2013) Diverse Autophagosome Membrane Sources Coalesce in Recycling Endosomes. Cell 154(6):1285-99

Puri C, Renna M, Bento CF, *et al.* (2014) ATG16L1 meets ATG9 in recycling endosomes. Autophagy 10(1):182-4

Raftopoulou M, Hall A (2004) Cell migration: Rho GTPases lead the way. Dev Biol. 265:23-32

Ravikumar B, Moreau K, Jahreiss L, *et al.* (2010) Plasma membrane contributes tot he formation of pre-autophagosomal structures. Nat Cell Biol. 12(8):747-57

Ridley AJ (1997) The GTP-binding Protein Rho. Int J Biochem Cell Biol. 29(11):1225-29

Riedl J, Crevenna AH, Kessenbrock K, *et al.* (2008) Lifeact: a versatile marker to visualize F-actin. Nat Methods 5(7):605

Rogers AL, Wiedemann U, Stuurman N, Vale RD (2003) Molecular requirements for actin-based lamella formation in *Drosophila* S2 cells. J Cell Biol. 162(6):1079-88

Romero S, Le Clainche C, Didry D, *et al.* (2004) Formin Is a Processive Motor that Requires Profilin to Accelerate Actin Assembly and Associated ATP Hydrolysis. Cell 119:419-29

Rosati A, Leone A, Del Valle L, *et al.* (2007) Evidence for BAG3 Modulation of HIV-1 Gene Transcription. J Cell Physiol. 210(3):676-83

Rosati A, Di Salle E, Luberto L, *et al.* (2009) Identification of a Btk-BAG3 complex induced by oxidative stress. Leukemia 23:823-24

Rosati a, Graziano V, Dee Laurenzi V, *et al.* (2011) BAG3: a multifaceted protein that regulates major cell pathways. Cell Death and Disease 2:e141

Ross JL, Ali MY, Warshaw DM (2008) Cargo Transport: Molecular Motors Navigate a Complex Cytoskeleton. Curr Opin Biol. 20(1):41-7

Rüdiger S, Buchberger A, Bukau B (1997) Interaction of Hsp70 chaperones with substrates. Nat Struct. Biol. 4:342−349

Saftig P, Klumperman J (2009) Lysosome biogenesis and lysosomal membrane proteins: trafficking meets fnction. Nature Reviews Mol Cell Biol. 10:623-635

Salah Z, Aqeilan RI (2011) WW domain interactions regulate the Hippo tumor suppressor pathway. Cell Death and Diesease 2:e172

Schiwek D, Endlich N, Holzman L, *et al.* (2004) Stable expression of nephrin and localization to cell-cell contacts in novel murine podocyte cell lines. Kidney Intern. 66:91-101

Schroeter MM, Beall B, Heid HW, Chalovich JM (2008) The Actin Binding Protein Fesselin, is a Member of the Synaptopodin Family. Biochem Biophys Res Commun. 371(3):582-6

Selcen D, Muntoni F, Burton BK, *et al.* (2009) Mutation in BAG3 Causes Severe Dominant Childhood Muscular Dystrophy. Ann Neurol. 65(1):83-9

Shi H, Xu H, Li Z *et al.* (2016) BAG3 regulates cell proliferation, migration, and invasion in human colorectal cancer. Tumor Biol. 37(4):5591-97

Snider J, Lin F, Rodionov V, *et al.* (2004) Intracellular actin-based transport: How far you go depends on ow often you switch. PNAS. 101(36):13204-09

Sondermann H, Scheufler C, Schneider C, Höhfeld J, *et al.* (2001) Structure of a Bag/Hsc70 Complex: Convergent Functional Evolution of Hsp70 Nucleotide Exchange Factors. Science 291:1553-7

Sternlicht H, Farr GW, Sternlicht ML, *et al.* (1993) The t-complex polypeptide 1 complex is a chaperonin for tubulin and actin in vivo. Cell Biol. 90:9422-26

Stetak A., Hajnal A (2011) The C. elegans MAGI-1 protein is a novel component of cell junctions that is required for junctional compartmentalization. Dev. Biol. 350:24–31

Suleiman HY, Roth R, Jain S, *et al.* (2017) Injury-induced actin cytoskeleton reorganization in podocytes revealed by super-resolution microscopy. JCI Insight 2(16):e94137

Takayama S, Sato T, Krajewski S, *et al.* (1995) Cloning and Functional Analysis of BAG-1: A Novel Bcl-2 Binding Protein with Anti-Cell Death Activity. Cell 80:279-84

Takayama S, Xie Z, Reed JC (1999) An Evolutionarily Conserved Family of Hsp70/Hsc70 Molecular Chaperone Regulators. J Biol Chem. 274(2):781-86

Tang V, Brieher WM (2013) FSGS3/CD2AP is a barbed-end capping protein that stabilizes actin and strengthens adherens junctions. J Cell Biol. 203(5):815-33

Tanida I, Ueno T, Kominami E (2008) LC3 and Autophagy. Methods Mol Biol. 445, 77-88

Theriot JA, Mitchison T, Tilney LG, Portnoy DA, (1992) The rate of actin-based motility of intracellular Listeria monocytogenes equals the rate of actin polymerization. Nature 357:257-260

Tojkander S, Gateva G, Schevzov G, *et al.* (2011) A Molecular Pathway for Myosin II Recruitment to Stress Fibers. Curr Biol 21:539-50

Tojkander S, Gateva G, Lappalainen P (2012) Actin stress fibers – assembly, dynamics and biological roles. J Cell Sci. 125:1855-64

Ulbricht A (2013) PhD Thesis: Chaperon-assistierte, selective Autophagie – Bedeutung für die Mechanotransduction. Retrieved from the group of Prof. Höhfeld, University of Bonn.

Ulbricht A, Eppler F, Tapia VE, *et al.* (2013) Cellular Mechanotransduction Relies on Tension-Induced and Chaperone-Assisted Autophagy. Curr Biol. 23:430-35

Ulbricht A, Gehlert S, Leciejewski B, *et al.* (2015) Induction and adaptation of chaperone-assisted selective autophagy CASA in response to resistance exercise in human skeletal muscle. Autophagy 11(3):538-46

Vasmant D, Maurice M, Feldmann G (1984) Cytoskeleto Ultrastructure of Podocytes and Glomerular Endothelial Cells in Man and in the Rat. Anat Rec. 210(1):17-24

Villard E, Perret C, Gary F, *et al.* (2011) A genome-wide association study identifies two loci associated with heart failure due to dlated cardiomyopathy. Europ Heart J. 32:1065-76

Vincente-Manzanares M, Ma X, Adelstein RS, Horwitz AR (2009) Non-muscle myosin II takes centre stage in cell adhesion and migration. Nat Rev Mol Cell Biol. 10(11):778-90

Virador VM, Davidson B, Czechowicz J, *et al.* (2009): The Anti-Apoptotic Activity of BAG3 is Restricted by Caspases and the Proteasome. PLoS ONE 4(4):e5136

Waelter S, Boeddrich A, Lurz R, *et al.* (2001) Accumulation of Mutant Huntingtin Fragments in Aggresome-like Inclusion Bodies as a Result of Insufficient Protein Degradation. Mol Biol Cell 12:1393-407

Wang HQ, Liu HM, Zhang HY, *et al.* (2008) Transcriptional upregulation of BAG3 upon proteasome inhibition. Biochem Biophys Res Commun 365:381-5

Wang J, Farr GW, Zeiss CJ, *et al.* (2009) Progressive aggregation despite chaperone associations of a mutant SOD1-YFP in transgenic mice that develop ALS. PNAS 106(5):1392-97

Wang Y, Yu A, Yu FX (2017) The Hippo pathway in tissue homeostasis and regeneration. Protein Cell 8(5):349-59

Watanabe TM, Higuchi H (2007) Stepwise Movements in Vesicle Transport of HER2 by Motor Proteins in Living Cells. Biophys J. 92:4109-20

Wegener AD, Jones LR (1984) Phosphorylation-induced Mobility Shift in Phospholamban in Sodium Dodecyl Sulfate-Polyacrylamide Gels. J Biol Chem. 259(3):1834-41

Weins A, Schwarz K, Faul C, *et al.* (2001) Differentiation- and stress-dependent nuclear cytoplasmic redistribution of myopodin, a novel actin-bundling protein. J Cell Biol. 155(3):393-403

Welsch T, Endlich N, Kriz W, Endlich K (2001) CD2AP and p130Cas localize to different F-actin structures in podocytes. Am J Physiol Renal Physiol. 281:F769-77

Wong JS, Iorns E, Rheault MN, *et al.* (2012) Rescue of tropomyosin deficiency in Drosophila and human cancer cells by synaptopodin reveals a role of tropomyosin α in RhoA stabilization. EMBO Journal 31:1028-40

Wu C, Asokan SB, Berginski AE, et al. (2012) Arp2/3 Is Critical for Lamellipodia and Response to Extracellular Matrix Cues but Is Dispensable for Chemotaxis. Cell 148:973-87

Xiao K, Allison DF, Kottke MD, *et al.* (2003) Mechanisms of VE-cadherin Processing and Degradation in Microvascular Endothelial Cells. J Biol Chem. 278(21):19199-208

Xu Z, Graham K, Foote M, *et al.* (2013) 14-3-3 protein targets misfolded chaperone-associated proteins to aggresomes. J Cell Sci. 126: 4173-86

Yamamoto H, Kakuta S, Watanabe TM, *et al.* (2012) Atg9 vesicles are an important membrane source during early steps of autophagosome formation. J Cell Biol. 198(2):219-33

Yanagida-Asanuma E, Asanuma K, Kim K, *et al.* (2007) Synaptopodin Protects Against Proteinuria by Disrupting Cdc42:IRSp53:Mena Signaling Complexes in Kidney Podocytes. Am J Pathol 171(2): 415-27

Yen WL, Shintani T, Nair U, *et al.* (2010) The conserved oligomeric Golgi complex is involved in double-membrane vesicle formation during autophagy. J Cell Biol. 188(1):101-14

Ylä-Anttila P, Vihinen H, Jokitalo E, Eskelinen EL (2009) 3D tomography reveals connections between the phagophore and endoplasmic reticulum. Autophagy 5(8):1180-5

Youn DY, Lee DH, Lim MH, *et al.* (2008) Bis deficiency results in early lethality with metabolic deterioration and involution of spleen and thymus. Am J Physiol Endocrinal Metab 295:E1349-E57

Zhang Y, Wang JH, Lu Q, Wang YJ (2012) Bag3 promotes resistance to apoptosis through Bcl-2 family members in non-small cell lung cancer. Oncology Rep. 27:109-13

Online References

Ensembl	http://www.ensembl.org
NCBI	https://www.ncbi.nlm.nih.gov
protein BLAST	https://blast.ncbi.nlm.nih.gov/Blast.cgi
Uniprot	http://www.uniprot.org

Danksagung

Mein besonderer Dank gilt Herrn Prof. Dr. Jörg Höhfeld für die Möglichkeit meine Dissertation in seiner Arbeitsgruppe am Institut für Zellbiologie durchzuführen.

Herrn Prof. Dr. Dieter Fürst danke ich sehr für die Übernahme des Koreferats meiner Arbeit.

Ich glaube ich finde nicht die richtigen Worte um meinen unglaublichen Arbeitskollegen Dr. Barbara Kathage, Christina Klimek, Karen Himmelberg, Jan Daerr, Judtith Wördehoff, Dr. Anna Ulbricht, Dr. Annemarie Ulitzsch, Laura Lüdecke, Svenja Adrian und Dr. Riga Tawo zu danken. Ihr wart da, in allen Höhen und Tiefen, als Kollegen und als Freunde. Ich weiss, dass ich es ohne Euch nicht geschafft hätte. Die Zeit mit euch BFFFLs war einfach „awesome“!

Auch bei den lieben Arbeitskollegen der Arbeitsgruppen Fürst und Haas möchte ich mich für die gute Arbeitsatmosphäre und die Hilfsbereitschaft bedanken. Hier möchte ich mich besonders bei der coolsten Büro-Nachbarin aller Zeiten Dr. Sibylle Molt bedanken. Du warst immer eine super Ansprechpartnerin für alles Wissenschaftliche und Persönliche und bist vor allem eine tolle Freundin.

Ein riesiger Dank geht an meine Eltern, meine Oma und meine Stiefeltern. Danke dass ihr mich nicht nur in der Zeit meiner Dissertation immer bedingungslos unterstützt habt. Ihr wart immer für mich da und ihr seid die Besten auf der Welt. Ich hab Euch sehr lieb.

Riga, danke dass du an meiner Seite bist. Danke, für deine Unterstützung, deine Ehrlichkeit, dein Vertrauen, deine Geduld, und dafür dass ich immer auf dich zählen kann.

Liebe Betty, für dich ist diese Arbeit. Vielleicht hättest du selber mal so eine geschrieben, wer weiß das schon. Du bist immer bei mir und wirst es immer sein. Ich vermisse dich und bin so unendlich dankbar für die Jahre die uns gegeben waren.